

**THE EFFECT OF AUSTENITISING AND TEMPERING
PARAMETERS ON THE MICROSTRUCTURE AND
HARDNESS OF MARTENSITIC STAINLESS STEEL AISI 420**

by

LILIAN D. BARLOW

Submitted in partial fulfilment of the requirements for the degree of

MASTER OF SCIENCE (APPLIED SCIENCE): METALLURGY

**in the Faculty of Engineering, Built Environment and Information
Technology**

University of Pretoria

Supervisor: Professor M du Toit

April 2009

ABSTRACT

The effect of austenitising and tempering practice on the microstructure and mechanical properties of two martensitic stainless steels was examined with the aim of supplying heat treatment guidelines to the consumer or fabricator that, if followed, would result in a martensitic structure with minimal retained austenite, evenly dispersed carbides and a hardness of between 610 HV and 740 HV (hardness on the Vickers scale) after quenching and tempering. The steels examined during the course of this examination conform in composition to medium-carbon AISI type 420 martensitic stainless steel, except for the addition of 0.13% vanadium and 0.62% molybdenum to one of the alloys. The effect of various austenitising and tempering heat treatments was examined. Steel samples were austenitised at temperatures between 1000°C and 1200°C, followed by quenching in oil. The as-quenched microstructures were found to range from almost fully martensitic structures to martensite with up to 35% retained austenite after quenching, with varying amounts of carbide precipitates. The influence of tempering, double tempering, and sub-zero treatment was investigated. Optical and scanning electron microscopy was used to characterise the as-quenched microstructures, and X-ray diffraction analysis was employed to identify the carbide present in the as-quenched structures and to quantify the retained austenite contents. Hardness tests were performed to determine the effect of heat treatment on mechanical properties. As-quenched hardness values ranged from 700 HV to 270 HV, depending on the amount of retained austenite. Thermodynamic predictions (using the CALPHAD™ model) were used to explain these microstructures based on the solubility of the carbide particles in the matrix at various austenitising temperatures. The carbide particles were found to be mainly in the form of M_7C_3 at elevated temperatures, transforming to $M_{23}C_6$ on cooling.

Keywords: martensitic, stainless, austenitising temperature, retained austenite, M_7C_3 , $M_{23}C_6$, carbide

TABLE OF CONTENTS

<u>CHAPTER 1 - BACKGROUND</u>		p. 1
1. INTRODUCTION		p. 1
2. LITERATURE SURVEY		p. 3
2.1 Martensitic stainless steels – an overview		p. 3
2.2 The influence of alloying elements on the microstructure of martensitic stainless steels		p. 4
2.2.1 Chromium		p. 4
2.2.2 Carbon		p. 5
2.2.3 Molybdenum		p. 6
2.2.4 Vanadium		p. 6
2.3 The effect of alloying elements on the formation and stability of carbides		p. 7
2.4 Heat treatment of martensitic stainless steels		p. 8
2.4.1 Annealing		p. 8
2.4.2 Austenitising		p. 9
2.4.3 Quenching		p. 18
2.4.4 Tempering		p. 19
2.4.5 Cryogenic or sub-zero treatment		p. 19
2.4.6 Multiple tempering steps		p. 20
3. HEAT TREATMENT OPTIMISATION		p. 20
<u>CHAPTER 2 – OBJECTIVES OF THE INVESTIGATION</u>		p. 21
1. BACKGROUND		p. 21
2. OBJECTIVES OF THE INVESTIGATION		p. 21
<u>CHAPTER 3 – OVERVIEW OF THE EXPERIMENTAL PROCEDURE</u>		p. 23
1. STAINLESS STEEL ALLOYS STUDIED IN THIS INVESTIGATION		p. 23
1.1 Chemical compositions		p. 23
1.2 Plant heat treatment		p. 23
2. HEAT TREATMENTS USED IN THIS INVESTIGATION		p. 24
3. METALLOGRAPHIC INVESTIGATION		p. 24
3.1 Austenite grain size		p. 24
3.2 The average carbide diameter and carbide density		p. 25
4. HARDNESS MEASUREMENTS		p. 25
5. X-RAY DIFFRACTION		p. 25
6. THERMODYNAMIC PREDICTIONS		p. 25
<u>CHAPTER 4 – RESULTS AND DISCUSSION</u>		p. 27
1. AS-RECEIVED SAMPLES		p. 27
2. THE EFFECT OF AUSTENITISING TEMPERATURE ON THE AS-QUENCHED MICROSTRUCTURE AND PROPERTIES OF HEATS 1 AND 2		p. 29
3. THE EFFECT OF TEMPERING ON THE MICROSTRUCTURE AND PROPERTIES OF HEATS 1 AND 2		p. 46
3.1 Tempering after austenitising at 1150°C or 1175°C		p. 47
3.2 Double tempering		p. 48
3.3 Sub-zero treatments		p. 50
4. PRELIMINARY CONCLUSIONS		p. 56



<u>CHAPTER 5 – FINAL CONCLUSIONS AND RECOMMENDATIONS</u>	p. 57
1. FINAL CONCLUSIONS	p. 57
2. RECOMMENDATIONS	p. 59
<u>CHAPTER 6 – REFERENCES</u>	p. 60
APPENDIX A – CARBIDE DIAMETER MEASUREMENTS	p. 62
APPENDIX B – ASTM GRAIN SIZE NUMBER	p. 64
APPENDIX C – VICKERS HARDNESS MEASUREMENTS	p. 67
APPENDIX D – ADDITIONAL MICROGRAPHS	p. 69

LIST OF FIGURES

Figure 1.1	The binary Fe-Cr phase diagram.	p. 2
Figure 1.2	Optical micrograph of AISI 420 in the spheroidise annealed form. The microstructure consists of carbides in a ferrite matrix. Etchant: Vilella's reagent ¹⁶ .	p. 9
Figure 1.3	Scanning electron micrograph of AISI 420 annealed at 750 °C for 2 hours. The microstructure consists of carbides in a ferrite matrix. Etchant: Vilella's reagent ¹⁵ .	p. 9
Figure 1.4	The influence of the heating rate on the A_{cc} temperature ¹⁶ .	p. 12
Figure 1.5	The area percentage of carbides after quenching as a function of austenitising temperature ¹⁶ .	p. 13
Figure 1.6	Vickers hardness after austenitising for 60 seconds at various temperatures ¹⁶ .	p. 13
Figure 1.7	The effect of austenitising temperature on as-quenched hardness (from De Andrés ¹⁶ , Candelaria ¹⁹ and Latrobe (labelled Timken) ¹⁸).	p. 15
Figure 1.8	Optical photomicrograph of X45CrMoV14 in the as-quenched condition (austenitised at 1100 °C). The structure consists predominantly of carbides in a fine martensitic matrix. The hardness is 670 HV ⁶ .	p. 16
Figure 1.9	Optical photomicrograph of X45CrMoV14 in the as-quenched condition (austenitised at 1150 °C). The structure consists predominantly of carbides in a fine martensitic matrix. The hardness is 630 HV ⁶ .	p. 16
Figure 1.10	Optical photomicrograph of X45CrMoV14 in the as-quenched condition (austenitised at 1200 °C). The structure consists predominantly of retained austenite and some undissolved carbides in a fine martensitic matrix. The hardness is 580 HV ⁶ .	p. 16
Figure 1.11	Optical photomicrograph of X45CrMoV14 in the as-quenched condition (austenitised at 1250 °C). The structure consists predominantly of retained austenite in a fine martensitic matrix. The hardness is 580 HV ⁶ .	p. 16
Figure 1.12	Effect of austenitising temperature on the carbide volume fraction in martensitic stainless steels ⁶ .	p. 17
Figure 1.13	Retained austenite volume fraction as a function of the austenitising temperature ⁶ .	p. 18
Figure 4.1	The as-received microstructure of HEAT 1, consisting of coarse $M_{23}C_6$ carbides in a ferrite matrix (hardness: 209±7 HV). (Magnification: 50x).	p. 28
Figure 4.2	The as-received microstructure of HEAT 2, consisting of coarse $M_{23}C_6$ carbides in a ferrite matrix (hardness: 195±4 HV). (Magnification: 100x).	p. 28
Figure 4.3	Scanning electron micrograph of the as-received microstructure of HEAT 2. The microstructure consists of coarse, globular $M_{23}C_6$ carbides in a ferrite matrix.	p. 28
Figure 4.4	Scanning electron micrograph of HEAT 2 after austenitising for 15 minutes at <u>1000 °C</u> , followed by oil quenching. The microstructure consists of coarse $M_{23}C_6$ carbides in a fine martensite matrix. (Hardness: 639±10 HV).	p. 31
Figure 4.5	Optical micrograph of HEAT 1 after austenitising for 15 minutes at <u>1050 °C</u> , followed by oil quenching. The microstructure consists of $M_{23}C_6$ carbides in a fine martensite matrix. (Hardness: 678±9 HV). (Magnification: 200x).	p. 32
Figure 4.6	Scanning electron micrograph of HEAT 1 after austenitising for 15 minutes at <u>1075 °C</u> , followed by oil quenching. The microstructure consists of $M_{23}C_6$ carbides in a martensite matrix. (Hardness: 684±10 HV).	p. 33
Figure 4.7	Thermodynamic prediction of the equilibrium phase diagram of two heats of AISI 420 at an austenitising temperature of 1075 °C.	p. 34
Figure 4.8	Scanning electron micrograph of HEAT 1 after austenitising for 15 minutes at <u>1100 °C</u> , followed by oil quenching. The microstructure consists of $M_{23}C_6$ carbides in a martensite matrix containing 23% retained austenite. (Hardness: 653±8 HV).	p. 35
Figure 4.9	Scanning electron micrograph of HEAT 2 after austenitising for 15 minutes at <u>1100 °C</u> , followed by oil quenching. The microstructure consists of $M_{23}C_6$ carbides in a martensite matrix containing 12% retained austenite. (Hardness: 639±15 HV).	p. 36

Figure 4.10	Thermodynamic prediction of the equilibrium phase diagram of two heats of AISI 420 at an austenitising temperature of 1100°C.	p. 36
Figure 4.11	Scanning electron micrograph of HEAT 1 after austenitising for 15 minutes at 1130°C, followed by oil quenching. The microstructure consists of M ₂₃ C ₆ carbides in a martensite matrix containing 25% retained austenite. (Hardness: 474±7 HV).	p. 37
Figure 4.12	Scanning electron micrograph of HEAT 2 after austenitising for 15 minutes at 1130°C, followed by oil quenching. The microstructure consists of M ₂₃ C ₆ carbides in a martensite matrix containing 15% retained austenite. (Hardness: 620±4 HV).	p. 38
Figure 4.13	Thermodynamic prediction of the equilibrium phase diagram of two heats of AISI 420 at an austenitising temperature of 1130°C.	p. 38
Figure 4.14	Optical micrograph of HEAT 1 after austenitising for 15 minutes at 1150°C, followed by oil quenching. The microstructure consists of a small number of residual M ₂₃ C ₆ carbides in a martensite matrix containing 27% retained austenite. (Hardness: 308±6 HV). (Magnification: 100x).	p. 39
Figure 4.15	Scanning electron micrograph of HEAT 1 after austenitising for 15 minutes at 1175°C, followed by oil quenching. The microstructure consists of martensite and 29% retained austenite. (Hardness: 279±4 HV).	p. 40
Figure 4.16	Scanning electron micrograph of HEAT 2 after austenitising for 15 minutes at 1175°C, followed by oil quenching. The microstructure consists of martensite and 21% retained austenite. (Hardness: 488±3 HV).	p. 40
Figure 4.17	Thermodynamic prediction of the equilibrium phase diagram of two heats of AISI 420 at an austenitising temperature of 1175°C.	p. 41
Figure 4.18	The influence of austenitising temperature on the carbide density (number of carbides per mm ²) in HEATS 1 and 2.	p. 42
Figure 4.19	The influence of austenitising temperature on the as-quenched hardness of HEATS 1 and 2 (with 95% confidence interval).	p. 44
Figure 4.20	The influence of austenitising temperature on the as-quenched retained austenite content of HEATS 1 and 2.	p. 44
Figure 4.21	The influence of austenitising temperature on the average ASTM grain size of HEATS 1 and 2.	p. 45
Figure 4.22	The influence of austenitising temperature on the average carbide diameter in HEATS 1 and 2.	p. 46
Figure 4.23	Optical micrograph of HEAT 1 after austenitising at 1175°C, followed by oil quenching and tempering at 550°C for 30 minutes. The microstructure consists of martensite and retained austenite. (Hardness: 284±14 HV). (Magnification: 100x).	p. 48
Figure 4.24	Optical micrograph of HEAT 1 after austenitising at 1150°C, followed by oil quenching and double tempering at 650°C. The microstructure consists of martensite and retained austenite. (Hardness: 500±9 HV). (Magnification: 100x).	p. 49
Figure 4.25	The effect of sub-zero tempering on the hardness of HEATS 1 and 2 after austenitising at temperatures between 1100°C and 1175°C.	p. 51
Figure 4.26	Optical micrograph of HEAT 2 after austenitising at 1130°C, followed by oil quenching and sub-zero treatment in liquid nitrogen. The microstructure consists of martensite and a small amount of retained austenite. (Hardness: 741±18 HV). (Magnification: 200x).	p. 51
Figure 4.27	Optical micrograph of HEAT 1 after austenitising at 1130°C, followed by oil quenching, sub-zero treatment in liquid nitrogen and tempering at 550°C. The microstructure consists of martensite and 3% retained austenite. (Hardness: 673±6 HV). (Magnification: 200x).	p. 52
Figure 4.28	Optical micrograph of HEAT 1 after austenitising at 1150°C, followed by oil quenching, sub-zero treatment in liquid nitrogen and tempering at 550°C. The microstructure consists of martensite and 5% retained austenite. (Hardness: 651±14 HV). (Magnification: 200x).	p. 52

- Figure 4.29** Scanning electron micrograph of HEAT 1 after austenitising at 1175°C, followed by oil quenching, sub-zero treatment in liquid nitrogen and tempering at 550°C. The microstructure consists of martensite, 8% retained austenite and networks of intergranular $M_{23}C_6$ carbides. (Hardness: 649±9 HV). p. 53
- Figure 4.30** Optical micrograph of HEAT 2 after austenitising at 1130°C, followed by oil quenching, sub-zero treatment in liquid nitrogen and tempering at 550°C. The microstructure consists of martensite and 1% retained austenite. (Hardness: 626±4 HV). (Magnification: 200x). p. 54
- Figure 4.31** Scanning electron micrograph of HEAT 2 after austenitising at 1150°C, followed by oil quenching, sub-zero treatment in liquid nitrogen and tempering at 550°C. The microstructure consists of martensite and 3% retained austenite. (Hardness: 644±9 HV). p. 54
- Figure 4.32** Scanning electron micrograph of HEAT 2 after austenitising at 1175°C, followed by oil quenching, sub-zero treatment in liquid nitrogen and tempering at 550°C. The microstructure consists of martensite, 4% retained austenite and networks of intergranular $M_{23}C_6$ carbides. (Hardness: 647±12 HV). p. 54
- Figure 4.33** Optical micrograph of HEAT 2 after austenitising at 1130°C, followed by oil quenching, sub-zero treatment in liquid nitrogen and tempering at 700°C. The microstructure consists of martensite and retained austenite. (Hardness: 333±2 HV). (Magnification: 500x). p. 55

LIST OF TABLES

Table 1.1	Typical chemical composition of AISI 420 martensitic stainless steel (weight percentage, balance Fe) ⁷ .	p. 4
Table 1.2	The chemical compositions (wt %) of X45Cr13 martensitic stainless steel ⁶ , AISI 420 ¹⁷ , LSS 420 HC ¹⁸ and a Ni-Mo martensitic steel ¹⁵ , balance Fe (nr = not reported).	p. 11
Table 3.1	Chemical composition of the AISI 420 heats examined during the course of this investigation (weight %, balance Fe).	p. 23
Table 4.1	A summary of the results obtained for HEAT 1 and HEAT 2 after various austenitising heat treatments.	p. 30
Table 4.2	The effect of tempering on the hardness of HEATS 1 and 2 after austenitising at 1150°C and 1175°C.	p. 48
Table 4.3	The effect of double tempering on the hardness of HEATS 1 and 2 after austenitising at 1150°C and 1175°C.	p. 49
Table 4.4	The effect of sub-zero treatment and tempering on the hardness of HEATS 1 and 2 after austenitising at 1130°C, 1150°C and 1175°C.	p. 55

ACKNOWLEDGEMENTS

I would like to express my gratitude and appreciation to the following people and companies for their assistance during the course of this project:

- My parents, Len and Julia Helfrich, and my children, Nicholas, Nadine, Bryan and Marianka, for their patience, love, support and their faith in me.
- Professor Madeleine du Toit for her patience, supervision and invaluable advice.
- Professor Chris Pistorius for his advice.
- Columbus Stainless Steel for financial sponsorship of the project.
- The University of Pretoria for providing laboratory facilities.
- My colleagues and friends in the Department of Materials Science and Metallurgical Engineering, in particular Prof Andrie Garbers-Craig, Mrs Sarah Havenga and Mr Markus Erwee, for their help and continuous encouragement.

CHAPTER 1 - BACKGROUND

1. INTRODUCTION

Martensitic stainless steels were developed to satisfy a need in industry for corrosion resistant alloys that respond to hardening through heat treatment. These steels are alloyed with at least 10.5% chromium and up to 0.6% carbon, and are designed to be fully austenitic at elevated temperatures. The austenite can be hardened by quenching or cooling to room temperature from the austenitising temperature¹, which enables transformation to martensite^{1,2}. Due to their high alloying element content, martensitic stainless steels demonstrate excellent hardenability and are normally considered to be air hardening.

To develop optimal mechanical and corrosion properties in martensitic stainless steels, complete transformation to martensite on cooling is essential. The alloy therefore has to be fully austenitic at elevated temperatures, with a martensite transformation range above room temperature to allow the transformation to martensite to go to completion on cooling. Chromium imparts corrosion resistance to stainless steels, but is a strong ferrite-forming element, favouring ferrite at the expense of austenite at higher temperatures. The requirement for a fully austenitic structure at high temperature therefore limits the maximum chromium content of martensitic stainless steels to that defined by the stable austenite region on the binary Fe-Cr phase diagram (the γ -phase field in Figure 1.1³). Carbon is added to martensitic stainless steels to increase hardness and wear resistance, but also acts as a powerful austenite-former (it promotes austenite at the expense of ferrite). Carbon therefore expands the γ -phase field to higher chromium contents, allowing the addition of higher levels of chromium for improved corrosion resistance without compromising the stability of austenite at higher temperatures. The austenite phase field extends to about 18% chromium with the addition of 0.6% carbon. By definition martensitic stainless steels therefore lie within the chromium range of 11.5 to 18%, with the lower limit being governed by corrosion resistance and the upper limit by the requirement for the alloy to convert fully to austenite on heating.

In addition to chromium and carbon, martensitic stainless steels may also contain additions of molybdenum and vanadium. These alloying elements increase the

hardenability, temper resistance and high temperature hardness of the steel⁴. Like chromium, molybdenum and vanadium are strong carbide-formers⁵. The austenitising temperature employed during heat treatment determines the partitioning of carbon and alloying elements between the austenite and carbide phases, with an increase in temperature leading to increased carbide dissolution and higher dissolved alloying element contents. When in solid solution at temperatures above the carbide dissolution temperature, these carbide-forming elements affect the transformation to martensite by depressing the martensite transformation range and reducing the martensite start (M_s) and martensite finish (M_f) temperatures. If the M_f temperature is depressed to below room temperature or even to below 0°C , retained austenite may be present in the as-quenched microstructure as a result of the martensite transformation not going to completion². Retained austenite reduces the as-quenched hardness and may transform to brittle martensite during subsequent tempering operations.

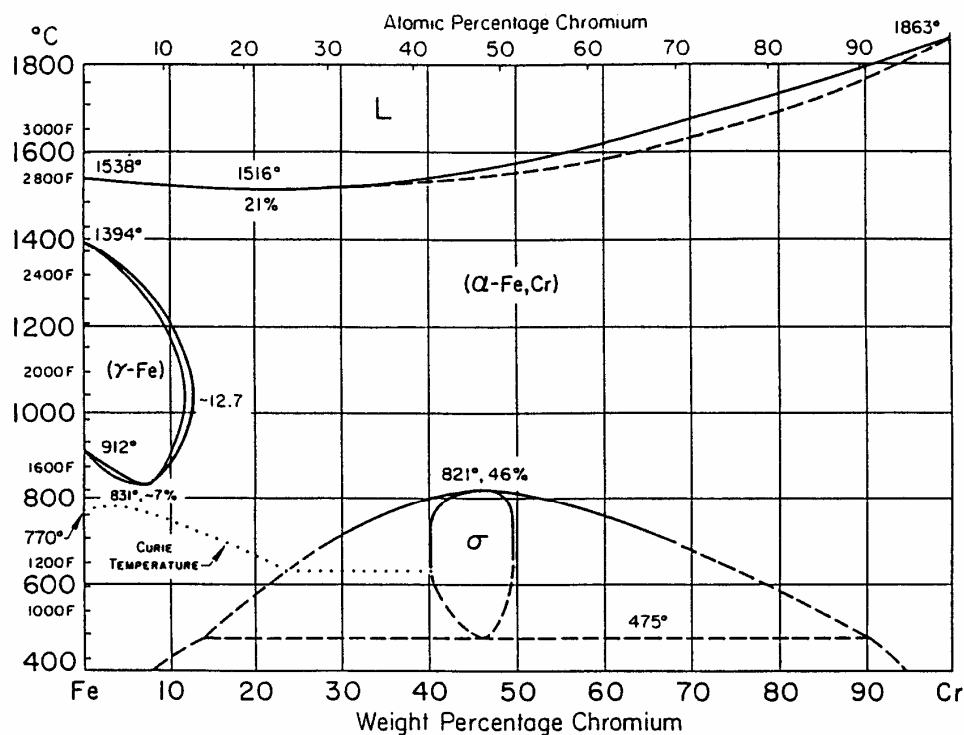


Figure 1.1: The binary Fe-Cr phase diagram.

The composition of martensitic stainless steels and their response to heat treatment therefore determine the resulting mechanical and corrosion properties. An overview of the relevant available literature on the metallurgy and heat treatment of these steels is given below.

2. LITERATURE OVERVIEW

In 1822, Michael Faraday initiated an investigation with the aim of producing an alloy steel for the manufacture of cutting tools and non-corrodable metals for reflectors. At this time only so-called plain-carbon steels were available – steels which do not perform satisfactorily in applications requiring high strength and corrosion resistance. One hundred years later, in 1922, Brearley discovered the stainless (“corrosion resistant”) properties of high-chromium steels. These high-chromium corrosion resistant alloy steels are now referred to as “stainless steels”⁴.

2.1 Martensitic stainless steels – an overview:

Martensitic stainless steels contain between 11.5% and 18% chromium, and are deliberately alloyed with up to 0.6% carbon. The development of this group of stainless steels was prompted by the need for corrosion resistant stainless steels that are hardenable by heat treatment. The resulting martensitic stainless steels are austenitic at elevated temperatures and harden through transformation to martensite during quenching or cooling to room temperature⁵. This results in an excellent combination of moderate to good corrosion resistance, high hardness and strength, good resistance to thermal and mechanical fatigue and excellent wear resistance.

The martensitic stainless steels are magnetic, can be cold-worked and hot-worked (especially at lower carbon contents), can be machined satisfactorily, display high toughness and possess good corrosion resistance to weather and some chemicals. They attain their best corrosion resistance in the hardened condition, but are generally not as corrosion resistant as the austenitic or ferritic stainless steels. Among corrosion-resistant applications, martensitic stainless steels are used in coal handling and in mining equipment, where advantage is taken of their high abrasion resistance and moderate corrosion resistance^{1,5}. The martensitic grades are usually hardened by heating above the transformation range to temperatures in the region of 1000°C, followed by cooling in air or oil. Time at temperature must be minimised to prevent decarburisation or excessive grain growth. In order to obtain mechanical properties suitable for engineering applications, the steels are tempered after quenching. The resulting mechanical properties depend strongly on the tempering temperature.

For a martensitic stainless steel to possess adequate hardness, wear resistance and corrosion resistance, no δ -ferrite should be present at the austenitising temperature (950°C to 1010°C), the martensite transformation range should be above room temperature (to reduce the risk of forming retained austenite) and the steel should exhibit maximum temper resistance. As the martensitic transformation is the dominant strengthening mechanism in these steels, the heat treatment of the alloy must be designed to ensure that no, or at best, minimal retained austenite is present after cooling⁶. This is complicated by the chemistry of the steel, and in particular the presence of additional alloying elements, which often depress the martensite finish temperature to below 0°C.

For applications involving wear or which require retention of sharp cutting surfaces in finished products, steels containing 11 to 14% chromium and between 0.3 and 0.4% carbon are preferred³. The medium to high carbon contents of these steels ensure the high as-quenched hardness values required in these applications. AISI 420 is a low-chromium, medium-carbon member of the martensitic family of stainless steels. In the hardened and tempered condition, AISI 420 has high strength and excellent wear resistance, which makes it the ideal choice for applications such as cutlery, hand tools, dental and surgical instruments, valve trim and parts, shafts, and plastic moulding. The typical chemical composition range specified for medium-carbon AISI 420 is shown in Table 1.1⁷. The steel is alloyed primarily with chromium and carbon. A brief discussion of these and other alloying elements routinely added to AISI 420 martensitic stainless steel is given below.

Table 1.1: Typical chemical composition of AISI 420 martensitic stainless steel (weight percentage, balance Fe)⁷.

C	Cr	Mn	Si	Mo	Ni	P	S
0.5 max.	12.0 to 14.0	1.0 max.	1.0 max.	1.0 max.	1.0 max.	0.04 max.	0.03 max.

2.2 The influence of alloying elements on the microstructure of martensitic stainless steels:

2.2.1 Chromium:

Chromium is the principal alloying element in stainless steels, added in amounts greater than approximately 10.5% to improve corrosion resistance and promote

passivation. Chromium is a strong ferrite-forming element and tends to restrict the austenite phase field and suppress the ferrite to austenite transformation during heating⁵. In binary Fe-Cr alloys, the austenite phase field extends to a maximum chromium content of approximately 12.7% (as shown in Figure 1.1). Beyond this chromium content, austenite is not thermodynamically stable.

This limits the amount of chromium that can be added to austenitic and martensitic stainless steels (these alloys have to transform completely to austenite at higher temperatures). In alloys requiring higher chromium contents for improved corrosion resistance, the austenite phase field can be expanded to higher chromium levels by adding strong austenite-forming elements, such as carbon, nitrogen or nickel. In the presence of sufficient carbon, steels containing in excess of 12% chromium can be fully austenitic above a certain temperature (this temperature being dependant on the carbon:chromium ratio)⁸. As shown in Table 1.1, AISI 420 contains 12 to 14% chromium. Chromium is also instrumental in increasing the hardness and wear resistance of the steel. It increases the hardenability and temper resistance of the steel³ and facilitates the formation of secondary chromium-rich alloy carbides, such as M_7C_3 or $M_{23}C_6$ ⁴.

2.2.2 Carbon:

Carbon is the single most important alloying element in steels and plays an important role in martensitic stainless steels. It is a strong austenite-forming element, promoting the formation of an austenitic structure at elevated temperatures at the expense of ferrite. An increase in carbon content up to approximately 1% enlarges the austenite phase field and allows steels with up to 16% chromium to be fully martensitic after appropriate hardening treatment¹. The carbon content of martensite also determines the hardness of the martensite, with the hardness increasing with an increase in carbon concentration (provided retained austenite does not form in significant amounts). Higher carbon steels are therefore preferred for applications requiring high hardness and wear resistance. The hardness of high-carbon martensitic steels can be increased further through precipitation of carbides on slow cooling from the austenite region³. However, the formation of massive chromium-rich $M_{23}C_6$ carbides lowers the corrosion resistance of the steel, a phenomenon known as sensitisation. These chromium-rich carbide particles introduce a second phase into

the metal which promotes galvanic corrosion⁹, and cause chromium depletion adjacent to the grain boundaries. Medium-carbon AISI 420 stainless steel contains up to 0.5% carbon for optimal hardness and wear resistance.

2.2.3 Molybdenum:

Although the standard AISI 420 stainless steel grades do not contain molybdenum as a deliberate alloying addition, this alloying element imparts certain beneficial properties to martensitic stainless steels that may justify its addition to AISI 420. Alloying with molybdenum results in a general improvement in corrosion resistance, machinability and mechanical properties. Molybdenum increases the hardness and temper resistance of the steel at higher temperatures⁴ and promotes secondary hardening during tempering.

Molybdenum in solid solution is a strong ferrite-forming element which enlarges the austenite phase field and retards the transformation of ferrite to austenite on heating. The addition of molybdenum to martensitic stainless steels therefore needs to be balanced with the addition of a suitable austenite-forming element to ensure a fully austenitic structure at elevated temperatures where molybdenum is more likely to be in solid solution. Molybdenum forms carbides readily and reacts with carbon to form various alloy carbides, such as Mo_2C , $\text{Fe}_4\text{Mo}_2\text{C}$ and $\text{Fe}_{21}\text{Mo}_2\text{C}_6$ ⁴. Molybdenum may also form part of the complex M_{23}C_6 carbide that precipitates on slow cooling from the austenite phase field.

2.2.4 Vanadium:

Vanadium has an important grain refining function in martensitic stainless steels, with as little as 0.1% effectively restricting grain growth during normal hardening heat treatments. Vanadium is a strong carbide-former and is normally present in the microstructure as finely dispersed carbides or carbonitrides which inhibit excessive grain growth⁴. On dissolving in the steel at higher temperatures, vanadium acts as an effective ferrite-forming element.

Since the stability of alloy carbides and their dissolution at higher temperatures have an important influence on the as-quenched microstructure and properties of martensitic stainless steels, the effect of alloying elements on the stability of carbides in these stainless steels is briefly considered below.

2.3 The effect of alloying elements on the formation and stability of carbides:

Alloying elements added to stainless steel either dissolve in the ferrite or austenite matrix, or react with carbon to form alloy carbides. Elements known to dissolve preferentially include aluminium, copper, silicon, phosphorous, nickel and zirconium. Those elements with a strong tendency to form carbides include, amongst others, chromium, tungsten, molybdenum, vanadium and titanium¹⁰. The partitioning of these carbide-forming elements between the matrix and carbide particles plays an important role in determining the microstructure and properties of martensitic stainless steels.

Higher chromium contents result in improved corrosion resistance, while higher carbon contents increase the strength, hardness and wear resistance of the steel. The presence of higher carbon contents in martensitic stainless steels is, however, associated with several disadvantages, including lower toughness, degradation of weldability and a reduction in corrosion resistance due to the formation of chromium-rich carbides. Higher carbon contents tend to increase the volume fraction of carbides present after cooling, often necessitating the use of high austenitising temperatures which result in grain growth and reduced impact properties².

Various authors have published reports detailing investigations into the nature of the different carbides that form in martensitic stainless steels^{6,11}. It has been shown that steels with more than 0.2% carbon and between 12 and 13% chromium (including AISI 420) typically contain M_3C , M_7C_3 and $M_{23}C_6$ carbides. The precipitation of these carbides is time dependent, and appears to occur in a typical precipitation sequence that involves initial precipitation of M_3C , followed by M_7C_3 and then $M_{23}C_6$ ¹¹. The addition of approximately 1% molybdenum to 12% chromium steels retards the coarsening of the carbide particles.

The stability of these carbides and their gradual dissolution at higher temperatures control the partitioning of carbon and alloying elements between the austenite matrix and the carbide precipitates. Dissolution of carbides during heat treatment reduces the M_s and M_f temperatures of the steel, and may result in the presence of significant amounts of retained austenite after cooling. The heat treatment of these grades of martensitic stainless steel therefore has a major influence on the microstructure and properties of the alloys, and is described in more detail below.

2.4 Heat treatment of martensitic stainless steels:

Heat treatment of steel causes internal physical changes which produce a wide range of microstructures in the alloy. These transformations affect the mechanical properties of the steel, and the heat treatment procedure can usually be manipulated to obtain a wide range of strength, toughness and hardness values¹².

The typical heat treatment sequence for martensitic stainless steels includes annealing to soften the steel in preparation for subsequent cold work or machining, austenitising to form an austenitic structure and fully or partially dissolve carbides, cooling or quenching to transform the austenite to martensite, followed by tempering of the martensitic structure to improve toughness and ductility. The final microstructure of AISI 420 is very dependent on the prior heat treatment that the steel received, and typically consists of martensite, undissolved and/or reprecipitated carbides and retained austenite. The volume fraction and size of the carbide particles present in the steel and the amount of retained austenite play a major role in determining the hardness, strength, toughness, corrosion resistance and wear resistance of the steel¹³. The typical heat treatments used in the processing of martensitic stainless steels are discussed below.

2.4.1 Annealing:

Martensitic stainless steel is often supplied in the fully annealed condition, allowing the material to be easily formed and machined by the fabricator or user. Once the component is in its final and near-final form, the fabricator or user performs the required hardening heat treatments to develop the desired strength, hardness and wear properties.

Annealing is defined as the process whereby a material is heated to and held at a suitable temperature and then cooled at a well-defined rate to reduce hardness, improve machinability, facilitate cold work, produce a specific microstructure, or obtain desired mechanical, physical or other properties¹⁴. Annealing of AISI 420 martensitic stainless steel softens the steel by producing a fully ferritic matrix with the majority of the carbon precipitated as coarse, globular carbide particles. Since the precipitation of chromium carbide is diffusion-controlled, the annealing conditions of AISI 420 have to be optimised to ensure sufficient softening within a reasonable

annealing time. Calliari *et al*¹⁵ reported that the best compromise between annealing temperature and holding time is obtained by annealing at a temperature of 750 °C for 2 hours, which yields hardness values in the region of 284 HV (hardness on the Vickers scale). Actual plant data supplied by Columbus Stainless for the annealing of AISI 420 indicate that a spheroidise annealing treatment at 860 °C, followed by further annealing at a reduced temperature of 775 °C, yields hardness values of 195 HV to 210 HV. Annealing at higher temperatures has been shown to reduce the hardness even further, but excessive annealing temperatures increase the risk of adverse grain growth.

Type AISI 420 stainless steel is often supplied in the spheroidise annealed condition to facilitate cold work and machining. De Andrés *et al*¹⁶ observed randomly dispersed globular carbides ($M_{23}C_6$) within a ferrite matrix in AISI 420 stainless steel after extended times at the annealing temperature (as illustrated in Figure 1.2). A scanning electron micrograph of AISI 420 after annealing at 750 °C for 2 hours (consisting of ferrite and chromium-rich $M_{23}C_6$ carbides) is shown in Figure 1.3.

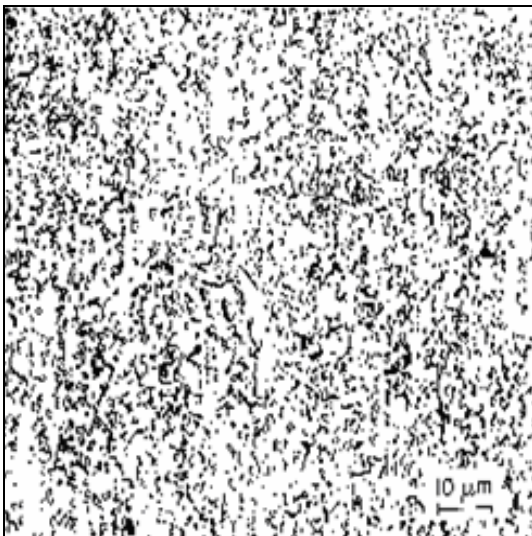


Figure 1.2: Optical micrograph of AISI 420 in the spheroidise annealed form. The microstructure consists of carbides in a ferrite matrix. Etchant: Vilella's reagent¹⁶.

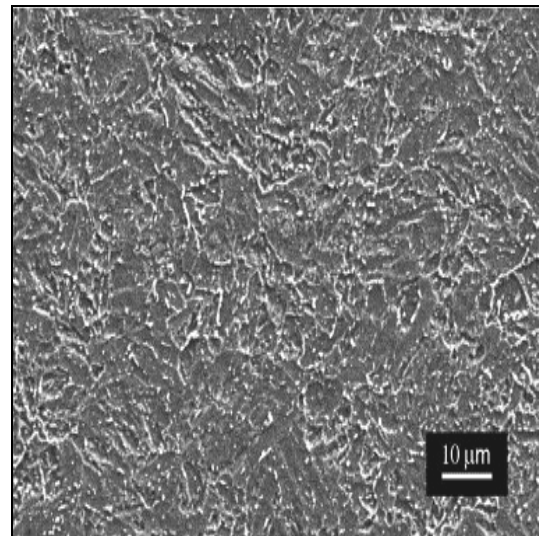


Figure 1.3: Scanning electron micrograph of AISI 420 annealed at 750 °C for 2 hours. The microstructure consists of carbides in a ferrite matrix. Etchant: Vilella's reagent¹⁵.

2.4.2 Austenitising:

The hardening heat treatment specified for martensitic stainless steels typically consists of heating to a temperature high enough to ensure an austenitic structure

with carbon in solid solution, followed by rapid cooling (air cooling or oil quenching) to form martensite. Air cooling of a fully austenitic structure usually produces full hardening in AISI 420, but oil quenching is used for larger sections to ensure complete transformation to martensite.

The austenitising treatment is of critical importance in the hardening of martensitic stainless steels. During austenitising, the final alloying element partitioning occurs between the austenite matrix (that transforms to martensite on cooling) and the retained carbides. An excessively high austenitising temperature will cause alloy carbides to coarsen or dissolve, resulting in undesirable grain growth. Alloying elements in solid solution in the austenite matrix also affect the hardenability, M_s and M_f temperatures, retained austenite content and secondary hardening potential of the steel. The volume fraction and size of undissolved carbides not only influence the wear resistance, but also affect the austenite grain size.

The effect of austenitising temperature on the microstructure and properties of martensitic stainless steels has been the subject of several investigations. Calliari *et al*¹⁵ reported that the maximum as-quenched hardness in AISI 420 martensitic stainless steel is found after austenitising at a temperature of 1050°C, as complete carbide dissolution is assumed to have occurred at this temperature. Tavares *et al*¹⁷ proposed austenitising temperatures in the range of 980°C to 1100°C for an AISI 420 martensitic steel (containing 0.4 wt% C, 13.5 wt% Cr and 0.008 wt% S). This range is considered to be too wide to guarantee consistent as-quenched hardness values, particularly in view of the strict requirements stated for the steels examined in the current investigation. Latrobe¹⁸ reported in their data sheet for LSS 420 HC stainless steel that the steel is fully austenitic after heating above 860°C, with a hardness peak of 660 HV and minimal retained austenite after air cooling from 1025°C. (The chemical compositions of the steels examined by De Andrés *et al*⁶, Calliari *et al*¹⁵, Tavares *et al*¹⁷ and Latrobe¹⁸ are shown in Table 1.2).

De Andrés *et al*⁶ investigated the effect of carbide-forming elements on the response to thermal treatment of two medium-carbon AISI 420 martensitic stainless steels. The steel designated X45Cr13 in this investigation conforms in composition to that specified for medium-carbon AISI 420, whereas the grade referred to as X45CrMoV14 contain deliberate additions of molybdenum and vanadium (refer to

Table 1.2 for the chemical compositions of these steels). Dilatometer tests were performed on small samples (12 mm in length and 2 mm in diameter) during heat treatment carried out by heating the specimens at a constant rate of 0.5°C per second to austenitising temperatures in the range of 1000°C to 1250°C, soaking for 60 seconds, followed by cooling at a constant rate of 2°C per second.

Table 1.2: The chemical compositions (wt %) of X45Cr13 martensitic stainless steel⁶, AISI 420¹⁷, LSS 420 HC¹⁸ and a Ni-Mo martensitic steel¹⁵, balance Fe (nr = not reported).

Grade	C	Si	Mn	P	S	Cr	Ni	Mo	V
X45CrMoV14 ⁶	0.460	0.46	0.44	0.018	0.003	14.3	0.16	0.51	0.13
X45Cr13 ⁶	0.450	0.32	0.44	0.030	0.016	13.0	0.38	nr	nr
AISI 420 ¹⁷	0.400	nr	nr	nr	0.008	13.5	nr	nr	nr
LSS 420 HC ¹⁸	0.460	0.40	0.40	nr	nr	13.0	nr	nr	0.30
Ni-Mo martensitic steel ¹⁵	0.195	nr	0.21	nr	nr	12.9	1.07	1.71	nr

The steels examined by De Andrés *et al*⁶ were observed to form $M_{23}C_6$ precipitates at the prior austenite grain boundaries on heating to temperatures of 550°C or higher. The authors contended that, as AISI 420 is an air-hardening steel, the as-quenched microstructure will always consist of martensite and complex carbides. It should be noted, however, that the austenitising temperature plays a major role in determining the as-quenched microstructure of the steel and the risk of retained austenite increases with an increase in austenitising temperature.

In a different study, De Andrés *et al*¹⁶ examined the effect of heating rate on the microstructure of AISI 420. The authors reported that dissolution of the $M_{23}C_6$ carbides in the austenite phase starts during heating of the steel to the austenitising temperature. They noted that the temperature at which all the carbides are dissolved (designated the A_{cc} temperature) is a function of the heating rate, as illustrated in Figure 1.4. It is evident that the temperature required for total dissolution of the carbides increases dramatically with an increase in heating rate, with the carbides dissolving completely at 1110°C for a heating rate of 0.5°C per second.

In an earlier phase of the investigation, De Andrés *et al*¹⁶ examined the effect of austenitising temperature on the as-quenched microstructure and properties of AISI 420 stainless steel at a constant heating rate of 0.5°C per second. This heating rate was selected as it is representative of heating rates commonly used in continuous

heat treatment plants in industry. The samples were held at various austenitising temperatures for 60 seconds, followed by oil quenching.

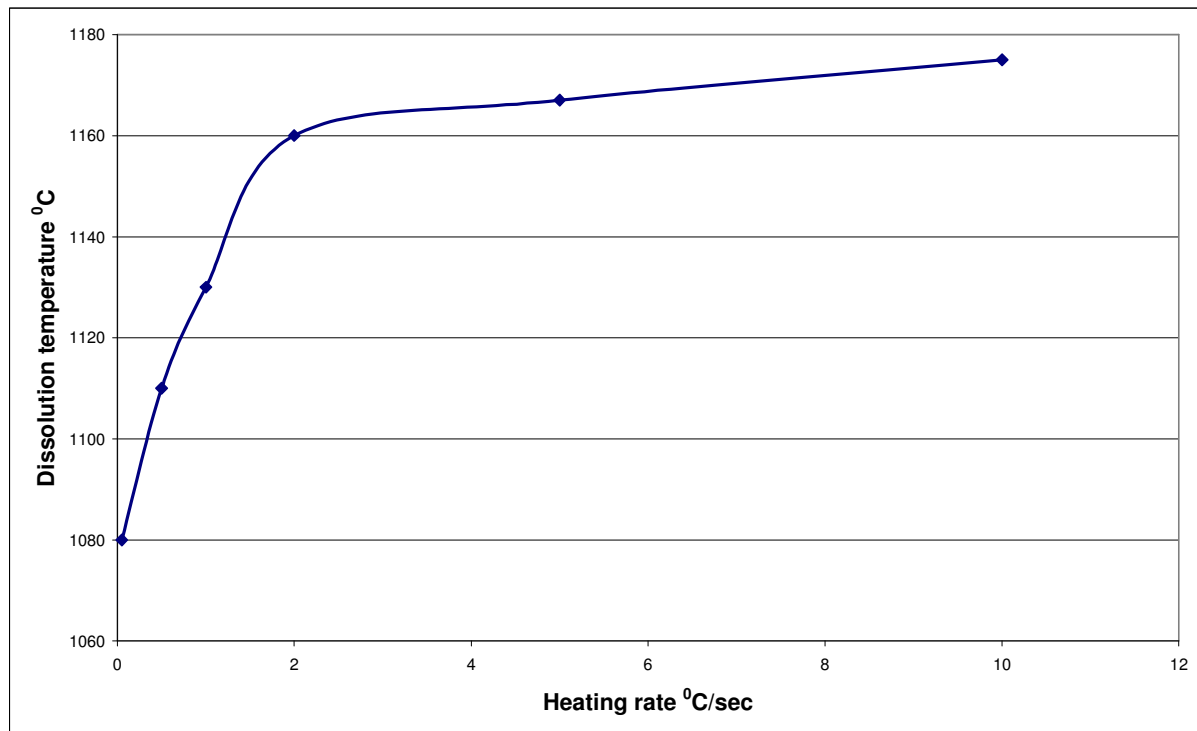


Figure 1.4: The influence of the heating rate on the A_{cc} temperature¹⁶.

The area percentage of carbides within the microstructure was measured by means of image analysis techniques and was shown to decrease with an increase in austenitising temperature (as illustrated in Figure 1.5). As more carbides dissolve at higher austenitising temperatures, it is expected that the risk of retained austenite in the as-quenched microstructure will increase. The gradual dissolution of $M_{23}C_6$ results in enrichment of carbide-forming elements and carbon in the austenite matrix, which may depress the martensite transformation range to below 0°C.

De Andrés *et al*¹⁶ reported that AISI 420 exhibits as-quenched peak hardness values of approximately 710 HV after austenitising at 1120°C for the grade containing no molybdenum, and 1130°C for the molybdenum-containing grade (as shown in Figure 1.6). The carbide volume fraction is less than 1% in both alloys after austenitising at these temperatures. As the austenitising temperature is raised further, the presence of retained austenite – which is considerably softer than martensite – reduces the as-quenched hardness values to 560 HV and 660 HV, respectively. Complete dissolution of the carbide precipitates requires a higher austenitising temperature in the presence of molybdenum.

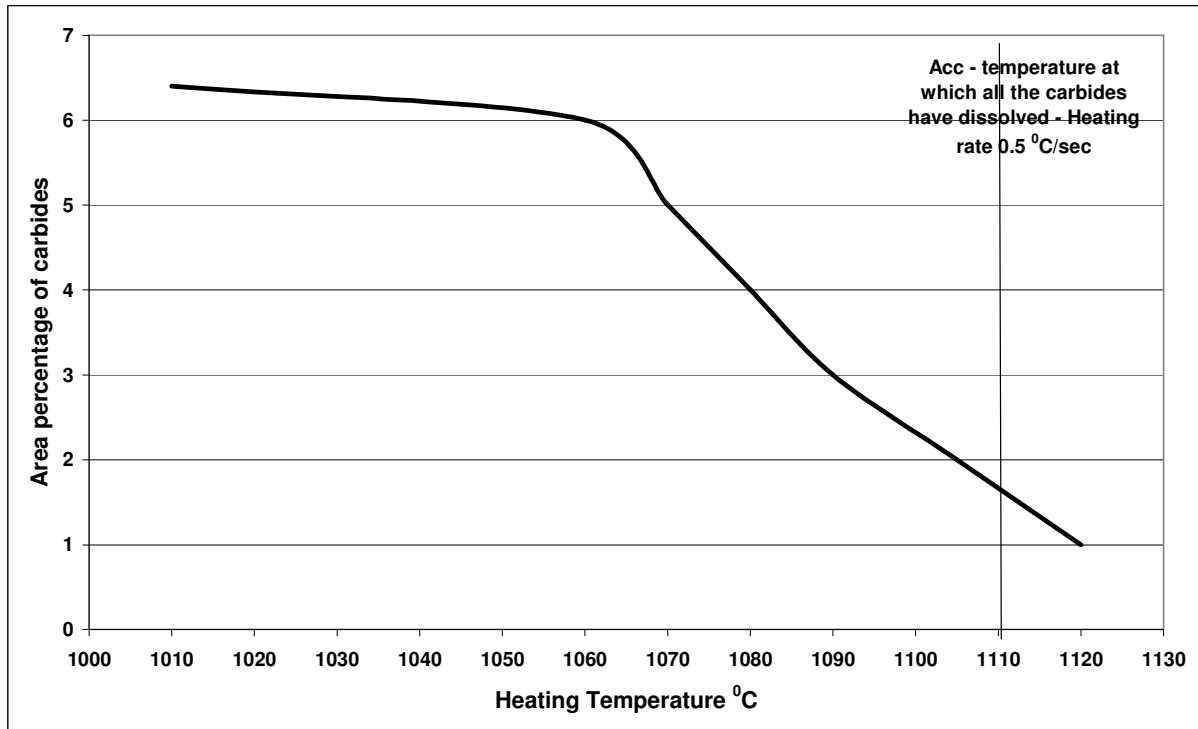


Figure 1.5: The area percentage of carbides after quenching as a function of austenitising temperature¹⁶.

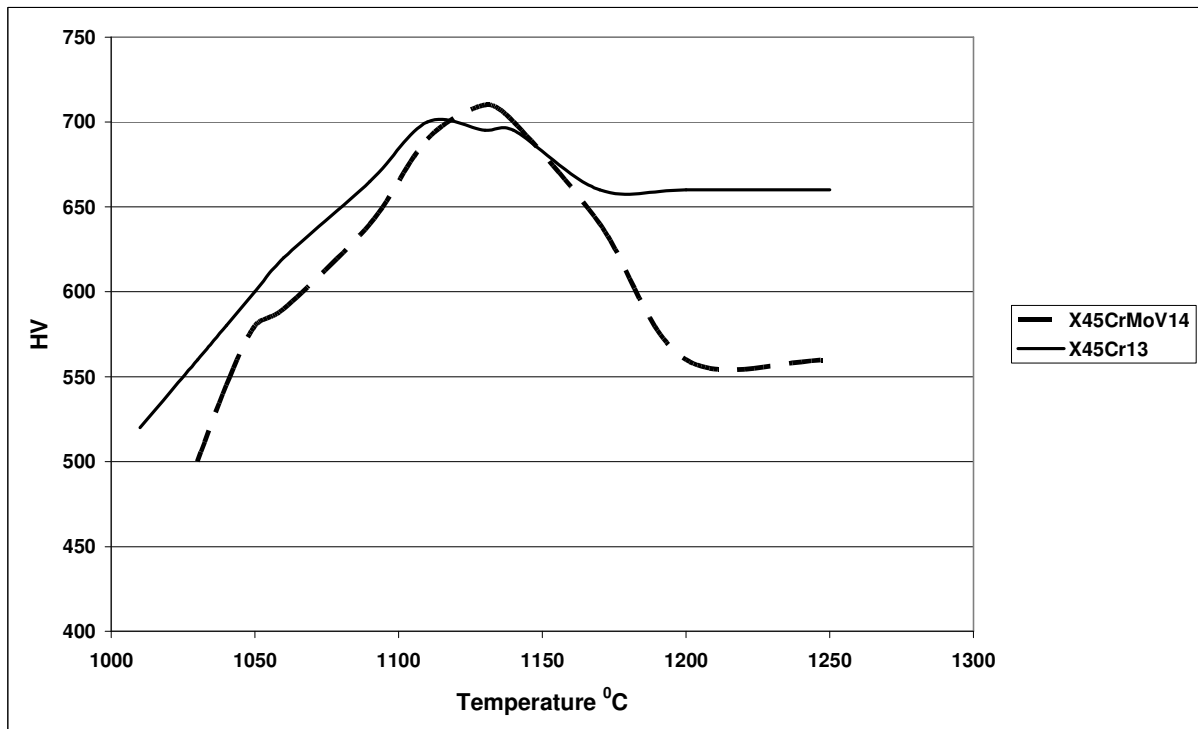


Figure 1.6: Vickers hardness after austenitising for 60 seconds at various temperatures¹⁶.

Candelaria *et al*¹⁹ reported complete dissolution of $M_{23}C_6$ carbides after oil quenching from austenitising temperatures between 900°C and 1100°C. The as-quenched

hardness increases with higher austenitising temperatures up to 1050°C. This is attributed to the gradual dissolution of $M_{23}C_6$ which increases the level of carbon supersaturation in the austenite phase, resulting in higher as-quenched martensite hardness values. At austenitising temperatures higher than approximately 1100°C, the hardness decreases as the high concentration of carbide-forming elements and carbon in solid solution in the austenite due to carbide dissolution reduces the martensite transformation range below 0°C. The martensite transformation does not go to completion and the as-quenched microstructure contains increasing amounts of retained austenite.

The influence of soaking time on the as-quenched microstructure and properties is less apparent. The Latrobe Steel¹⁸ data sheet for AISI 420 martensitic stainless steel states that a slow reduction in hardness is observed on increasing the soaking time at the austenitising temperature. This conclusion is apparently contradicted by the results shown in Figure 1.7, which indicate that longer austenitising times of 30 and 60 minutes, as used by Latrobe¹⁸ and Candelaria¹⁹, result in very similar peak hardness values as the results obtained by De Andrés *et al*¹⁶ for a soaking time of 60 seconds. The peak hardness values were, however, achieved at much higher austenitising temperatures in the investigation by De Andrés *et al*. The kinetics of carbide dissolution is governed by both time and temperature, and despite the small sample sizes used by De Andrés *et al*, the short 60 second austenitising time was probably insufficient to develop peak as-quenched hardness values at the same austenitising temperatures as those reported for the other two investigations.

Once the steels had been austenitised, quenching or cooling to below the martensite transformation range results in the formation of martensite⁶. The M_s temperature of AISI 420 martensitic stainless steel is reported to be in the range of 300°C to 70°C, whereas the M_f temperature is estimated to be approximately 150°C to 200°C lower than the M_s temperature. Almost all alloying elements in solid solution reduce the M_s and M_f temperatures, with carbon having the greatest effect. If the M_f temperature is depressed to below room temperature or even 0°C, the more highly alloyed martensitic steels may contain retained austenite after quenching due to the sub-zero temperatures required to transform all the austenite to martensite.

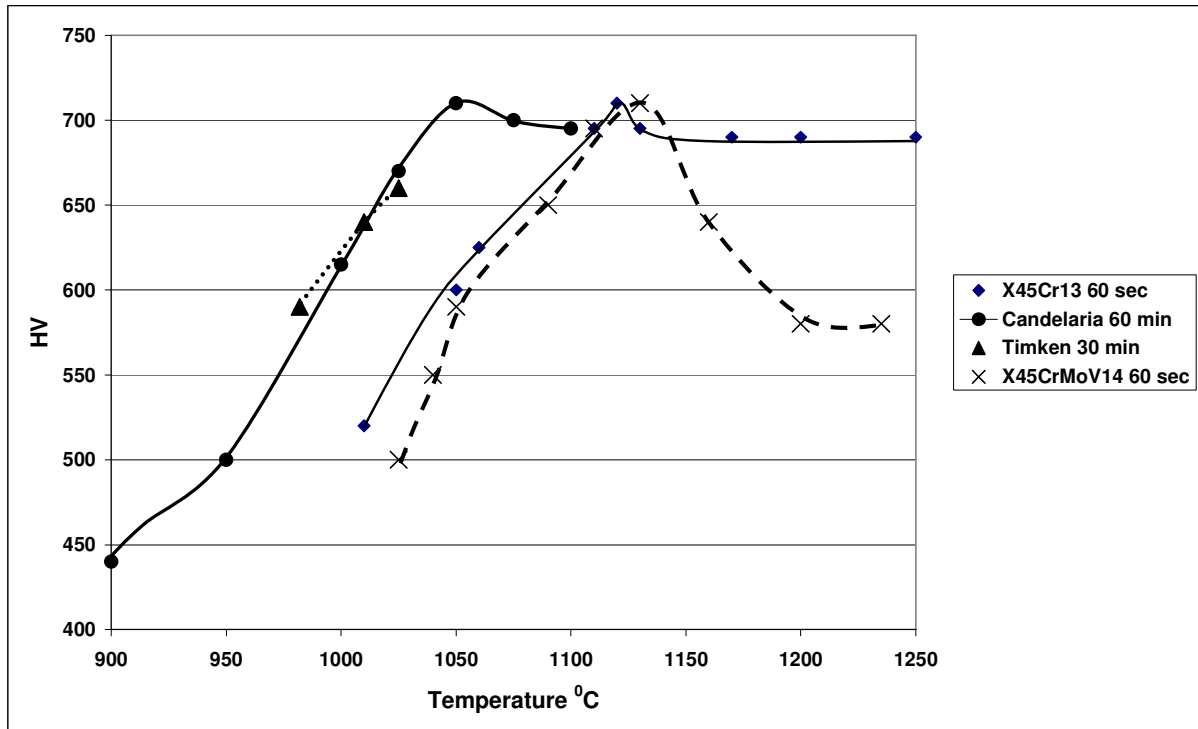


Figure 1.7: The effect of austenitising temperature on as-quenched hardness (from De Andrés¹⁶, Candelaria¹⁹ and Latrobe (labelled Timken)¹⁸).

De Andres *et al*⁶ reported no measurable retained austenite in either grade of martensitic stainless steel after austenitising at temperatures up to 1150°C. Austenitising at temperatures above 1150°C resulted in as-quenched microstructures containing lath martensite and retained austenite. Excessive grain growth was observed at austenitising temperatures above 1120°C, with a corresponding decrease in carbide volume fraction to approximately 1%. The temperatures required for complete carbide dissolution were reported to be 1130°C for X45Cr13 (no deliberate molybdenum addition) and 1170°C for X45CrMoV14 (alloyed with molybdenum).

Figures 1.8 to 1.11 show the as-quenched microstructures of X45CrMoV14 after austenitising at various temperatures for 60 seconds. An increase in retained austenite content is evident with an increase in austenitising temperature, and at austenitising temperatures of 1200°C or higher the microstructures contained no visible carbide particles. The conclusion was drawn that all carbides had dissolved at the higher heat treatment temperatures, reducing the martensite transformation range and favouring retained austenite. The lower carbide volume fraction also allowed uncontrolled grain growth during the austenitising treatment.

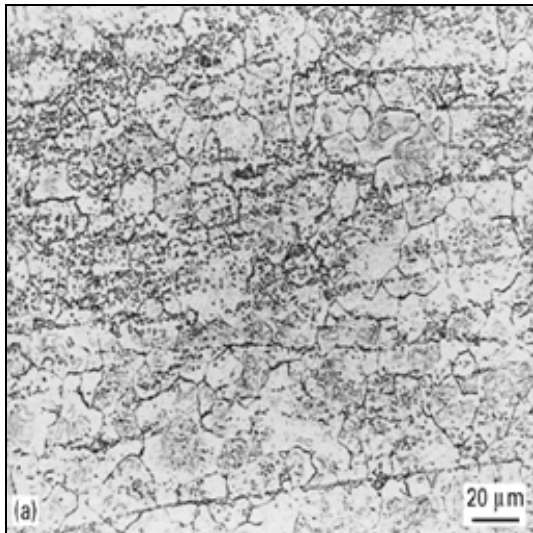


Figure 1.8: Optical photomicrograph of X45CrMoV14 in the as-quenched condition (austenitised at 1100 °C). The structure consists predominantly of carbides in a fine martensitic matrix. The hardness is 670 HV⁶.

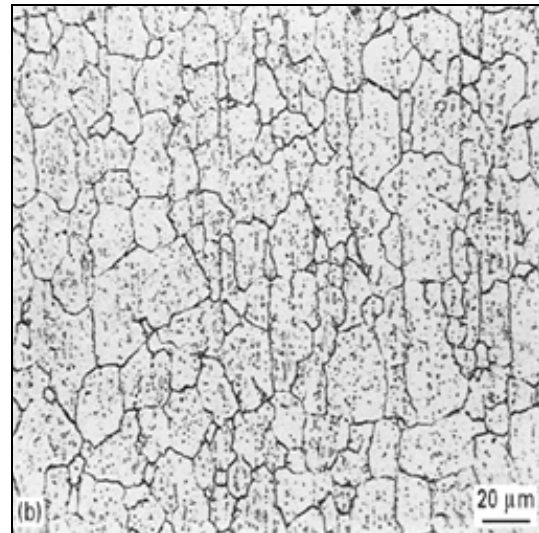


Figure 1.9: Optical photomicrograph of X45CrMoV14 in the as-quenched condition (austenitised at 1150 °C). The structure consists predominantly of carbides in a fine martensitic matrix. The hardness is 630 HV⁶.

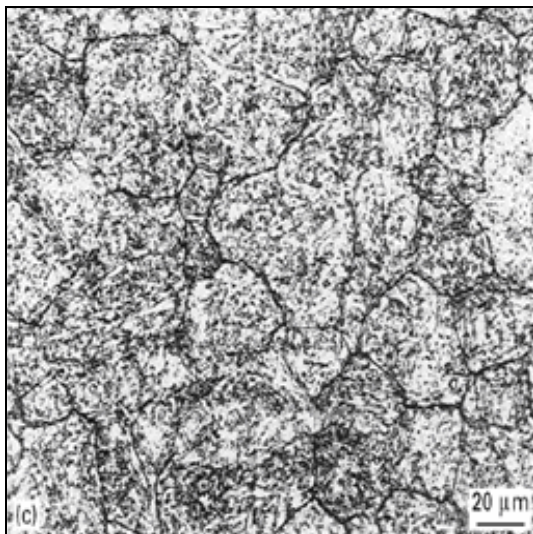


Figure 1.10: Optical photomicrograph of X45CrMoV14 in the as-quenched condition (austenitised at 1200 °C). The structure consists predominantly of retained austenite and some undissolved carbides in a fine martensitic matrix. The hardness is 580 HV⁶.

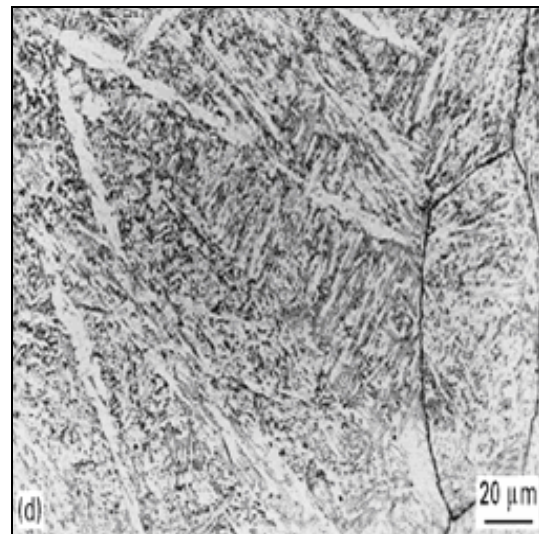


Figure 1.11: Optical photomicrograph of X45CrMoV14 in the as-quenched condition (austenitised at 1250 °C). The structure consists predominantly of retained austenite in a martensitic matrix. The hardness is 580 HV⁶.

Figure 1.12 demonstrates the effect of austenitising temperature on the carbide volume fraction in these steels, as determined by De Andrés *et al*⁶. It is evident that the volume fraction of carbide particles decreases from almost 7% at an austenitising

temperature of 1060 °C, to less than 2% at 1130 °C and 1120 °C for X45CrMoV14 and X45Cr13, respectively. This confirms that the carbide particles gradually dissolve with increasing austenitising temperatures.

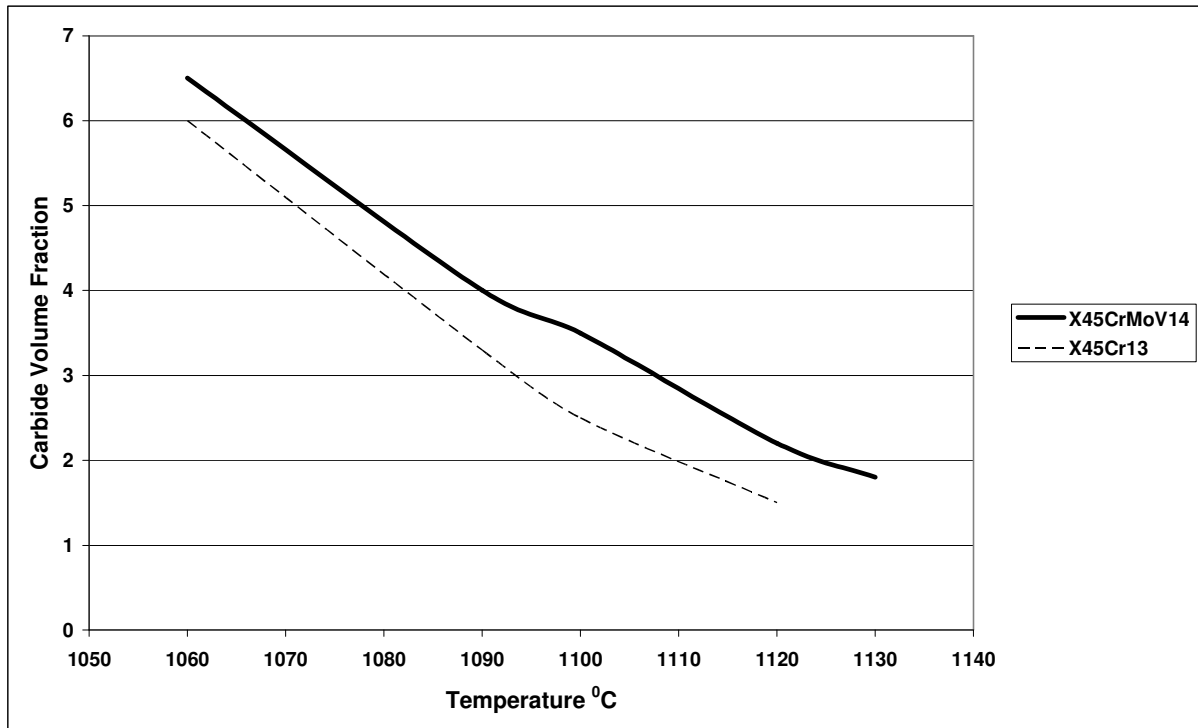


Figure 1.12: Effect of austenitising temperature on the carbide volume fraction in martensitic stainless steels⁶.

Figure 1.12 also illustrates that the volume fraction of carbides in the molybdenum-containing steel (X45CrMoV14) is consistently higher than that of the steel with no molybdenum addition. Molybdenum is reported to combine with carbon to form Mo_2C or to form part of the chromium-rich M_{23}C_6 carbide that is commonly observed in martensitic stainless steels. The presence of molybdenum is expected to retard the coarsening and dissolution of M_{23}C_6 . Higher austenitising temperatures are therefore required for complete dissolution of carbides in the presence of molybdenum.

Figure 1.13 shows the volume fraction of retained austenite as a function of the austenitising temperature for X45CrMoV14, the molybdenum-alloyed grade studied by De Andrés *et al*⁶. As the austenitising temperature increases and the carbides go into solution, the M_s transformation temperature is depressed with a corresponding increase in the volume fraction retained austenite in the as-quenched steel. Figure 1.13 indicates that retained austenite is observed after quenching from austenitising temperatures in excess of approximately 1100 °C in this alloy. This temperature

corresponds well with the temperature range in which increasing dissolution of carbides was observed in this alloy. In the molybdenum-containing alloy the percentage retained austenite stabilises at approximately 34% at temperatures above 1200 °C.

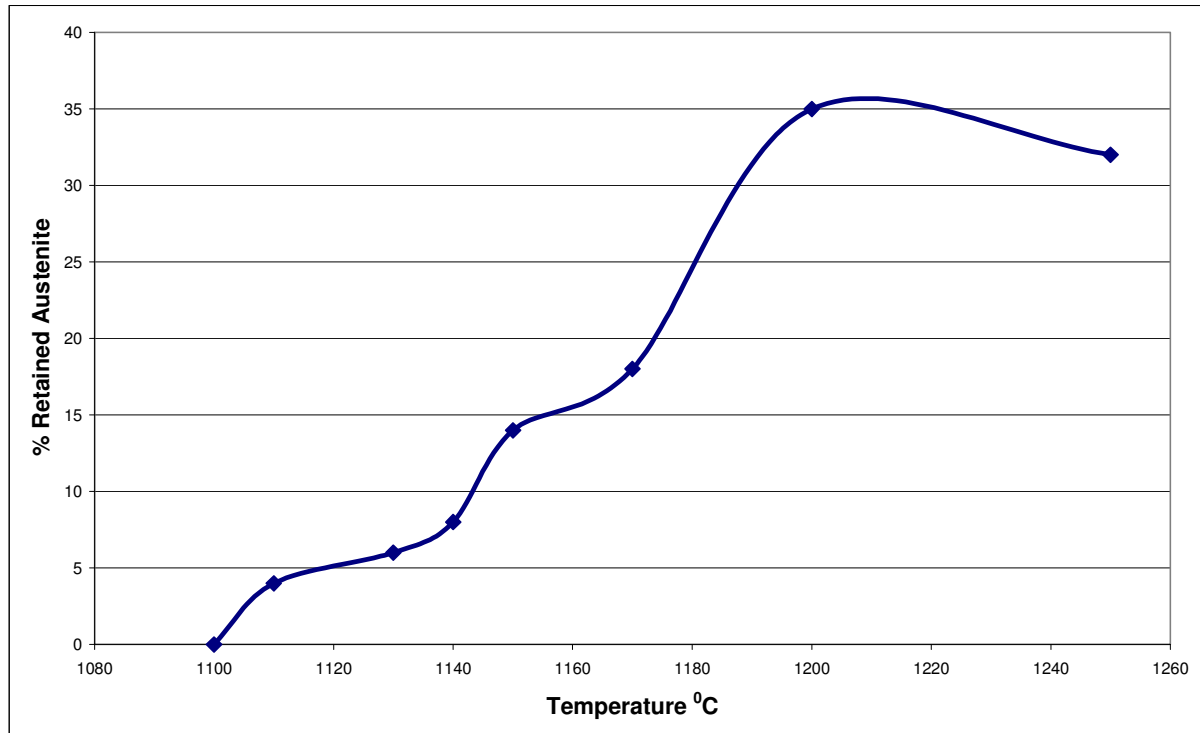


Figure 1.13: Retained austenite volume fraction as a function of the austenitising temperature⁶.

2.4.3 Quenching:

After austenitising the steel is cooled or quenched to form martensite. Most martensitic stainless steels are air-hardening, but larger sections are routinely oil quenched to ensure full transformation to martensite. Slow cooling rates promote precipitation or incomplete hardening, whereas excessive cooling rates may cause distortion or quench cracking. An unwelcome complication of AISI 420 is, as described earlier, the tendency to retain austenite after quenching. As shown in Figure 1.13, this steel may contain up to 35% retained austenite after quenching. The presence of significant amounts of retained austenite reduces the as-quenched hardness of the alloy, and may promote embrittlement if fresh, untempered martensite forms during tempering. Multiple tempering steps can be used to temper the fresh martensite, or cryogenic (sub-zero) tempering²⁰ can be used to reduce the retained austenite content prior to tempering.

2.4.4 Tempering:

In its “as-quenched” martensitic condition, the steel is hard and brittle and may contain pockets of retained austenite. Quenching is therefore followed by tempering to reduce brittleness, increase ductility and toughness and reduce residual stresses. During tempering the steel is kept at a temperature below the austenite transformation range, and cooled at a prescribed rate²¹. Tempering allows controlled precipitation of fine carbide particles, transformation of retained austenite, and recovery and recrystallisation of the highly distorted martensite matrix. Due to its high temper resistance, AISI 420 martensitic stainless steel is usually tempered at temperatures higher than approximately 550°C. Secondary hardening due to the precipitation of alloy carbides may increase the hardness during the tempering of martensitic stainless steels.

If the steel contains a significant volume fraction of retained austenite after quenching, carbide precipitation during tempering may reduce the alloying element content of the austenite, thereby increasing the M_s temperature and promoting transformation of retained austenite to martensite on cooling after tempering. This martensite is untempered and may reduce the toughness of the tempered structure. The formation of fresh martensite during tempering can be prevented using a cryogenic treatment after quenching to transform any retained austenite to martensite prior to tempering, or by using multiple tempering steps.

2.4.5 Cryogenic or sub-zero treatment:

AISI 420 martensitic stainless steel is likely to retain as much as 35% by volume retained austenite in the as-quenched structure. The ASM Handbook²² reports that the cold treating of steel is widely accepted as a treatment to promote the transformation of austenite to martensite after quenching. To complete the transformation of retained austenite to martensite, the steel needs to be cooled to a temperature below the M_f temperature. In cryogenic treatment²¹, the temperature of the steel is reduced from room temperature to temperatures well below 0°C. Refrigeration or cooling in dry ice or liquid nitrogen is commonly used, and slow cooling rates in the region of 2°C per minute are recommended to prevent thermal shock. The material must be kept at this temperature for a period of 24 to 36 hours. At sub-zero temperatures, austenite converts to martensite very slowly, but more

complete transformation to martensite may be obtained provided the cryogenic treatment temperature is below the M_f temperature of the steel.

2.4.6 Multiple tempering steps:

Multiple tempering steps can be used to temper martensite that forms as a result of the transformation of retained austenite during tempering. Carbide precipitation during tempering reduces the alloying element content of the austenite, thereby increasing the M_s temperature and promoting transformation of retained austenite to martensite on cooling after tempering. This martensite will be untempered and may reduce the toughness of the tempered structure. A second (or even third) tempering step is required to temper this fresh martensite. Tempering, or multiple tempering, of martensitic stainless steels appears to be more effective when preceded by a sub-zero quench²³.

3. HEAT TREATMENT OPTIMISATION

The preceding discussion emphasised the importance of heat treatment in developing the desired mechanical properties in martensitic stainless steels. Since these steels are often supplied in the annealed condition to facilitate machining or cold work, the consumer or fabricator is required to perform the final hardening heat treatments to ensure high hardness and wear resistance in the final component. Well-defined heat treatment guidelines are therefore required to assist the consumer or fabricator in performing appropriate hardening heat treatments in order to develop optimal properties. Although such guidelines are available in literature, the published heat treatment parameters are often inconsistent and the recommended temperature ranges too wide to ensure consistent properties.

During the course of this investigation, the heat treatment of two alloys conforming in composition to the range specified for medium-carbon type AISI 420 martensitic stainless steel was optimised with the aim of obtaining fully martensitic microstructures with minimal retained austenite and hardness values between 610 and 740 HV. More details on the primary objectives of this investigation are given in Chapter 2.

CHAPTER 2 – OBJECTIVES OF THE INVESTIGATION

1. BACKGROUND

AISI 420 is a low-chromium martensitic stainless steel that is often recommended for use in applications requiring a combination of corrosion resistance, high hardness and good wear resistance. Two heats of medium-carbon AISI 420 material were supplied by Columbus Stainless, a primary steel mill in South Africa, for the purpose of this investigation. These steels, with internal heat numbers of 349628 and 350052, are referred to as HEAT 1 and HEAT 2 in the remainder of this report. The chemistry of the two heats (to be considered in more detail in Chapter 3) are similar except that HEAT 1 contains 14.33% chromium and 0.62% molybdenum, whereas HEAT 2 contains 13.48% chromium and 0.025% molybdenum.

A percentage of the AISI 420 stainless steel produced by Columbus Stainless is earmarked for the production of razor blades. For optimal wear resistance and good edge retention in this application, the steel is required to have a fully martensitic structure with minimal retained austenite, a final hardness of between 610 and 740 HV after hardening, and evenly dispersed spherical carbides.

The plant heat treatment of this grade of stainless steel consists of a standard spheroidise annealing treatment to facilitate the formation of globular carbides in a ferrite matrix and to obtain maximum softness in preparation for further cold working or machining operations. The steel is supplied to the consumer in the annealed condition and the consumer or fabricator is required to perform the hardening heat treatments to ensure high hardness and wear resistance in the final component. Well-defined heat treatment guidelines are therefore required to assist the consumer or fabricator in performing the hardening treatments in such a way that optimal properties are achieved.

2. OBJECTIVES OF THE INVESTIGATION

This investigation aimed at identifying the heat treatment parameters (including the austenitising temperature, austenitising time, temper temperature and temper time) required to produce a martensitic structure, with minimal retained austenite and evenly dispersed spherical carbides, and hardness of between 610 HV and 740 HV

(hardness on the Vickers scale) in two medium-carbon AISI 420 martensitic stainless steels.

To examine the influence of these critical heat treatment parameters, two heats of AISI 420 martensitic stainless steel were subjected to various heat treatments. Different austenitising and temper treatments were used to form a detailed picture of the effect of heat treatment parameters on the properties and microstructure of the steels. Vickers hardness measurements were performed on all the samples to determine the hardness of the steel in each heat treatment condition. Optical and scanning electron microscopy was used to characterise the as-quenched and tempered microstructures. The average austenite grain size was determined by means of the mean lineal intercept method and the average carbide diameter was measured using image analysis techniques. The average number of carbides in a given area was determined, and the carbides were identified using X-ray diffraction techniques.

Once the effect of the heat treatment parameters on the microstructure and properties of the two heats had been established, thermodynamic predictions (using the CALPHAD™ model) of the solubility of the carbide particles in the matrix at various austenitising temperatures were used to explain the results obtained.

The experimental procedure used during the course of this investigation is described in Chapter 3.

CHAPTER 3 – OVERVIEW OF THE EXPERIMENTAL PROCEDURE

This chapter provides an overview of the experimental procedure followed during the course of this investigation. This procedure aimed at identifying the heat treatment parameters required to fully austenitise the steel, dissolve the majority of the carbides and convert the austenite to martensite on cooling. For optimal performance, the resulting microstructures are required to be martensitic, with minimal retained austenite and evenly dispersed spherical carbides, and a hardness of between 610 HV and 740 HV (hardness on the Vickers scale). More detailed information on the experimental procedure is supplied in Chapter 4.

1. STAINLESS STEEL ALLOYS STUDIED IN THIS INVESTIGATION

1.1 Chemical compositions:

Grade AISI 420 martensitic stainless steel is commercially available in a low-carbon version (with a specified carbon content of less than 0.15%), and a medium-carbon version (with a maximum carbon content of 0.5%). Two medium-carbon heats of AISI 420 martensitic stainless steel (containing approximately 0.47% carbon) were supplied by Columbus Stainless for the purpose of this investigation. As shown in Table 3.1, the steels contain 13.48% and 14.33% chromium, respectively, with small additions of copper, nickel and vanadium. The major difference between the two heats is the deliberate addition of molybdenum to HEAT 1. Molybdenum is expected to increase the hardenability, raise the temper resistance and improve the high temperature strength of the alloy.

Table 3.1: Chemical compositions of the AISI 420 heats examined during the course of this investigation (weight %, balance Fe).

Heat	C	Mn	Si	Cu	Mo	Cr	Ni	N	V
1	0.472	0.62	0.41	0.10	0.623	14.33	0.22	0.0165	0.13
2	0.471	0.62	0.33	0.08	0.025	13.48	0.17	0.0120	0.10

1.2 Plant heat treatment:

The two steels were received in the spheroidise annealed condition, involving heat treatment at 860 °C for 20 hours, followed by slow cooling to 770 °C to facilitate the

formation of globular carbides in a ferrite matrix and to obtain maximum softness for forming. The steels were supplied in the form of 5 mm thick plate material.

2. HEAT TREATMENTS USED IN THIS INVESTIGATION

Samples with dimensions of 5 mm x 10 mm x 5 mm were sectioned from the as-supplied plate material. The samples were austenitised in a muffle furnace at various temperatures between 1000 °C and 1200 °C. An average heating rate of approximately 0.2 °C per second and a holding time of 15 minutes were used. The austenitising heat treatment was followed by oil quenching in all cases.

Tempering heat treatments were performed at various temperatures for samples austenitised at 1075 °C, 1150 °C and 1175 °C. The effect of double tempering on the retained austenite content and hardness was investigated for samples austenitised at 1150 °C and 1175 °C.

Samples austenitised at 1100 °C, 1130 °C, 1150 °C and 1175 °C were sub-zero treated in liquid nitrogen at -196 °C. After sub-zero treatment in liquid nitrogen, the samples were tempered for one hour at 550 °C, 650 °C or 700 °C.

3. METALLOGRAPHIC INVESTIGATION

Each heat treated sample was sectioned and mounted in black phenolic resin. The mounted samples were ground, diamond polished to a mirror finish and etched using Vilella's reagent (consisting of 1 g picric acid, 10 ml hydrochloric acid and 100 ml ethanol) to reveal the general microstructure. The etched samples were examined microscopically using optical and scanning electron microscopes, and photomicrographs were taken of each sample. Following the general microscopic examination, the austenite grain size, average carbide diameter and the carbide density of the samples were determined, as described below.

3.1 Austenite grain size:

The mean lineal intercept method was used to estimate the ASTM grain size (G) of the metallographic samples. Five uniformly distributed test lines were drawn across a printed micrograph, and the number of times a given line intersected the grain boundaries was recorded. Equation (3.1) was used to calculate the mean lineal intercept length, L_L .

$$L_L = \frac{L_T}{PM} \quad \dots(3.1)$$

where: L_L is the mean lineal intercept length,
 L_T is the total length of the test lines,
 P is the total number of grain boundary intersections, and
 M is the magnification.

The ASTM grain size, G , was then determined using equation (3.2).

$$G = -3.2877 - 6.6439 \log L_L \quad \dots(3.2)$$

(This method is based on an article presented by George Vander Voort on the occasion of the 75th anniversary of Committee E-4 on Metallography, and originally appeared in *ASTM Standardization News*, May 1991, as "Committee E-4 and Grain Size Measurements").

3.2 The average carbide diameter and carbide density:

The average diameter of the carbide particles observed in each heat treated sample was measured using image analysis techniques. To determine the carbide density, scanning electron micrographs were divided into squares with a total area of 2300 μm^2 . The number of carbides in each square was determined, and the carbide density was reported as the number of carbides per mm^2 .

4. HARDNESS MEASUREMENTS

Calibrated Vickers hardness measurements with an applied load of 10 kg were performed on all the heat treated samples. The results were reported as the average of five tests per sample.

5. X-RAY DIFFRACTION

In order to quantify the volume fraction of retained austenite present in various heat treated samples, X-ray diffraction (XRD) analyses were performed. XRD was also used to identify the carbide particles observed in the samples. Since the carbide particles were too small to be identified using SEM-EDS analysis, and too large for TEM (transmission electron microscope) analysis, the carbides were extracted by dissolving the martensitic matrix in hydrochloric acid. The sediment was filtered

through glass-fibre micropaper, washed in distilled water and rinsed with acetone. The carbide residue was collected and subjected to XRD analysis.

6. THERMODYNAMIC PREDICTIONS

Computational simulations were performed using CALPHAD™ software, and phase diagrams of the two heats of AISI 420 martensitic stainless steel were compiled at four austenitising temperatures (1075°C, 1100°C, 1130°C and 1175°C) to determine the phase stability and the equilibrium dissolution temperatures of the carbides.

Chapter 4 provides more detail on the experimental procedure and presents the results of this investigation.

CHAPTER 4 – RESULTS AND DISCUSSION

This chapter describes the influence of various heat treatment parameters on the microstructure and hardness of two heats of medium-carbon AISI 420 martensitic stainless steel. The metallographic investigation characterised each heat treated sample by reporting the general microstructure, carbide density, average carbide diameter, ASTM grain size and the percentage retained austenite. Additional data is presented in Appendix A to C. Representative micrographs are shown in this chapter, with the remaining microstructures displayed in Appendix E. The type of carbide present in the as-quenched microstructures was identified using X-ray diffraction techniques and the hardness of each sample was recorded as the average of five measurements (with the 95% confidence interval calculated and reported in each case). Thermodynamic predictions using the CALPHAD™ model are reported for austenitising temperatures between 1075°C and 1175°C.

1. AS-RECEIVED SAMPLES

The two heats of medium-carbon AISI 420 material were supplied by Columbus Stainless in the spheroidise annealed condition. The measured as-received hardness was 209±7 HV for HEAT 1 and 195±4 HV for HEAT 2. As shown in Figures 4.1 to 4.3, the microstructures of both steels consist of coarse, globular carbides in a ferrite matrix.

De Andrés *et al*¹⁶ reported that the only carbide present in the spheroidise annealed microstructure of AISI 420 is $M_{23}C_6$, however, according to Bjarbo *et al*¹¹ steels with more than 0.2% carbon and 12 to 13% chromium contain M_3C , M_7C_3 and $M_{23}C_6$ carbides. The precipitation of the carbides is reported to be dependent on time with M_3C precipitating first, followed by M_7C_3 and then $M_{23}C_6$. In this investigation only $M_{23}C_6$ carbides were identified, with M consisting mainly of iron and chromium.

The higher chromium and molybdenum contents of HEAT 1 result in a higher volume fraction of carbides compared to HEAT 2. The presence of a high volume fraction of carbides is likely to affect the austenitising treatment of both heats. According to the available literature²⁴, chromium-rich $M_{23}C_6$ carbides dissolve in the 950°C to 1050°C temperature range, whereas M_7C_3 carbides dissolve in the 1050°C to 1150°C

temperature range. A higher austenitising temperature therefore causes more carbides to dissolve. This raises the alloy content of the austenite and depresses the martensite transformation range, increasing the likelihood of retained austenite after quenching.

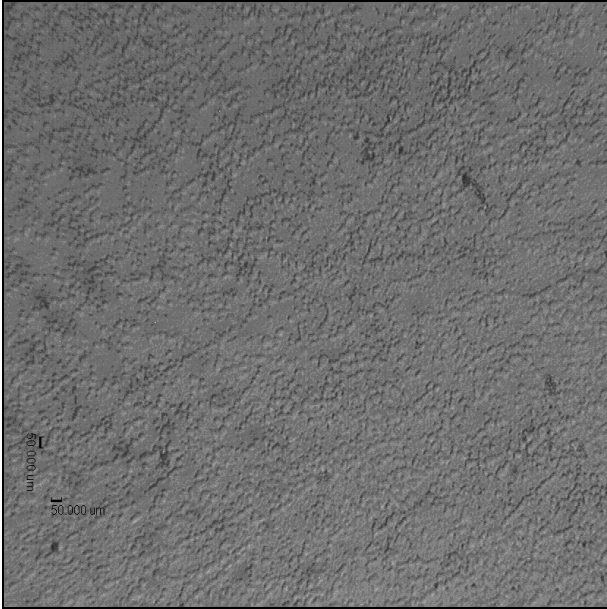


Figure 4.1: The as-received microstructure of HEAT 1, consisting of coarse $M_{23}C_6$ carbides in a ferrite matrix (hardness: 209 ± 7 HV). (Magnification: 50x).

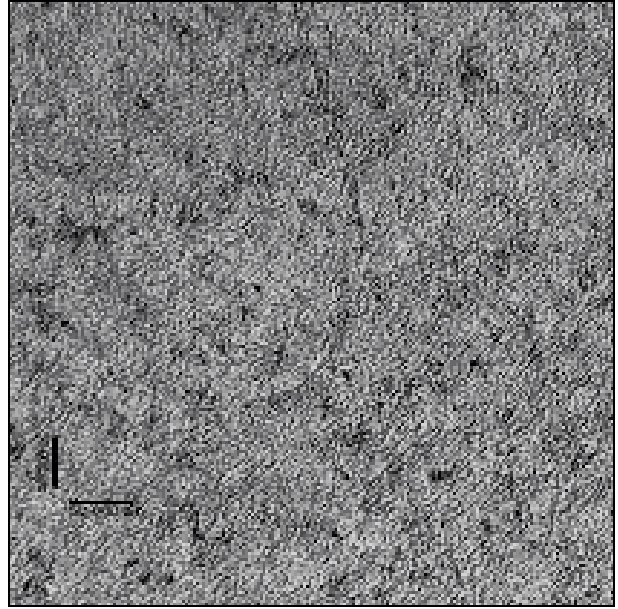


Figure 4.2: The as-received microstructure of HEAT 2, consisting of coarse $M_{23}C_6$ carbides in a ferrite matrix (hardness: 195 ± 4 HV). (Magnification: 100x).

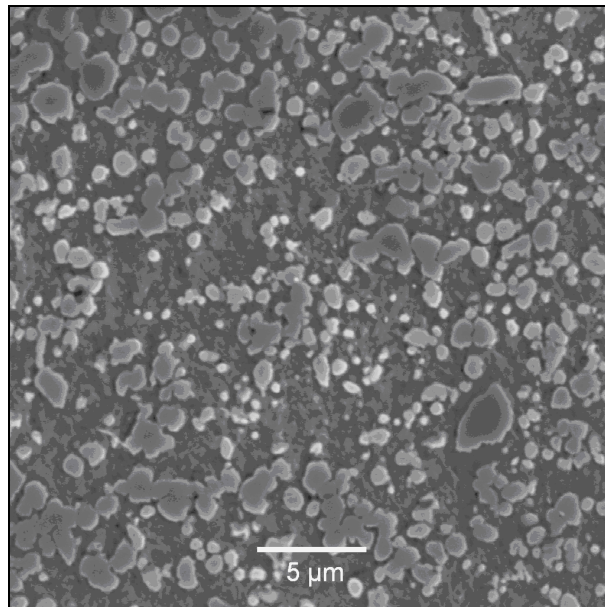


Figure 4.3: Scanning electron micrograph of the as-received microstructure of HEAT 2. The microstructure consists of coarse, globular $M_{23}C_6$ carbides in a ferrite matrix.

2. THE EFFECT OF AUSTENITISING TEMPERATURE ON THE AS-QUENCHED MICROSTRUCTURE AND PROPERTIES OF HEATS 1 AND 2

When alloying elements dissolve in the steel at high temperatures, the martensite transformation temperatures are depressed. This is illustrated by the equation (4.1), which illustrates the effect of various alloying elements on the M_s (martensitic start) temperature of 12% chromium steels (all alloy contents in weight percentage)².

$$M_s(°C) = 500 - 333C - 34Mn - 35V - 20Cr - 17Ni - 11Mo - 10Cu - 5W - 15Co + 30Al \dots(4.1)$$

Equation (4.1) yields predicted martensite start temperatures of 21 °C for HEAT 1 and 46 °C for HEAT 2. These temperatures are close to ambient, suggesting that the martensite transformation is unlikely to go to completion (unless sub-zero treated) if all the alloying elements are in solution in the two stainless steel grades examined. Since the carbides in AISI 420 increasingly dissolve with an increase in austenitising temperature, the martensite start temperature is expected to decrease with higher austenitising temperatures. As shown in Chapter 1, the risk of retained austenite therefore increases with an increase in austenitising temperature. The presence of additional molybdenum in HEAT 1 depresses the martensite start temperature to well below that of HEAT 2, predicting a higher risk of retained austenite after quenching to room temperature.

Table 4.1 displays a summary of the results obtained in this investigation after various austenitising heat treatments. These results are considered in more detail below.

Tavares *et al*¹⁷ reported that the austenitising treatment of AISI 420 should be performed in the temperature range of 980 °C to 1100 °C. Based on a preliminary investigation (not included in this report), a slightly higher austenitising temperature range of 1000 °C to 1200 °C was selected for the purpose of this investigation. Samples of both heats were austenitised at 1000 °C, 1050 °C, 1075 °C, 1100 °C, 1130 °C, 1150 °C, 1175 °C and 1200 °C for 15 minutes. As small samples were used and enough time was allowed for the sample temperature to equalise in the furnace, a 15 minute soaking time was considered to be sufficient for complete austenitising. This was confirmed as part of an unpublished preliminary investigation into the effect of soaking time on as-quenched hardness.

Table 4.1: A summary of the results obtained for HEAT 1 and HEAT 2 after various austenitising heat treatments.

HEAT 1

Austenitising temperature	Hardness (HV)	Observed microstructure	% Retained austenite	Carbide density per mm ²
1000°C	664	Martensite, retained austenite and carbides	4	181
1050°C	678	Martensite, retained austenite and carbides	5	131
1075°C	684	Martensite, retained austenite and carbides	15	87
1100°C	653	Martensite, retained austenite and carbides	23	84
1130°C	474	Martensite, retained austenite and carbides	25	81
1150°C	308	Martensite and retained austenite	27	43
1175°C	279	Martensite and retained austenite	29	0
1200°C	270	Martensite and retained austenite	33	0

HEAT 2

Austenitising temperature	Hardness (HV)	Observed microstructure	% Retained austenite	Carbide density per mm ²
1000°C	639	Martensite, retained austenite and carbides	4	227
1050°C	665	Martensite, retained austenite and carbides	6	184
1075°C	674	Martensite, retained austenite and carbides	10	117
1100°C	639	Martensite, retained austenite and carbides	12	63
1130°C	620	Martensite, retained austenite and carbides	15	32
1150°C	609	Martensite and retained austenite	17	14
1175°C	488	Martensite and retained austenite	21	0
1200°C	459	Martensite and retained austenite	24	0

In order to verify the results reported in literature, HEATS 1 and 2 were austenitised at 1000°C for 15 minutes, a temperature too low to dissolve significant amounts of $M_{23}C_6$. As only a small percentage of carbides goes into solution during heat treatment, very little retained austenite is expected after quenching. This was confirmed by XRD analysis which shows that 4% retained austenite was present in both HEATS 1 and 2 after austenitising at 1000°C (as shown in Table 4.1). The as-quenched microstructure, shown in Figure 4.4, consists of coarse, globular carbides in a fine martensitic matrix. The shape and distribution of the carbide particles suggest that they are undissolved precipitates (from the spheroidise annealing treatment), rather than reprecipitated carbides. The carbide density in HEATS 1 and 2, austenitised at 1000°C, was determined as 181 and 227 carbides per mm²,

respectively. The carbides have an average diameter of 1.28 μm in HEAT 1 and 0.75 μm in HEAT 2. The measured hardness values are high at 664 ± 12 HV for HEAT 1 and 639 ± 10 HV for HEAT 2. These high hardness values can be attributed to the fine martensitic matrix and the low levels of retained austenite.

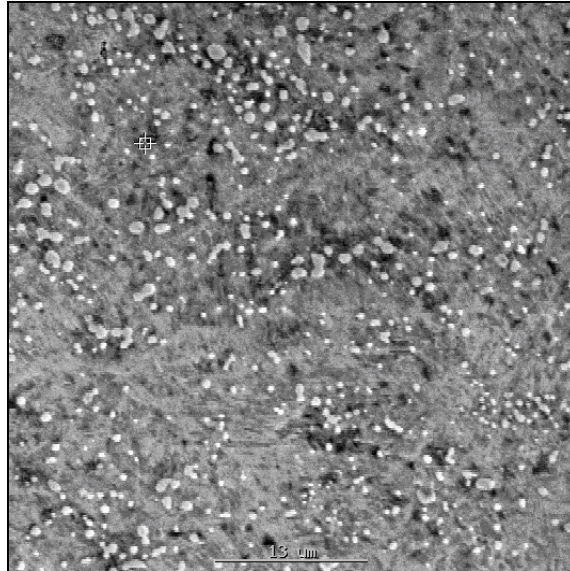


Figure 4.4: Scanning electron micrograph of HEAT 2 after austenitising for 15 minutes at 1000°C , followed by oil quenching. The microstructure consists of coarse M_{23}C_6 carbides in a fine martensite matrix. (Hardness: 639 ± 10 HV).

According to Pickering², the equilibrium carbide dissolution temperature in AISI 420 (without added molybdenum) is 1050°C . The heating rate used by Pickering was, however, not reported. According to De Andres *et al*¹⁶ the total carbide dissolution temperature is, to a certain degree, dependent on the heating rate. A carbide dissolution temperature of 1110°C was reported for a heating rate of 0.5°C per second. Due to furnace constraints, a heating rate of approximately 0.2°C per second was used for the purpose of this investigation, and a relatively high percentage of carbides is therefore expected in the as-quenched microstructure after austenitising at 1050°C . Based on published literature, the carbide dissolution temperature, using a 0.2°C per second heating rate, is expected to be approximately 1090°C .

To determine the extent of carbide dissolution at 1050°C , samples from HEAT 1 and HEAT 2 were austenitised at 1050°C for 15 minutes, followed by quenching in oil. A representative optical photomicrograph of HEAT 1 in the as-quenched condition is

shown in Figure 4.5. The microstructure consists of well-defined carbide particles in a martensitic matrix. This confirms that an austenitising temperature of 1050°C is still below the temperature required to completely dissolve the $M_{23}C_6$ precipitates in the two heats examined. Carbide densities of 131 and 184 carbides per mm^2 were obtained for HEAT 1 and HEAT 2, respectively. These densities are lower than those observed in samples quenched from 1000°C, implying that partial dissolution of the carbides had occurred. The measured hardness values are 678 ± 9 HV for HEAT 1 and 665 ± 9 HV for HEAT 2. These hardness values are somewhat higher than those measured after quenching from 1000°C. This increase in hardness is attributed to an increase in the carbon content of the martensite phase due to the partial dissolution of carbides. The martensite is therefore harder due to its higher carbon content, but the amount of carbon and alloying elements in solid solution was not high enough to depress the martensite transformation range below 0°C. The retained austenite contents of the two heats therefore remain low at 5% and 6%.

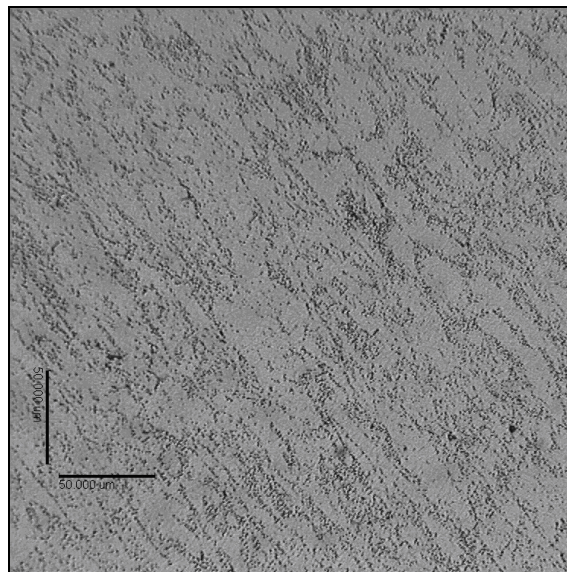


Figure 4.5: Optical micrograph of HEAT 1 after austenitising for 15 minutes at 1050°C, followed by oil quenching. The microstructure consists of $M_{23}C_6$ carbides in a fine martensite matrix. (Hardness: 678 ± 9 HV). (Magnification: 200x).

Austenitising at a temperature of 1075°C yields as-quenched hardness values of 684 ± 10 HV for HEAT 1 and 674 ± 12 HV for HEAT 2. As shown in Figure 4.6, the microstructures of the two heats are predominantly martensitic, with well-defined carbide particles. Carbide densities of 87 and 117 carbides per mm^2 were

determined for HEATS 1 and 2, respectively. Although these densities are somewhat lower than those measured after austenitising at 1050°C, suggesting that partial dissolution of carbides had occurred, the results suggest that 1075°C is still below the complete carbide dissolution temperature. The average carbide particle diameters of 0.93 µm (HEAT 1) and 0.58 µm (HEAT 2) are very similar to those observed at lower austenitising temperatures. Partial dissolution of carbides increased the carbon and alloying element contents of the austenite, resulting in slightly higher as-quenched hardness values (compared to those recorded after quenching from 1050°C) and higher retained austenite levels of 15% and 10% in HEATS 1 and 2, respectively.

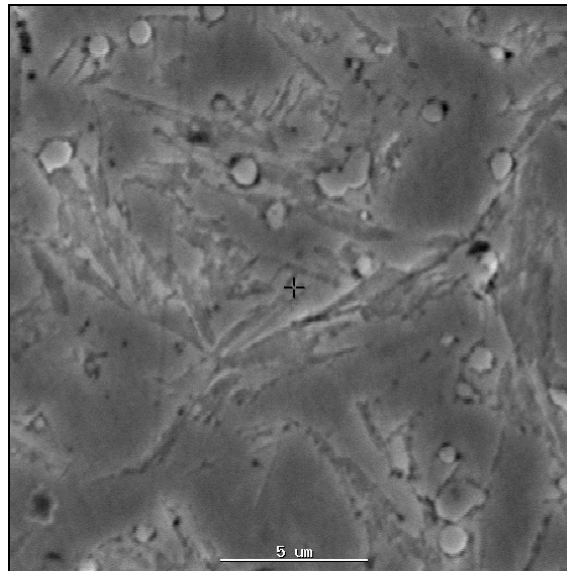


Figure 4.6: Scanning electron micrograph of HEAT 1 after austenitising for 15 minutes at 1075°C, followed by oil quenching. The microstructure consists of $M_{23}C_6$ carbides in a martensite matrix. (Hardness: 684 ± 10 HV).

Published literature^{1,6,16} suggests that extensive carbide dissolution should occur in both heats during austenitising at 1075°C. In order to explain the observed discrepancy between published dissolution temperatures and the microstructures observed after austenitising at 1075°C, thermodynamic predictions (using the CALPHAD™ model) of the austenite and carbide stabilities in the two heats during austenitising were used. Figure 4.7 shows the predicted equilibrium phase diagram for HEATS 1 and 2 at 1075 °C. In this figure, the # symbol denotes the position of HEAT 1 in terms of percentage chromium and percentage carbon, whereas *

denotes the position of HEAT 2. The solid lines represent the calculated phase boundaries for HEAT 1 and the broken lines the boundaries for HEAT 2. It is evident from Figure 4.7 that the higher molybdenum and chromium contents of HEAT 1 restrict the austenite phase field (both elements are strong ferrite-formers).

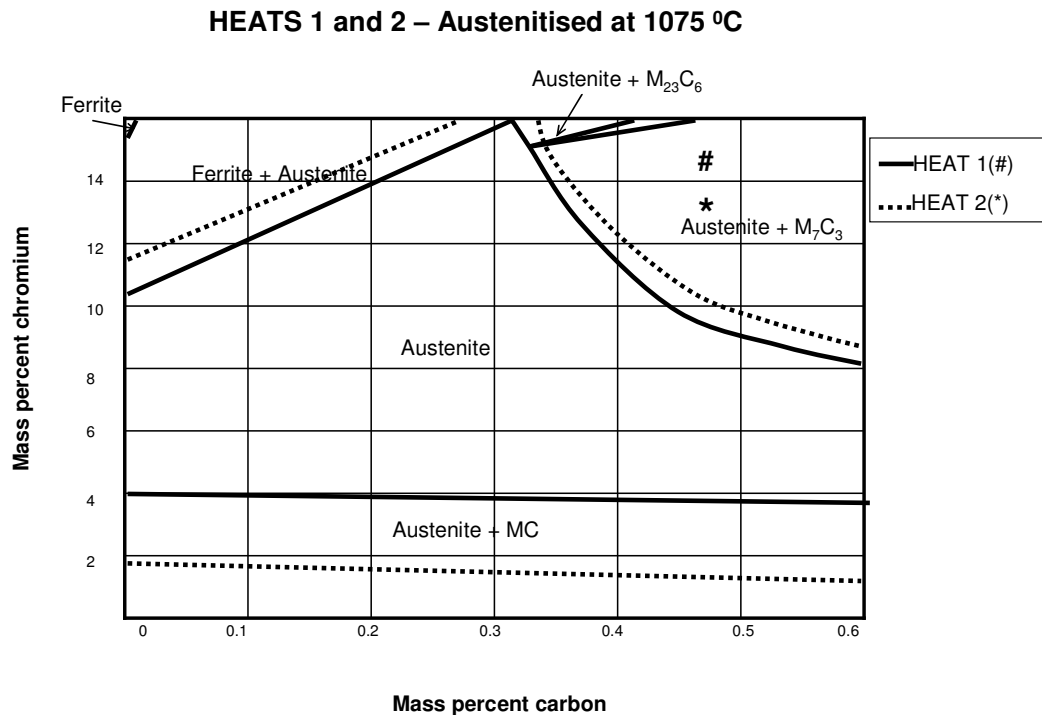


Figure 4.7: Thermodynamic prediction of the equilibrium phase diagram of two heats of AISI 420 at an austenitising temperature of 1075 °C.

Figure 4.7 predicts that both heats contain austenite and M_7C_3 carbides during austenitising at 1075 °C. According to the predicted phase diagram all $M_{23}C_6$ carbides are in solution at this temperature. This is in agreement with the observations of Salem²⁴, who reported that $M_{23}C_6$ chromium carbides dissolve in the 950 °C to 1050 °C temperature range, whereas M_7C_3 carbides dissolve in the 1050 °C to 1150 °C temperature range. Partial dissolution of M_7C_3 carbides is therefore likely at 1075 °C. Information derived from the CALPHAD model predicts 1.23% M_7C_3 in HEAT 1 at 1075 °C, and 0.91% M_7C_3 in HEAT 2. No $M_{23}C_6$ is expected in these steels at 1075 °C, but $M_{23}C_6$ forms during cooling on conversion of the M_7C_3 carbides. The presence of $M_{23}C_6$ carbide in the as-quenched microstructures of the steels was confirmed by XRD analysis. No M_7C_3 was observed in any of the steels after cooling from the austenitising temperature.

Available literature predicts that increasing the austenitising temperature to 1100°C should result in a large percentage of carbides going into solution. The critical temperature for complete carbide solution in AISI 420 (without molybdenum) was recorded as 1110°C at a heating rate of 0.5°C per second¹⁶. At the 0.2°C per second heating rate used in the current investigation, a carbide dissolution temperature of approximately 1090°C is predicted. Figures 4.8 and 4.9 indicate, however, that carbides remain present in the as-quenched microstructures of both HEAT 1 and HEAT 2. The carbide densities were estimated as 84 carbides per mm² for HEAT 1 and 63 carbides per mm² for HEAT 2. XRD analysis reported 23% retained austenite in HEAT 1, and 12% retained austenite in HEAT 2. The increase in retained austenite content accounts for the lower as-quenched hardness values of 653±8 HV for HEAT 1 and 639±8 HV for HEAT 2.

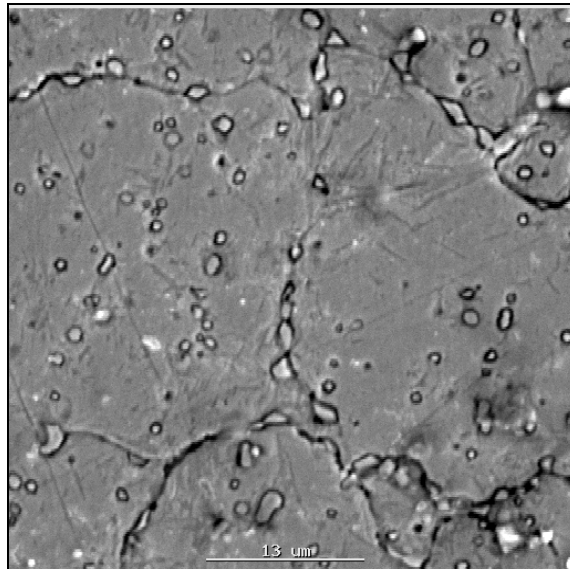


Figure 4.8: Scanning electron micrograph of HEAT 1 after austenitising for 15 minutes at 1100°C, followed by oil quenching. The microstructure consists of $M_{23}C_6$ carbides in a martensite matrix containing 23% retained austenite. (Hardness: 653±8 HV).

This inconsistency between the reported carbide dissolution temperatures and those determined during the course of this investigation was investigated further by examining the predicted phase diagram at 1100°C (shown in Figure 4.10). At this temperature, both steels are located in the dual-phase region where austenite and M_7C_3 carbides are stable, suggesting that the temperature is not high enough to completely dissolve all carbides. Extensive carbide dissolution does, however, take place at this temperature, with the CALPHAD model predicting 0.62% M_7C_3 in HEAT

1 and 0.27% in HEAT 2 at 1100 °C. The increased dissolution of carbides depresses the martensite transformation range, resulting in the formation of higher levels of retained austenite.

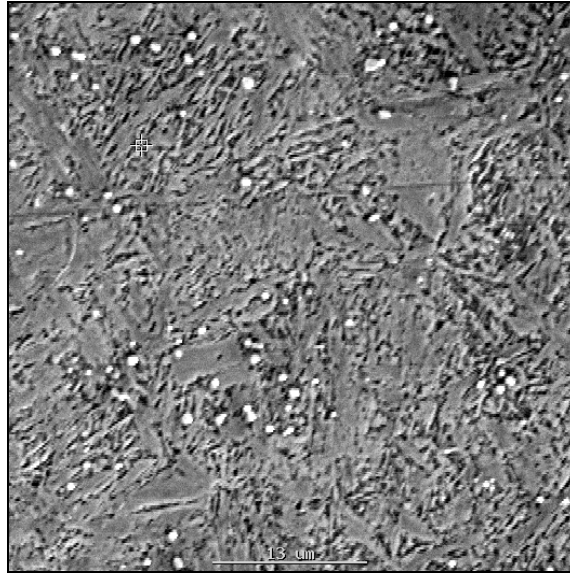


Figure 4.9: Scanning electron micrograph of HEAT 2 after austenitising for 15 minutes at 1100 °C, followed by oil quenching. The microstructure consists of $M_{23}C_6$ carbides in a martensite matrix containing 12% retained austenite. (Hardness: 639 ± 15 HV).

HEATS 1 and 2 – Austenitised at 1100 °C

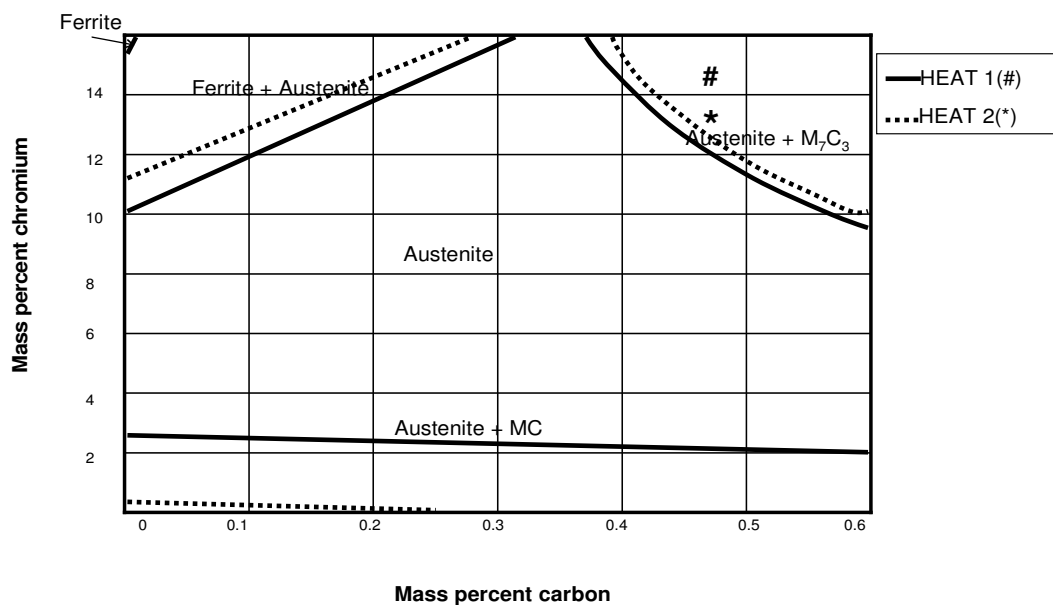


Figure 4.10: Thermodynamic prediction of the equilibrium phase diagram of two heats of AISI 420 at an austenitising temperature of 1100 °C.

Scanning electron micrographs of HEATS 1 and 2 after austenitising at 1130°C are shown in Figures 4.11 and 4.12. Contrary to published predictions, carbides remain visible in the as-quenched microstructures, with measured carbide densities of 81 carbides per mm² for HEAT 1 and 32 carbides per mm² for HEAT 2. The hardness of HEAT 1 is, however, significantly lower than that of HEAT 2 at 474±7 HV. This can be attributed to the presence of a significant volume fraction of retained austenite (25%) after austenitising at 1130°C. The hardness of HEAT 2 remains high at 620±4 HV, which is in agreement with the measured retained austenite content of 15%. A significant increase in ASTM grain size is observed at this austenitising temperature, with ASTM grain size numbers of 8.6 for HEAT 1 and 6.9 for HEAT 2. This increase in grain size can be attributed to the higher austenitising temperature and the increased dissolution of grain pinning carbides.

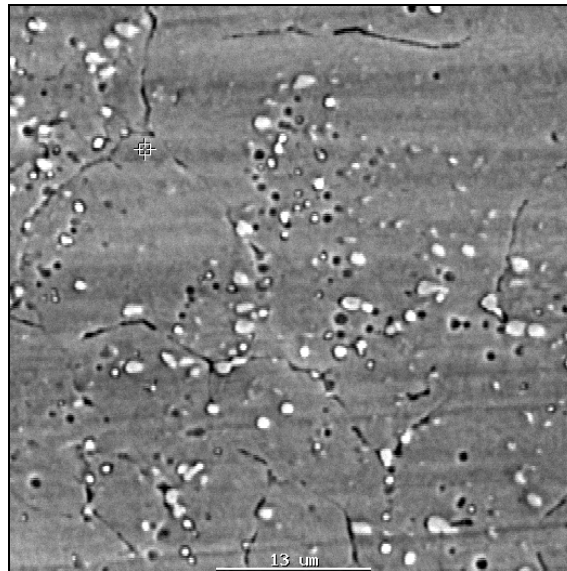


Figure 4.11: Scanning electron micrograph of HEAT 1 after austenitising for 15 minutes at 1130°C, followed by oil quenching.

The microstructure consists of $M_{23}C_6$ carbides in a martensite matrix containing 25% retained austenite. (Hardness: 474±7 HV).

The predicted phase diagrams for HEATS 1 and 2 at 1130°C are shown in Figure 4.13. HEAT 1 is located on the boundary between the austenite and (austenite + M_7C_3) phase fields, whereas HEAT 2 is located well within the single-phase austenite region. The CALPHAD model therefore predicts complete dissolution of carbides during austenitising at 1130 °C. This suggests that equilibrium was not reached during heat treatment, resulting in the presence of retained carbides, or that the model does not predict the phase boundaries to the desired level of accuracy.

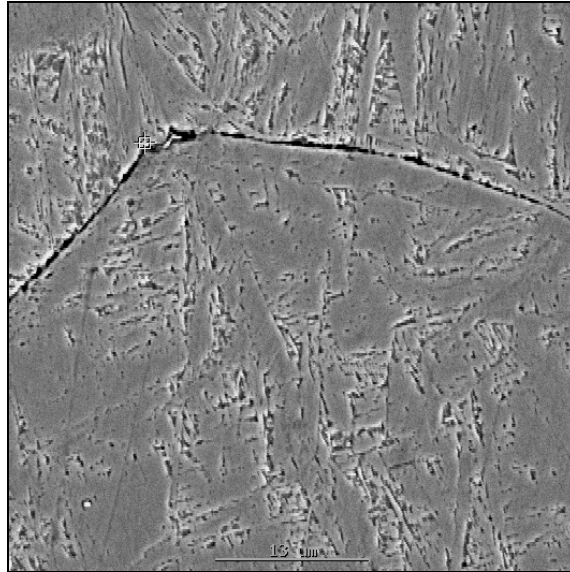


Figure 4.12: Scanning electron micrograph of HEAT 2 after austenitising for 15 minutes at 1130 °C, followed by oil quenching. The microstructure consists of $M_{23}C_6$ carbides in a martensite matrix containing 15% retained austenite. (Hardness: 620 ± 4 HV).

HEATS 1 and 2 – Austenitised at 1130 °C

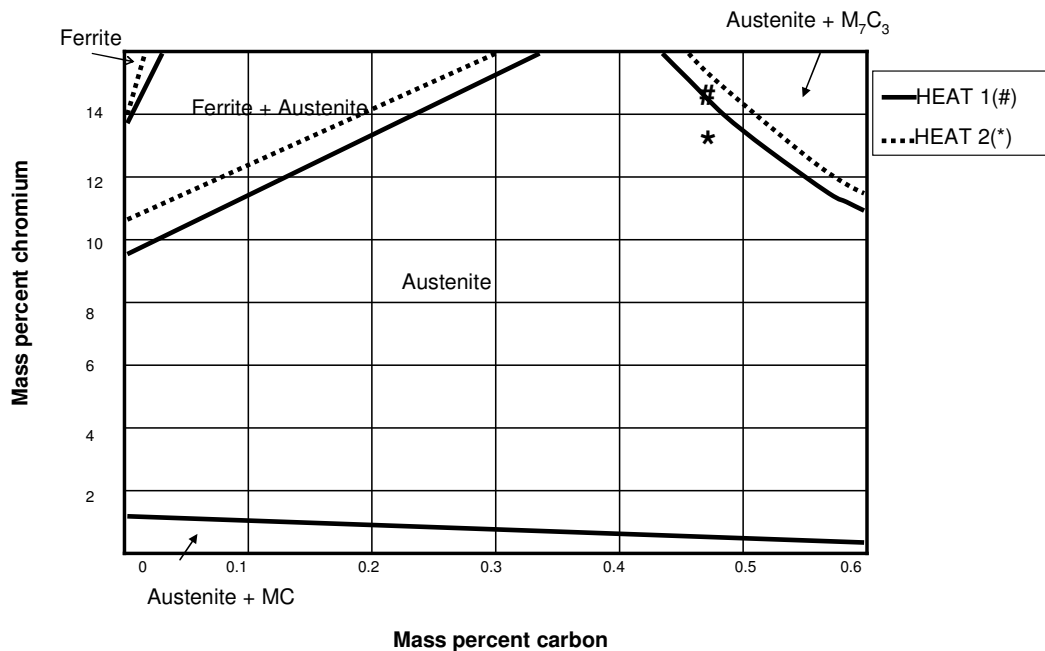


Figure 4.13: Thermodynamic prediction of the equilibrium phase diagram of two heats of AISI 420 at an austenitising temperature of 1130 °C.

Austenitising at a temperature of 1150°C results in a significant increase in retained austenite after quenching. HEAT 1 contains 27% retained austenite (see Figure 4.14), resulting in a low as-quenched hardness of 308 ± 6 HV. HEAT 2 contains approximately 17% retained austenite and displays a higher hardness of 609 ± 10 HV. The carbides have almost completely gone into solution, with residual carbide densities of 43 and 14 carbides per mm^2 for HEATS 1 and 2, respectively. Due to the higher austenitising temperature and the dissolution of grain pinning carbides, considerable grain growth is observed and the average ASTM grain size number decreases to 6.3 for HEAT 1 and 5.1 for HEAT 2.

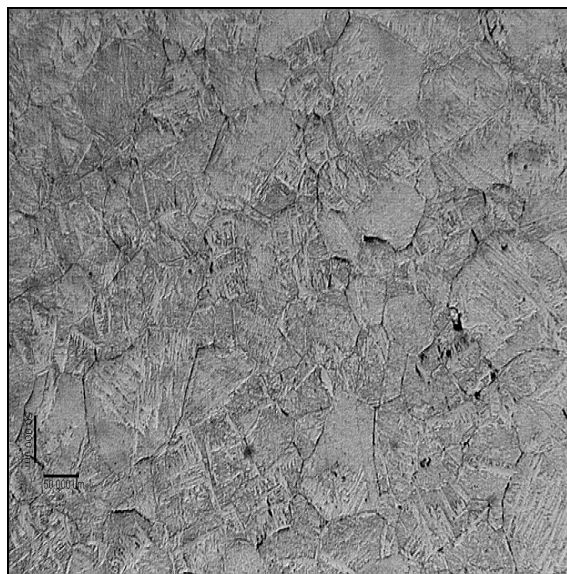


Figure 4.14: Optical micrograph of HEAT 1 after austenitising for 15 minutes at 1150°C, followed by oil quenching. The microstructure consists of a small number of residual $M_{23}C_6$ carbides in a martensite matrix containing 27% retained austenite. (Hardness: 308 ± 6 HV). (Magnification: 100x).

No phase diagram was calculated for an austenitising temperature of 1150°C , but both heats are expected to be located well within the austenite phase field at this temperature.

Scanning electron micrographs of HEATS 1 and 2 after austenitising at 1175°C are shown in Figures 4.15 and 4.16. Both heats contain martensite and retained austenite (29% retained austenite in HEAT 1 and 21% in HEAT 2). No carbide particles are visible, suggesting that this temperature is above the temperature for complete carbide dissolution in both alloys. Excessive grain growth is evident in both

heats, with average ASTM grain size numbers of 4 and 3.4 for HEATS 1 and 2. The high percentage retained austenite resulted in low hardness values of 279 ± 4 HV for HEAT 1 and 488 ± 3 HV for HEAT 2.

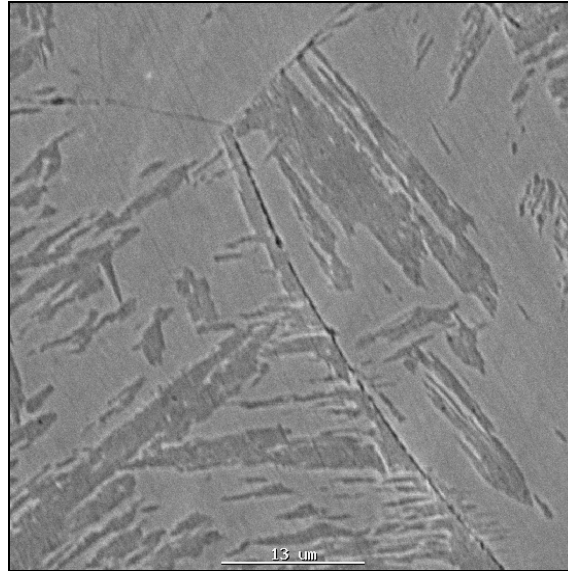


Figure 4.15: Scanning electron micrograph of HEAT 1 after austenitising for 15 minutes at 1175°C , followed by oil quenching. The microstructure consists of martensite and 29% retained austenite. (Hardness: 279 ± 4 HV).

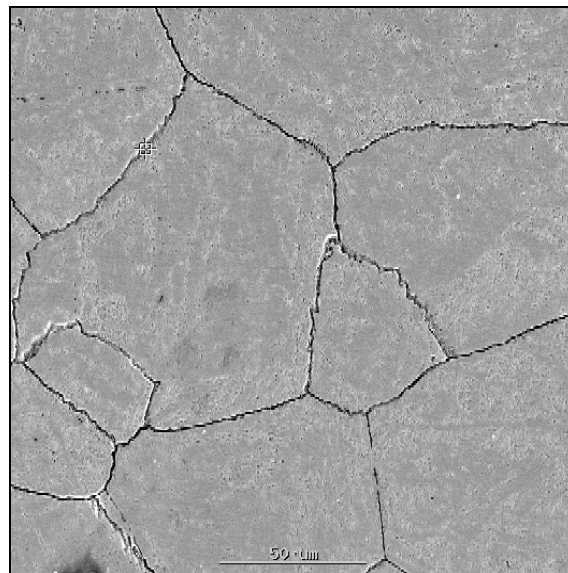


Figure 4.16: Scanning electron micrograph of HEAT 2 after austenitising for 15 minutes at 1175°C , followed by oil quenching. The microstructure consists of martensite and 21% retained austenite. (Hardness: 488 ± 3 HV).

The CALPHAD model predicts that no carbides are present in either heat at an austenitising temperature of 1175°C. As shown in Figure 4.17, both alloys are located well within the austenite phase field. The complete dissolution of carbides during heat treatment depresses the martensite transformation range and results in high levels of retained austenite.

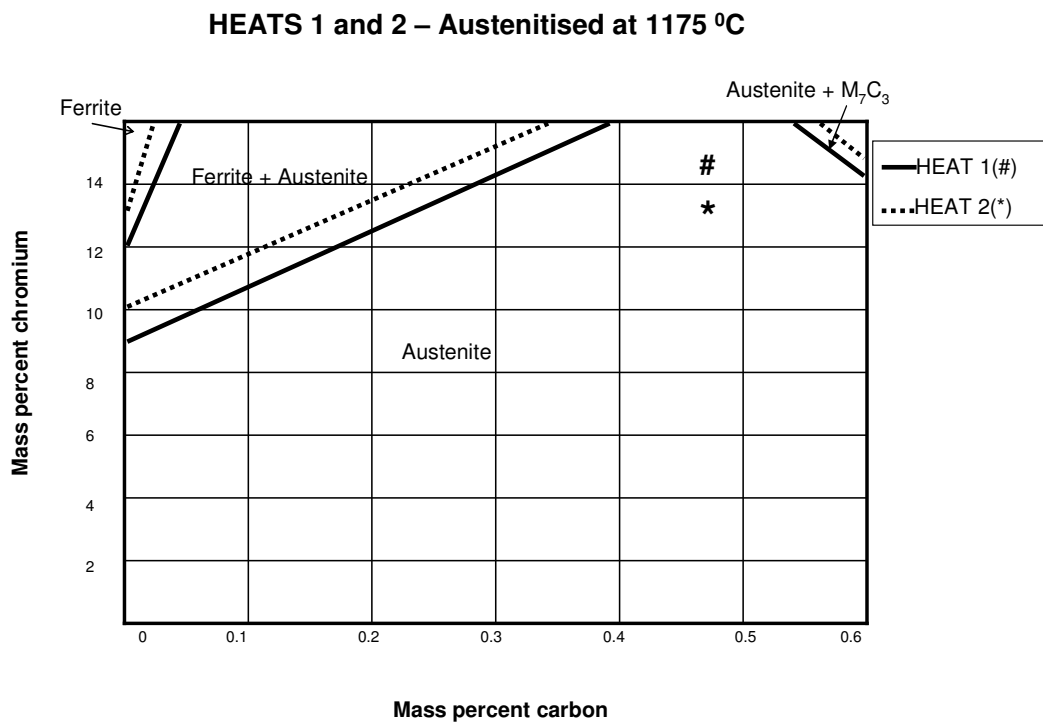


Figure 4.17: Thermodynamic prediction of the equilibrium phase diagram of two heats of AISI 420 at an austenitising temperature of 1175 °C.

At 1200°C, all carbides are in solution in the austenite, resulting in as-quenched microstructures containing martensite and retained austenite. HEAT 1 contains 33% retained austenite, whereas HEAT 2 contains 24%. Hardness values of 270±12 HV for HEAT 1 and 459±2 HV for HEAT 2 were measured. The higher hardness of HEAT 2 can be attributed to the higher martensite content after quenching. Excessive grain growth occurs at the austenitising temperature, yielding average as-quenched ASTM grain size numbers of 2.8 and 3.2 for HEATS 1 and 2, respectively.

A brief summary of these results is given below.

Table 4.1 confirms that an increase in austenitising temperature is associated with a decrease in carbide density and an increase in the percentage retained austenite. Figure 4.18 shows the effect of austenitising temperature on the carbide density in HEATS 1 and 2. The carbide densities in both steels decrease with an increase in austenitising temperature. At austenitising temperatures between 1000°C and 1050°C, the carbide densities of both heats decrease at similar rates, suggesting the progressive dissolution of $M_{23}C_6$ carbides ($M_{23}C_6$ is reported to dissolve at temperatures between 950°C and 1050°C). HEAT 2 has a higher initial carbide density, but at temperatures higher than 1050°C the carbide density decreases at a faster rate than that of HEAT 1. This suggests that the increased molybdenum content of HEAT 1 retards carbide dissolution at higher austenitising temperatures, possibly due to the higher stability of M_7C_3 in the molybdenum-containing alloy (as confirmed by phase diagrams constructed using the CALPHAD model). Molybdenum appears to stabilise and promote the equilibrium M_7C_3 carbide at temperatures higher than 1050°C, retarding carbide coarsening and dissolution. Complete carbide dissolution takes place at temperatures higher than 1175°C in both heats.

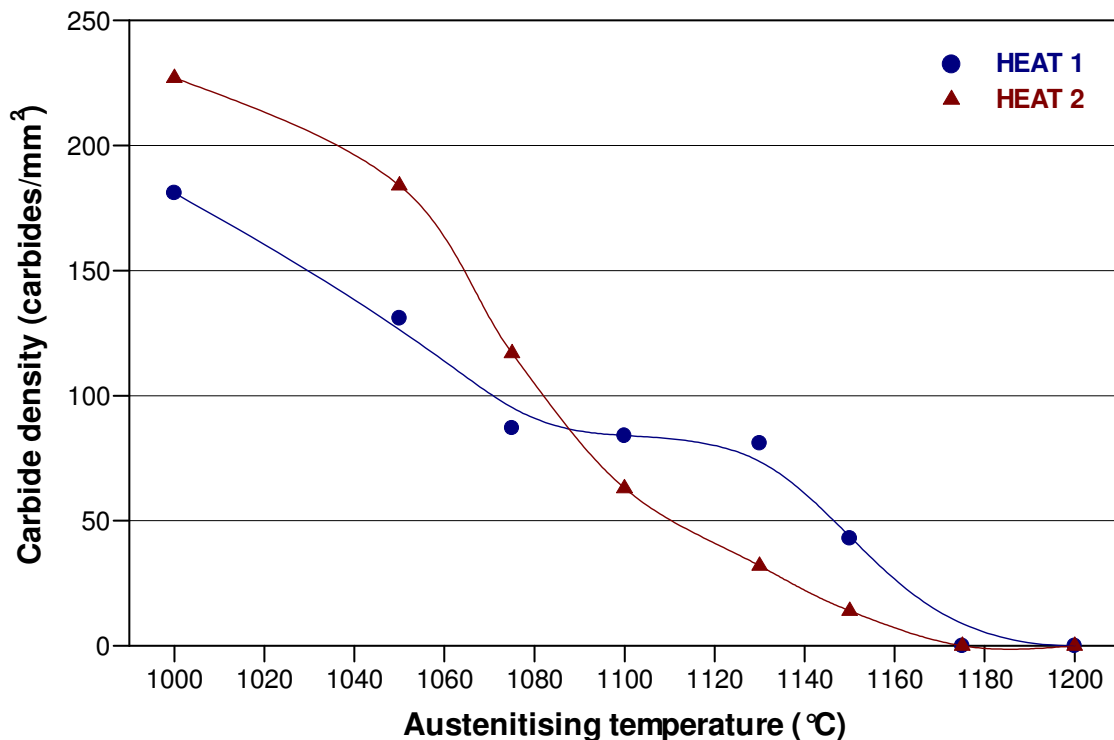


Figure 4.18: The influence of austenitising temperature on the carbide density (number of carbides per mm²) in HEATS 1 and 2.

The gradual dissolution of carbides up to austenitising temperatures of 1175°C (where complete carbide dissolution is observed in both heats) affects the measured retained austenite content, as-quenched hardness and grain size of the steels. The effect of austenitising temperature on the as-quenched hardness is shown in Figure 4.19. The measured hardness values of both heats increase slightly with an increase in austenitising temperature up to 1075°C. This can be attributed to the gradual dissolution of $M_{23}C_6$ carbides, which raises the carbon content of the austenite phase at elevated temperatures. On quenching a higher carbon martensite forms, which increases the as-quenched hardness of both heats. Although retained austenite is present in both heats after quenching from austenitising temperatures of 1075°C or lower, retained austenite is not present in high enough quantities to reduce the as-quenched hardness significantly. Higher austenitising temperatures raise the amount of carbon and alloying elements in solution in the austenite, and depress the martensite transformation range to lower temperatures. At temperatures higher than approximately 1075°C, increased carbide dissolution results in higher retained austenite contents (as shown in Figure 4.20), particularly in HEAT 1, and a considerable reduction in hardness. The higher retained austenite content and lower as-quenched hardness of HEAT 1 after austenitising at higher temperatures can probably be attributed to the higher alloying content of this steel. More molybdenum in solid solution causes a considerable reduction in the martensite transformation range, resulting in higher levels of retained austenite.

The dissolution of carbides during austenitising also affects the austenite grain size, as shown in Figure 4.21 for austenitising temperatures between 1000°C and 1100°C. The average ASTM grain size number remains stable at well above 9 for austenitising temperatures below about 1075°C. At austenitising temperatures between 1075°C and 1200°C, the grain size increases rapidly from an average ASTM grain size number of 9 to around 3. This increase in grain size is associated with the increase in temperature (providing a higher driving force for grain growth during heat treatment), compounded by coarsening and dissolution of grain pinning carbides. Grain growth in HEAT 1 is suppressed at temperatures below approximately 1120°C due to the higher stability of carbides in this steel. Once all the alloying elements are in solid solution due to the dissolution of carbides at higher temperatures, the austenite grain sizes of the two heats are similar.

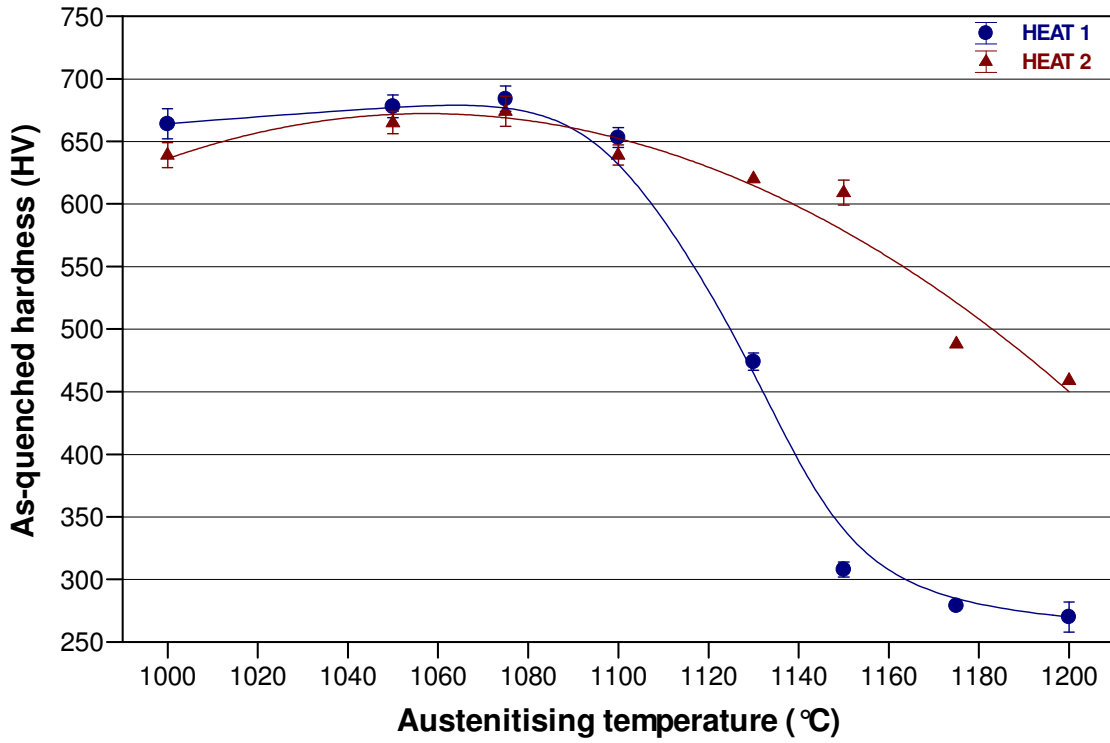


Figure 4.19: The influence of austenitising temperature on the as-quenched hardness of HEATS 1 and 2 (with 95% confidence interval).

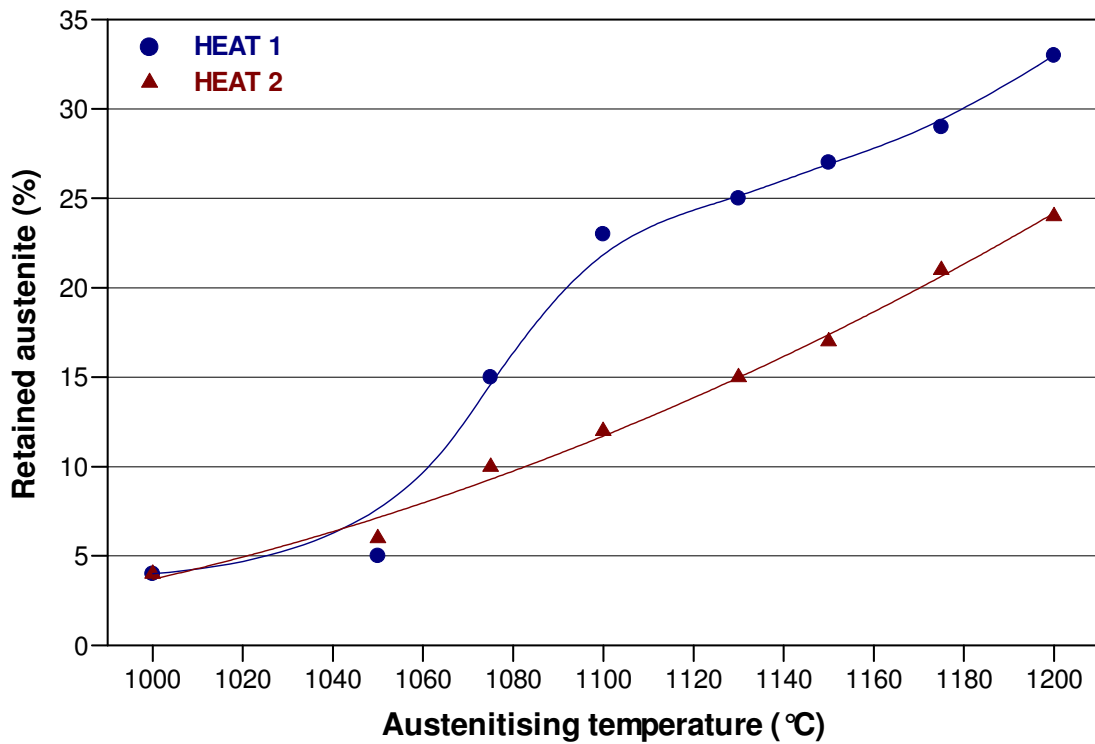


Figure 4.20: The influence of austenitising temperature on the as-quenched retained austenite content of HEATS 1 and 2.

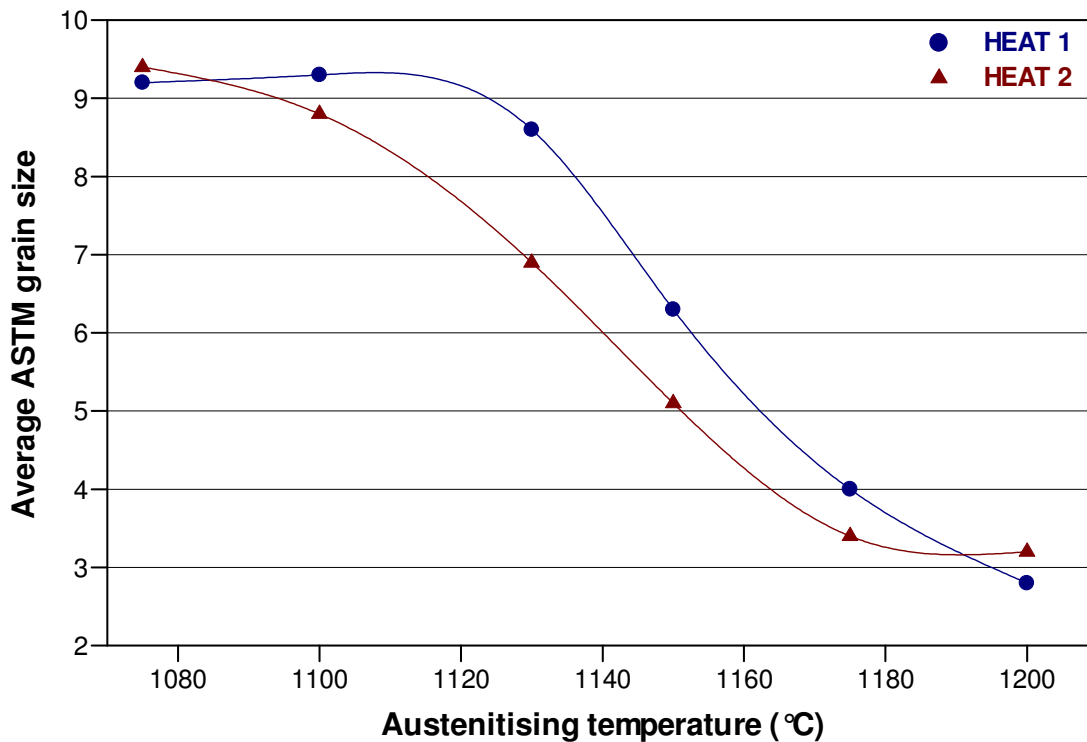


Figure 4.21: The influence of austenitising temperature on the average ASTM grain size of HEATS 1 and 2.

The average carbide diameters of the two heats are shown in Figure 4.22 as a function of austenitising temperature. The average carbide diameter measured in HEAT 1 decreases from approximately 1.3 μm at 1000°C to 0.8 μm at 1100°C. This reduction in average carbide diameter is less evident in HEAT 2, with the diameter decreasing from approximately 0.75 μm at 1000°C to below 0.6 μm diameter at 1100°C.

It is evident from Table 4.1 and Figure 4.19 that peak hardness values of 684 ± 10 HV and 674 ± 12 HV are obtained in HEAT 1 and HEAT 2, respectively, after quenching from an austenitising temperature of 1075°C. Although these hardness values are well above the minimum requirement of 610 HV stated in Chapter 2, the steels contain between 10 and 15% retained austenite after quenching. Since minimal retained austenite is specified as a requirement, the effect of tempering on the microstructure (and in particular the retained austenite content) and the properties of the two heats was investigated.

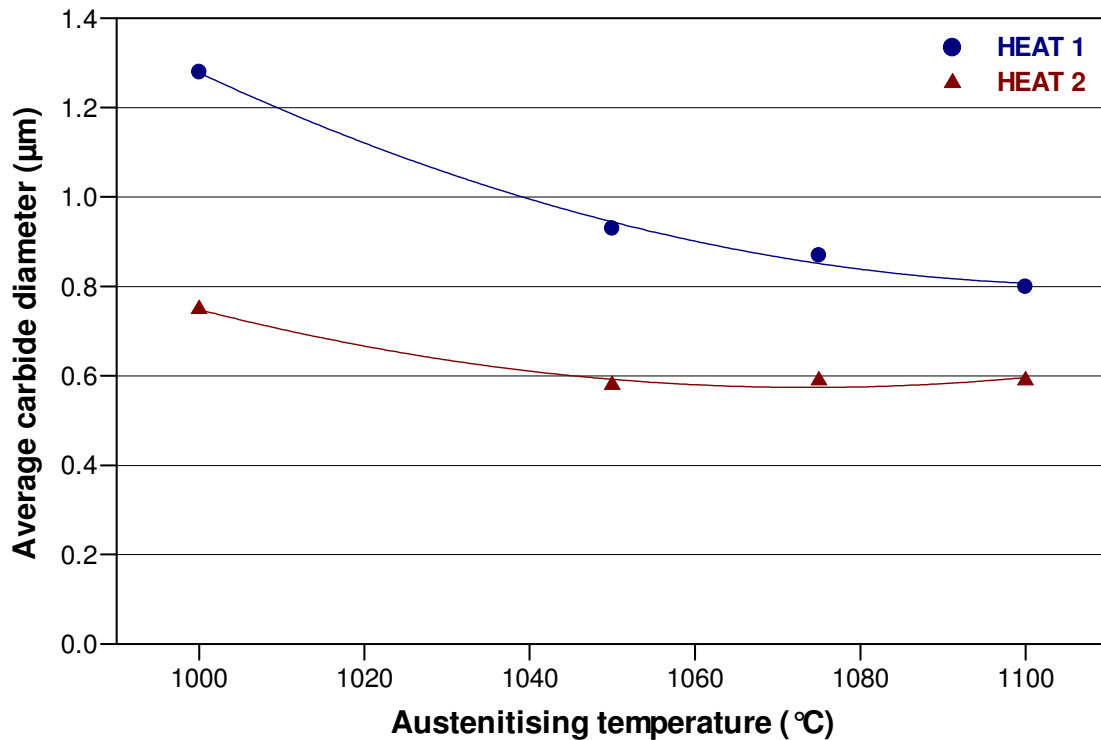


Figure 4.22: The influence of austenitising temperature on the average carbide diameter in HEATS 1 and 2.

3. THE EFFECT OF TEMPERING ON THE MICROSTRUCTURE AND PROPERTIES OF HEATS 1 AND 2

As stated in Chapter 2, a martensitic structure with minimal retained austenite, an evenly dispersed carbide structure and hardness values of between 610 HV and 740 HV are required to satisfy the design criteria for the steels examined during the course of this investigation. Austenitising at 1075°C for 15 minutes, followed by oil quenching, yields martensitic structures with dispersed carbides and hardness values well within the specified range for HEATS 1 and 2. The retained austenite contents of both steels are, however, higher than the desired levels.

To increase the toughness of the as-quenched martensitic structures, transform retained austenite and induce secondary hardening, both heats of medium-carbon AISI 420 martensitic stainless steel were tempered at three temper temperatures, namely 550°C, 650°C and 750°C, for 30 minutes. Since tempering reduces the as-quenched hardness of both heats to unacceptable levels after austenitising at temperatures below 1150°C, the following discussion considers only the results obtained on tempering HEATS 1 and 2 after austenitising at 1150°C and 1175°C.

3.1 Tempering after austenitising at 1150°C or 1175°C:

The hardness of HEAT 1 after quenching from 1150°C was 308 ± 6 HV. Tempering at 550°C has very little effect on the microstructure of this alloy. Retained austenite and martensite was observed in the tempered microstructure, and an average hardness of 299 ± 10 HV was recorded. Increasing the tempering temperature to 650°C increased the hardness to 362 ± 14 HV, whereas tempering at 750°C raised the hardness to 560 ± 10 HV. This increase in hardness can be attributed to the formation of secondary alloy carbides, and most likely the transformation of some retained austenite to martensite. These hardness values are, however, still well below the required hardness level. The as-quenched hardness of HEAT 2 after austenitising at 1150°C for 15 minutes was 609 ± 10 HV. Tempering at 550°C yielded a microstructure containing residual austenite and martensite, with a hardness of 513 ± 9 HV. Tempering at 650°C reduced the hardness to 482 ± 14 HV, while tempering at 750°C reduced the hardness even further to 400 ± 10 HV. This steel has a lower alloying element content (lower molybdenum level) and therefore does not respond to secondary hardening to the same extent as the molybdenum-alloyed HEAT 1. None of these treatments satisfy the requirements stated in Chapter 2.

Austenitising at 1175°C, followed by oil quenching, yielded hardness values of 279 ± 4 HV for HEAT 1 and 488 ± 3 HV for HEAT 2. Subsequent tempering of HEAT 1 at 550°C has very little effect on the microstructure of the sample (as shown in Figure 4.23), and an average hardness of 284 ± 14 HV was recorded. Raising the tempering temperature to 650°C raised the hardness to 409 ± 13 HV due to alloy carbide precipitation and partial transformation of retained austenite to martensite. Very little change in microstructure or hardness was observed for HEAT 2 after tempering at 550°C or 650°C. Due to the low hardness values recorded, tempering at 750°C was not performed.

The measured hardness values of HEATS 1 and 2 after austenitising at 1150°C and 1175°C, followed by tempering at 550°C, 650°C or 750°C, are compared in Table 4.2. The hardness values of HEAT 1 exhibit a characteristic increase during tempering. This suggests that the higher molybdenum content of HEAT 1 promoted secondary hardening in this alloy. The precipitation of fine alloy carbides during tempering is also expected to increase the martensite transformation range and

facilitate the partial transformation of retained austenite to martensite. The hardness of HEAT 2 decreased during tempering. The absence of molybdenum and the lower chromium content of this steel reduced the temper resistance of steel and limited the extent of secondary hardening.

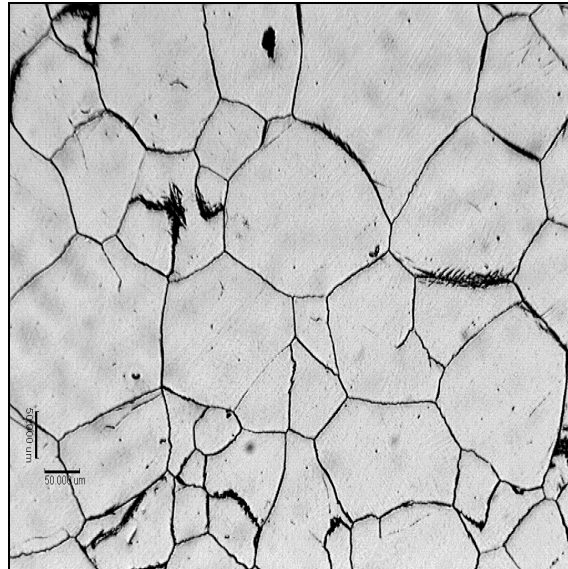


Figure 4.23: Optical micrograph of HEAT 1 after austenitising at 1175°C, followed by oil quenching and tempering at 550°C for 30 minutes. The microstructure consists of martensite and retained austenite. (Hardness: 284±14 HV). (Magnification: 100x).

Table 4.2: The effect of tempering on the hardness of HEATS 1 and 2 after austenitising at 1150°C and 1175°C.

Austenitising temperature	HEAT 1			HEAT 2		
	As-quenched hardness	Temper temperature	Hardness	As-quenched hardness	Temper temperature	Hardness
1150°C	308±6 HV	550°C	299±10 HV	609±10 HV	550°C	513±9 HV
		650°C	362±14 HV		650°C	482±14 HV
		750°C	560±10 HV		750°C	400±10 HV
1175°C	279±4 HV	550°C	284±14 HV	488±3 HV	550°C	446±5 HV
		650°C	409±13 HV		650°C	455±8 HV

3.2 Double tempering:

In order to promote the transformation of retained austenite to martensite, a second tempering step was introduced for samples austenitised at 1150°C and tempered at 650°C or 750°C, and for samples austenitised at 1175°C and tempered at 550°C or 650°C. These samples were tempered for a second time at the same temper

temperatures (for an additional 30 minutes). The results obtained after double tempering are summarised in Table 4.3.

Table 4.3: The effect of double tempering on the hardness of HEATS 1 and 2 after austenitising at 1150°C and 1175°C.

Austenitising temperature	HEAT 1			HEAT 2		
	Temper temperature	Hardness (1 st temper)	Hardness (2 nd temper)	Temper temperature	Hardness (1 st temper)	Hardness (2 nd temper)
1150°C	650°C	362±14 HV	500±9 HV	650°C	482±14 HV	360±5 HV
	750°C	560±10 HV	320±7 HV	750°C	400±10 HV	294±7 HV
1175°C	550°C	284±14 HV	295±14 HV	550°C	446±5 HV	522±5 HV
	650°C	409±13 HV	388±9 HV	650°C	455±8 HV	344±6 HV

With the exception of HEAT 1 austenitised at 1150°C and double tempered at 650°C, and HEAT 2 austenitised at 1175°C and double tempered at 550°C, double tempering did not result in any significant hardening in any of the samples tested. An optical photomicrograph of HEAT 1 after austenitising at 1150°C and double tempering at 650°C is shown in Figure 4.24. Even though double tempering results in a hardness increase in this sample, the microstructure still contains a significant amount of retained austenite after the double temper treatment. All hardness values in Table 4.3 are well below the required hardness values.

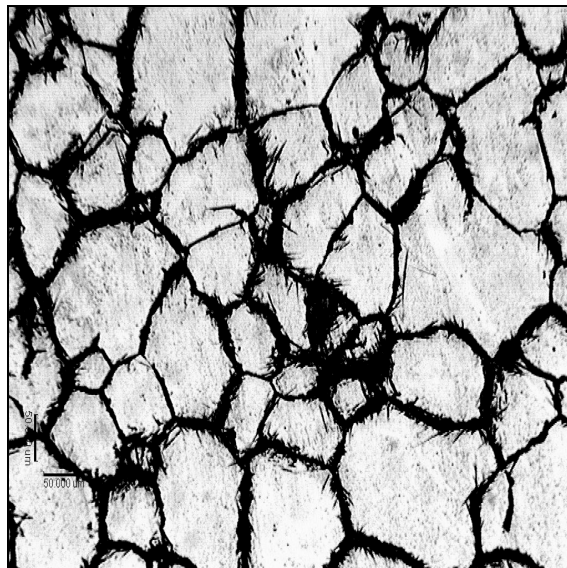


Figure 4.24: Optical micrograph of HEAT 1 after austenitising at 1150°C, followed by oil quenching and double tempering at 650°C. The microstructure consists of martensite and retained austenite. (Hardness: 500±9 HV). (Magnification: 100x).

It is apparent from the preceding discussion that the microstructure and properties obtained after tempering AISI 420 at temperatures between 550°C and 750°C after austenitising at 1150°C or 1175°C do not satisfy the requirements stated in Chapter 2. In order to facilitate a higher degree of transformation of retained austenite to martensite, cryogenic treatment was performed. The results of this investigation are described below.

3.3 Sub-zero treatments:

In order to determine the effect of sub-zero tempering on the microstructure and hardness of HEATS 1 and 2, samples austenitised at 1100°C, 1130°C, 1150°C and 1175°C were sub-zero tempered in liquid nitrogen at -196°C for 40 minutes after oil quenching.

The influence of sub-zero treatment after quenching is illustrated in Figure 4.25 as a function of austenitising temperature for HEATS 1 and 2. Treatment in liquid nitrogen raised the hardness values considerably in both HEAT 1 and HEAT 2, with final hardness values above 690 HV in all the samples evaluated. This suggests that the majority of the retained austenite in the as-quenched microstructures transformed to martensite during sub-zero treatment, resulting in a significant increase in hardness. All samples of HEAT 1 displayed hardness values higher than 700 HV, a substantial increase over those measured in the as-quenched condition (particularly at higher austenitising temperatures). The recorded hardness values of HEAT 2 ranged between 739 HV and 785 HV after sub-zero tempering, as opposed to 639 HV to 488 HV for the as-quenched samples. A representative example of the microstructure of HEAT 2 after sub-zero treatment is shown in Figure 4.26. The structure is predominantly martensitic, with a small percentage of retained austenite.

The results shown in Figure 4.25 suggest that sub-zero treatment in liquid nitrogen is effective in transforming most of the retained austenite to martensite. The final hardness values are, however, too high to satisfy the design requirements of the steel, and the newly transformed martensite most likely too brittle. HEATS 1 and 2 were therefore tempered at 550°C or 700°C after austenitising at 1130°C, 1150°C and 1175°C, oil quenching and sub-zero treatment at -196°C. A tempering time of 1 hour was used. The results of tempering after sub-zero treatment in liquid nitrogen are considered below.

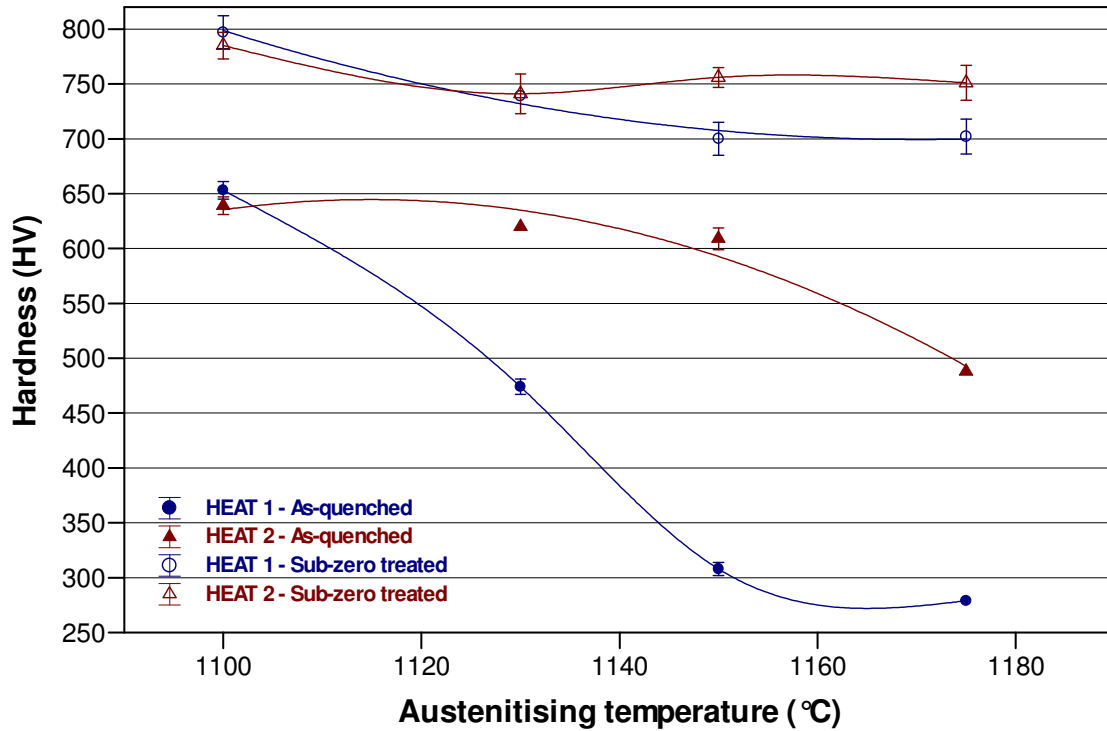


Figure 4.25: The effect of sub-zero tempering on the hardness of HEATS 1 and 2 after austenitising at temperatures between 1100°C and 1175°C.

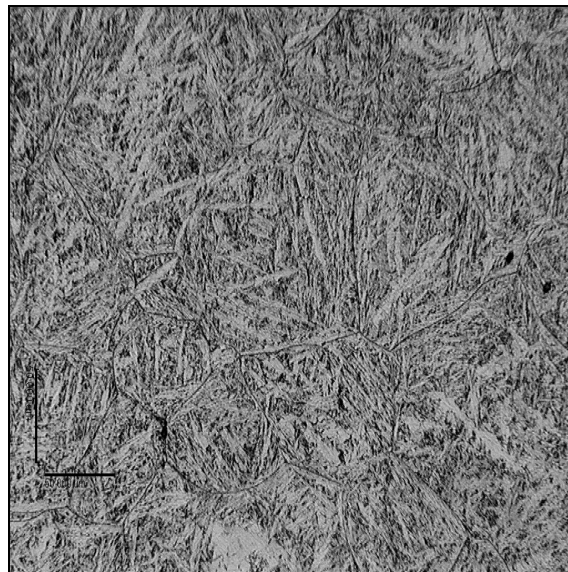


Figure 4.26: Optical micrograph of HEAT 2 after austenitising at 1130°C, followed by oil quenching and sub-zero treatment in liquid nitrogen. The microstructure consists of martensite and a small amount of retained austenite. (Hardness: 741 ± 18 HV). (Magnification: 200x).

HEAT 1, austenitised at 1130 °C to 1175 °C, oil quenched, sub-zero treated at -196 °C and tempered at 550 °C, has final hardness values between 649 HV and 673 HV. Micrographs of HEAT 1, austenitised at 1130 °C, 1150 °C or 1175 °C, sub-zero treated at -196 °C and tempered at 550 °C, are shown in Figures 4.27, 4.28 and 4.29.

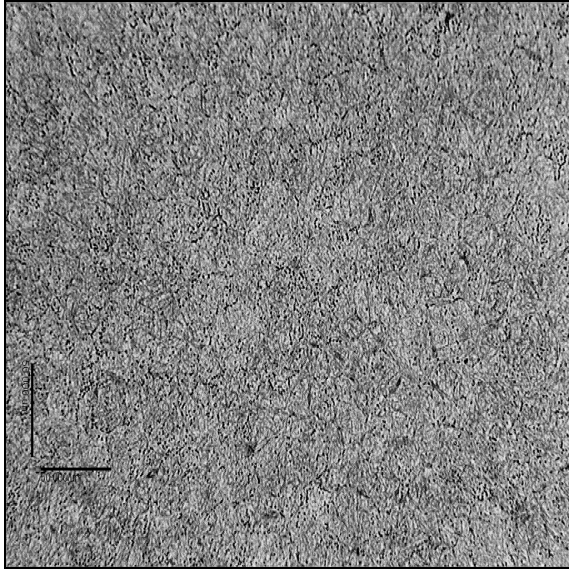


Figure 4.27: Optical micrograph of HEAT 1 after austenitising at 1130 °C, followed by oil quenching, sub-zero treatment in liquid nitrogen and tempering at 550 °C. The microstructure consists of martensite and 3% retained austenite. (Hardness: 673±6 HV). (Magnification: 200x).

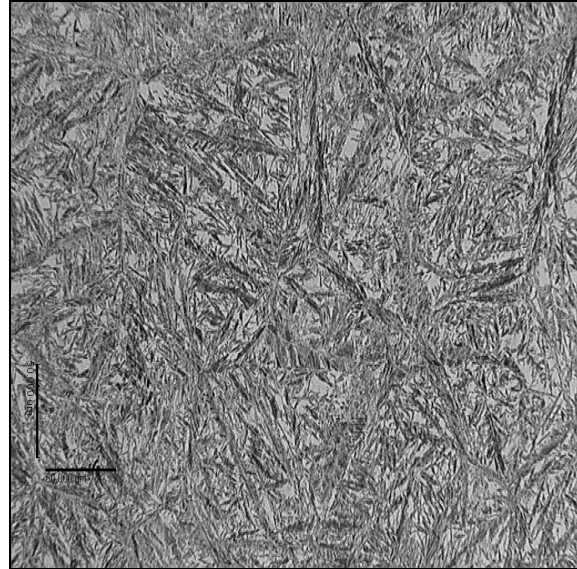


Figure 4.28: Optical micrograph of HEAT 1 after austenitising at 1150 °C, followed by oil quenching, sub-zero treatment in liquid nitrogen and tempering at 550 °C. The microstructure consists of martensite and 5% retained austenite. (Hardness: 651±14 HV). (Magnification: 200x).

The microstructures shown in Figures 4.27 and 4.28 (for austenitising temperatures of 1130 °C and 1150 °C, respectively) consist of martensite, retained austenite and a small number of carbides. Retained austenite levels of 3% (austenitised at 1130 °C) and 5% (austenitised at 1150 °C) were measured. The microstructure of HEAT 1, austenitised at 1175 °C and subjected to sub-zero treatment and tempering at 550 °C, is shown in Figure 4.29. This microstructure consists of martensite, approximately 8% retained austenite and grain boundary $M_{23}C_6$ carbide particles. The grain boundary $M_{23}C_6$ carbides precipitate during tempering from the carbon saturated matrix. Since the requirements stated in Chapter 2 specify an evenly dispersed carbide network, this sample is not considered acceptable in view of the alloy design criteria.

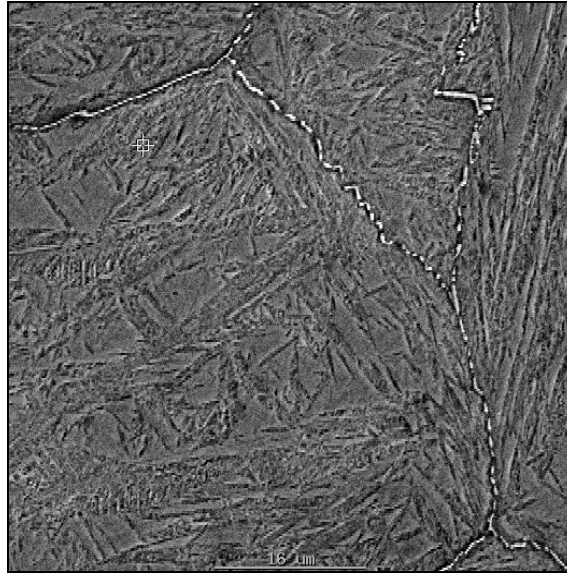


Figure 4.29: Scanning electron micrograph of HEAT 1 after austenitising at 1175°C, followed by oil quenching, sub-zero treatment in liquid nitrogen and tempering at 550°C. The microstructure consists of martensite, 8% retained austenite and networks of intergranular $M_{23}C_6$ carbides. (Hardness: 649 ± 9 HV).

HEAT 2, austenitised at 1130°C, 1150°C or 1175°C, followed by oil quenching, sub-zero treatment at -196°C and tempering at 550°C, displays final hardness values between 626 HV and 644 HV. The microstructures of samples austenitised at 1130°C and 1150°C are shown in Figures 4.30 and 4.31. These samples are shown to consist of martensite, small amounts of retained austenite and carbides. Retained austenite contents of 1% (austenitised at 1130°C) and 3% (austenitised at 1150°C) were measured. A scanning electron micrograph of HEAT 2 after austenitising at 1175°C, followed by oil quenching, sub-zero treatment and tempering at 550°C, is shown in Figure 4.32. This microstructure consists of martensite, approximately 4% retained austenite and a network of reprecipitated grain boundary $M_{23}C_6$ carbide particles. A structure with a pronounced grain boundary network of carbides does not satisfy the requirement of evenly dispersed carbides, as stated in Chapter 2.

A temper temperature of 700°C proved to be excessive for both heats, resulting in extensive softening. Tempering at this temperature after sub-zero treatment yielded hardness values well below 400 HV in both heats. A representative micrograph of HEAT 2, austenitised at 1130°C, sub-zero treated at -196°C and tempered at 700°C, is shown in Figure 4.33.

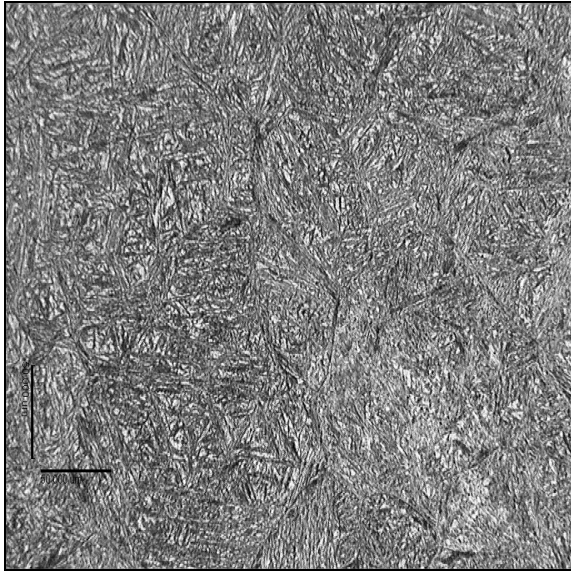


Figure 4.30: Optical micrograph of HEAT 2 after austenitising at 1130°C, followed by oil quenching, sub-zero treatment in liquid nitrogen and tempering at 550°C. The microstructure consists of martensite and 1% retained austenite. (Hardness: 626±4 HV). (Magnification: 200x).

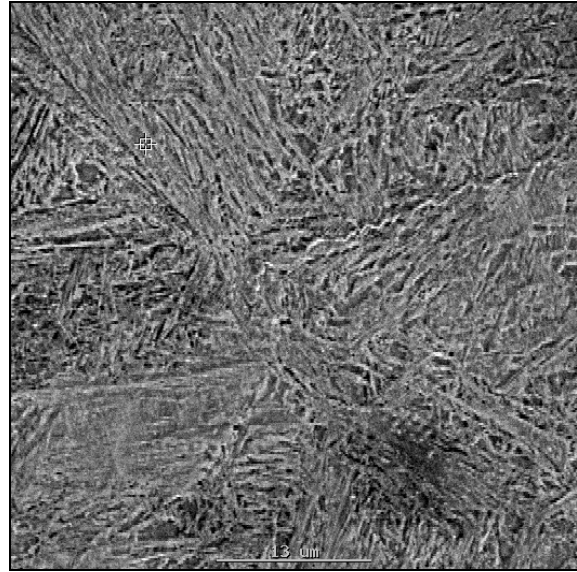


Figure 4.31: Scanning electron micrograph of HEAT 2 after austenitising at 1150°C, followed by oil quenching, sub-zero treatment in liquid nitrogen and tempering at 550°C. The microstructure consists of martensite and 3% retained austenite. (Hardness: 644±9 HV).

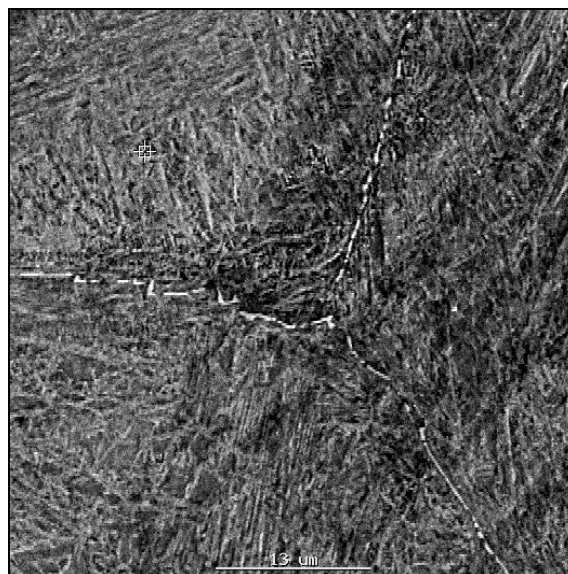


Figure 4.32: Scanning electron micrograph of HEAT 2 after austenitising at 1175°C, followed by oil quenching, sub-zero treatment in liquid nitrogen and tempering at 550°C. The microstructure consists of martensite, 4% retained austenite and networks of intergranular $M_{23}C_6$ carbides. (Hardness: 647±12 HV).

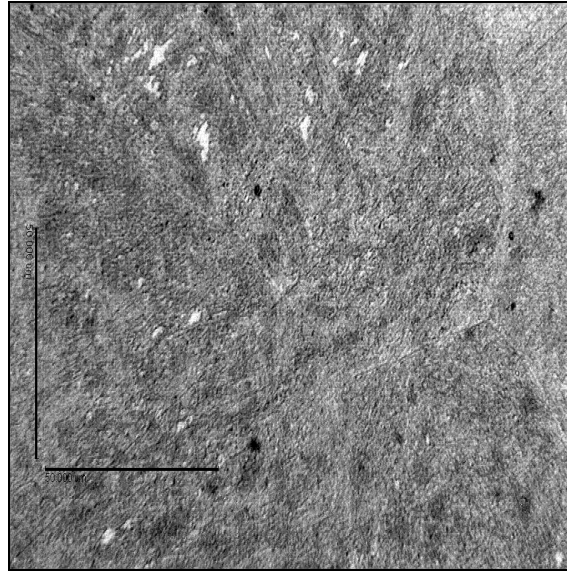


Figure 4.33: Optical micrograph of HEAT 2 after austenitising at 1130°C, followed by oil quenching, sub-zero treatment in liquid nitrogen and tempering at 700°C. The microstructure consists of martensite and retained austenite. (Hardness: 333±2 HV). (Magnification: 500x).

A summary of the effect of sub-zero treatment and tempering on the hardness of HEATS 1 and 2 is shown in Table 4.4. It is evident that austenitising at temperatures between 1130°C and 1175°C, followed by oil quenching, sub-zero treatment in liquid nitrogen and tempering at 550°C, satisfy the hardness requirements stated in Chapter 2.

Table 4.4: The effect of sub-zero treatment and tempering on the hardness of HEATS 1 and 2 after austenitising at 1130°C, 1150°C and 1175°C.

HEAT 1				
Austenitising temperature	As-quenched	Sub-zero treated	Tempered at 550°C	Tempered at 700°C
1130°C	474±7 HV	739±1 HV	673±6 HV	372±7 HV
1150°C	308±6 HV	700±15 HV	651±14 HV	380±4 HV
1175°C	279±4 HV	702±16 HV	649±9 HV	372±7 HV

HEAT 2				
Austenitising temperature	As-quenched	Sub-zero treated	Tempered at 550°C	Tempered at 700°C
1130°C	620±4 HV	741±18 HV	626±4 HV	333±2 HV
1150°C	609±10 HV	756±9 HV	644±9 HV	330±3 HV
1175°C	488±3 HV	751±16 HV	647±12 HV	326±6 HV

4. PRELIMINARY CONCLUSIONS

The results of this investigation therefore indicate that it is possible to obtain a martensitic structure with minimal retained austenite, evenly dispersed, spherical carbides, and hardness values between 610 HV and 740 HV in both heats of medium-carbon AISI 420 martensitic stainless steel supplied for the purpose of this investigation. The following heat treatment procedure is recommended to ensure these properties:

- Austenitise at temperatures between 1130°C and 1150°C.
- Oil quench.
- Sub-zero temper in liquid nitrogen at -196°C.
- Temper at 550°C for 1 hour.

The final structure is predominantly martensitic, with minimal retained austenite (between 3% and 5%) and evenly dispersed carbides. Austenitising at temperatures higher than 1150°C gives rise to the formation of a distinct grain boundary network of $M_{23}C_6$ carbides during tempering, and should be avoided.

The final conclusions and recommendations are discussed in Chapter 5.

CHAPTER 5 – FINAL CONCLUSIONS AND RECOMMENDATIONS

1. FINAL CONCLUSIONS

Medium-carbon AISI 420 martensitic stainless steel is recommended for use in applications requiring moderate corrosion resistance, high hardness, excellent wear resistance and good edge retention in cutting surfaces. The steel is usually supplied in the fully annealed condition, with a microstructure consisting of coarse, globular carbides in a ferrite matrix. Annealing softens the steel in preparation for further cold work or machining operations. After forming, the consumer or fabricator performs the final hardening treatments to develop optimal mechanical and corrosion properties. The microstructure and properties of medium-carbon AISI 420 martensitic stainless steel depend strongly on the hardening heat treatment, and in particular the austenitising treatment, that the steel receives. The austenitising temperature controls the partitioning of alloying elements between the austenite and carbides at elevated temperature, and affects the martensite transformation range, grain size, hardness and the retained austenite content of the steel in the as-quenched condition. This project aimed at identifying the heat treatment parameters required to produce a martensitic structure with minimal retained austenite and evenly dispersed carbides, and hardness values between 610 HV and 740 HV (hardness on the Vickers scale) in two heats of AISI 420 martensitic stainless steel. The following conclusions were drawn:

- Higher austenitising temperatures lead to increased carbide dissolution. The carbide densities in both steels decrease with an increase in austenitising temperature. The higher molybdenum content of HEAT 1 retards carbide dissolution at higher austenitising temperatures due to the increased stability of the carbides (as confirmed by phase diagrams constructed using the CALPHAD model). Complete carbide dissolution takes place at temperatures higher than 1175°C in both heats.
- The gradual dissolution of carbides at austenitising temperatures up to 1175°C (where complete carbide dissolution is observed in both heats) affects the measured retained austenite content, as-quenched hardness and grain size of the steels. The measured hardness values of both heats increase slightly with

an increase in austenitising temperature up to 1075°C. This can be attributed to the partial dissolution of $M_{23}C_6$ carbides, which raises the carbon content of the austenite phase, as a result of which a higher carbon martensite forms on quenching.

- Higher austenitising temperatures raise the amount of carbon and alloying elements in solution in the austenite, and depress the martensite transformation range to lower temperatures. At temperatures higher than approximately 1075°C, increased carbide dissolution results in higher retained austenite contents, particularly in HEAT 1, and a considerable reduction in hardness.
- The dissolution of carbides during austenitising affects the austenite grain size. The average ASTM grain size number remains stable at well above 9 for austenitising temperatures below about 1075°C. At austenitising temperatures between 1075°C and 1200°C, the grain size increases rapidly. This increase in grain size is associated with the increase in temperature (providing a higher driving force for grain growth during heat treatment), compounded by the dissolution of grain pinning carbides.
- Tempering at temperatures of 550°C, 650°C or 750°C after austenitising at 1150°C and 1175°C does not reduce the as-quenched retained austenite content or induce secondary hardening. Significant secondary hardening is observed only after tempering at 750°C in HEAT 1, but the hardness values are well below those required. Double tempering at the same temperatures is also not effective.
- Sub-zero treatment in liquid nitrogen after austenitising at 1130°C or 1150°C raises the hardness values considerably in both HEAT 1 and HEAT 2, with final hardness values above 690 HV in all the samples evaluated. This suggests that the majority of the retained austenite in the as-quenched microstructures transforms to martensite during sub-zero treatment, resulting in a significant increase in hardness. Tempering at 550°C after sub-zero treatment results in hardness values well within the range specified. The microstructure after tempering at 550°C consists of martensite with minimal retained austenite and evenly dispersed carbides. Austenitising at temperatures higher than 1150°C

gives rise to the formation of a distinct grain boundary network of $M_{23}C_6$ carbides, and should be avoided.

2. RECOMMENDATIONS

The results of this investigation confirm that it is possible to obtain a martensitic structure with minimal retained austenite, evenly dispersed, spherical carbides, and hardness values between 610 HV and 740 HV in both heats of medium-carbon AISI 420 martensitic stainless steel supplied for the purpose of this investigation. The following heat treatment procedure is recommended to ensure these properties:

- Austenitise at temperatures between 1130°C and 1150°C. Short soaking times of 15 minutes are sufficient for light sections, but the austenitising time needs to be adjusted for heavier sections.
- Oil quench.
- Sub-zero temper in liquid nitrogen at -196°C.
- Temper at 550°C for 1 hour.

The final structure is predominantly martensitic, with minimal retained austenite (between 3% and 5%), and contains evenly dispersed carbides. Austenitising at temperatures higher than 1150°C gives rise to the formation of a distinct grain boundary network of $M_{23}C_6$ carbides, and should be avoided.

CHAPTER 6 - REFERENCES

- [1] W.F. Smith, *Principles of Materials Science and Engineering*, Third Edition, McGraw-Hill, 1996, pp 517–551.
- [2] F.B. Pickering, *The Metallurgical Evolution of Stainless Steels, a discriminative selection of outstanding articles and papers from the scientific literature*, American Society for Metals, 1979, pp 2-44.
- [3] D.S. Clark and W.R. Varney, *Metallurgy for Engineers*, D. van Nostrand Company, 1965, pp 206-333.
- [4] R.A Higgins, *Engineering Metallurgy, Part 1 - Applied Physical Metallurgy*, Fifth Edition, Hodder and Stoughton, 1983, pp 295-319.
- [5] S.H. Avner, *Introduction to Physical Metallurgy*, International Student Edition, McGraw-Hill, 1974, pp 349-367.
- [6] C. Garcia de Andrés, L.F. Alvarez and V. Lopez, *Effects of carbide forming elements on the response to thermal treatment of the X45Cr13 martensitic stainless steel*, *Journal of Materials Science*, 33, 1998, pp 4095-4100.
- [7] Interlloy Pty Ltd, *Data Sheet for 420 Martensitic Stainless Steel Bar*, available at http://www.interlloy.com.au/data_sheets/stainless_steel/stainless_pdf/interlloy_420_Martensitic_Stainless_Steel_Bar.pdf.
- [8] L. Colombier, *Molybdenum in Stainless Steels and Alloys*, Climax Molybdenum Company Ltd.
- [9] S. Kalpakjian and S.R. Schmid, *Manufacturing Processes for Engineering Materials*, Fourth Edition, Prentice Hall, 2003, p 110.
- [10] R.E. Reed-Hill, *Physical Metallurgy Principles*, Third Edition, PWS Publishing Company, 1994, p 678.
- [11] A. Bjarbo and M. Hatterstrand, *Complex Carbides Growth, Dissolution, and Coarsening in a Modified 12 Pct Chromium Steel – an Experimental and Theoretical Study*, *Metallurgical and Materials Transactions A*, 32A, 2001, pp 19–27.
- [12] T. Sourmail and H.K.D.H. Bhadeshia, *Stainless Steels*, University of Cambridge, 2005, available at http://www.msm.cam.ac.uk/phase-trans/2005/Stainless_steels/stainless.html.

- [13] A. Rajasekhar, G.M. Reddy, T. Mohandas and V.S.R. Murti, *Influence of austenitising temperature on microstructure and mechanical properties of AISI 431 martensitic stainless steel electron beam welds*, Materials and Design, 2008, accepted manuscript.
- [14] S.H. Avner, *Introduction to Physical Metallurgy*, International Student Edition, McGraw-Hill, 1974, pp 667–668.
- [15] I. Calliari, M. Zanesco, M. Dabala, K. Brunelli and E. Ramous, *Investigation of microstructure and properties of a Ni-Mo martensitic stainless steel*, Materials and Design, 29(1), 2008, pp 246–250.
- [16] C. Garcia de Andrés, G. Caruna and L.F. Alvarez, *Control of $M_{23}C_6$ carbides in 0.45C-13Cr martensitic stainless steel by means of three representative heat treatment parameters*, Materials Science and Engineering A, A241, 1998, pp 211-215.
- [17] S.S.M. Tavares, D. Fruchart, S. Miraglia and D. Laborie, *Magnetic properties of an AISI 420 martensitic stainless steel*, Journal of Alloys and Compounds, 312(1-2), 2000, pp 307–314.
- [18] Latrobe Steel, *Datasheet for LSS 420 HC stainless steel*, 2008, available at <http://www.matweb.com/search/datasheet.aspx?matguid=ed94b14f5a6b463e8ffe7b89def0cec&ckck=1>.
- [19] A.F. Candelaria and C.E. Pinedo, *Influence of the heat treatment on the corrosion resistance of the martensitic stainless steel type AISI 420*, Journal of Materials Science Letters, 22(16), 2003, pp 1151–1153.
- [20] R.A Higgins, *Engineering Metallurgy, Part 1 - Applied Physical Metallurgy*, Fifth Edition, Hodder and Stoughton, 1983, p 175.
- [21] S. Kalpakjian and S.R. Schmid, *Manufacturing Processes for Engineering Materials*, Fourth Edition, Prentice Hall, 2003, p 243.
- [22] ASM Metals Handbook, *Volume 4 - Heat Treating*, ASM, Metals Park, Ohio, Revised 2001, pp 203-206.
- [23] J.R. Yang, T.H. Yu and C.H. Wang, *Martensitic transformations in AISI 440C stainless steel*, Materials Science and Engineering A, A438-440, 2006, pp 276–280.
- [24] S. Salem, *Alloyed steel intended for hot rolling mill rolls*, Metal Science and Heat Treatment, 35(11), 1993, pp 657–659.

APPENDIX A - CARBIDE DIAMETER MEASUREMENTS

THE MEASURED DIAMETERS OF THIRTEEN CARBIDE PARTICLES IN HEAT 1
AFTER QUENCHING FROM 1000°C, 1050°C, 1075°C AND 1100°C.

MEASURED CARBIDE DIAMETER, μm				
	Austenitised at 1000°C	Austenitised at 1050°C	Austenitised at 1075°C	Austenitised at 1100°C
	1.20	0.80	0.80	0.67
	1.47	1.20	0.80	0.53
	0.80	0.67	0.67	0.53
	0.93	0.67	0.93	0.93
	1.07	1.07	1.20	0.80
	1.47	1.20	0.67	0.80
	1.20	0.93	0.67	0.53
	0.93	0.93	0.93	0.93
	1.33	0.67	0.80	0.93
	3.20	0.93	0.67	1.33
	1.60	0.93	1.60	0.67
	0.67	1.07	1.07	0.53
	0.80	1.07	0.53	1.20
AVERAGE	1.28	0.93	0.87	0.80
Smallest	0.67	0.67	0.53	0.53
Largest	3.20	1.20	1.60	1.33



**THE MEASURED DIAMETERS OF THIRTEEN CARBIDE PARTICLES IN HEAT 2
AFTER QUENCHING FROM 1000°C, 1050°C, 1075°C AND 1100°C.**

MEASURED CARBIDE DIAMETER, μm			
Austenitised at 1000°C	Austenitised at 1050°C	Austenitised at 1075°C	Austenitised at 1100°C
0.40	0.67	0.67	0.67
0.67	0.67	0.53	0.40
0.53	0.40	0.67	0.53
0.93	0.53	0.53	0.67
0.80	0.67	0.53	0.53
1.07	0.40	0.00	0.67
0.67	0.40	0.00	0.67
1.33	0.40	0.00	0.53
0.93	0.40	0.00	0.67
0.53	0.80	0.00	0.00
0.67	0.67	0.00	0.00
0.53	0.67	0.00	0.00
0.67	0.93	0.00	0.00
AVERAGE	0.75	0.58	0.59
Smallest	0.40	0.40	0.40
Largest	1.33	0.93	0.67

APPENDIX B - ASTM GRAIN SIZE NUMBER

ASTM GRAIN SIZE NUMBER (*G*) OF HEAT 1 AS A FUNCTION OF AUSTENITISING TEMPERATURE

AUSTENISED AT 1075°C AND OIL QUENCHED					
Measurements	<i>L_T</i>	<i>P</i>	<i>M</i>	<i>L_L</i>	<i>G</i>
1	122	39	240	0.0130	9.235
2	122	40	240	0.0127	9.309
3	123	34	240	0.0151	8.816
4	122	38	240	0.0134	9.160
5	122	40	240	0.0127	9.309
95% confidence interval					0.25
Average ASTM grain size number, <i>G</i>					9.166
AUSTENISED AT 1100°C AND OIL QUENCHED					
Measurements	<i>L_T</i>	<i>P</i>	<i>M</i>	<i>L_L</i>	<i>G</i>
1	139	14	780	0.0127	9.304
2	139	16	780	0.0111	9.689
3	139	12	780	0.0149	8.859
4	139	13	780	0.0137	9.090
5	139	15	780	0.0119	9.503
95% confidence interval					0.41
Average ASTM grain size number, <i>G</i>					9.289
AUSTENISED AT 1130°C AND OIL QUENCHED					
Measurements	<i>L_T</i>	<i>P</i>	<i>M</i>	<i>L_L</i>	<i>G</i>
1	187	19	600	0.0164	8.572
2	185	19	600	0.0162	8.603
3	185	23	600	0.0134	9.154
4	189	14	600	0.0225	7.660
5	185	21	600	0.0147	8.892
95% confidence interval					0.7
Average ASTM grain size number, <i>G</i>					8.576
AUSTENISED AT 1150°C AND OIL QUENCHED					
Measurements	<i>L_T</i>	<i>P</i>	<i>M</i>	<i>L_L</i>	<i>G</i>
1	139	18	220	0.0351	6.377
2	139	14	220	0.0451	5.652
3	139	18	220	0.0351	6.377
4	139	18	220	0.0351	6.377
5	139	21	220	0.0301	6.822
95% confidence interval					0.52
Average ASTM grain size number, <i>G</i>					6.321
AUSTENISED AT 1175°C AND OIL QUENCHED					
Measurements	<i>L_T</i>	<i>P</i>	<i>M</i>	<i>L_L</i>	<i>G</i>
1	146	8	260	0.0702	4.377
2	140	7	260	0.0769	4.113
3	140	6	260	0.0897	3.668
4	140	6	260	0.0897	3.668
5	140	7	260	0.0769	4.113
95% confidence interval					0.39
Average ASTM grain size number, <i>G</i>					3.988



AUSTENISED AT 1200°C AND OIL QUENCHED					
Measurements	L_T	P	M	L_L	G
1	142	19	60	0.1246	2.722
2	142	21	60	0.1127	3.011
3	142	14	60	0.1690	1.841
4	142	21	60	0.1127	3.011
5	142	23	60	0.1029	3.274
95% confidence interval					0.69
Average ASTM grain size number, G					2.772

**ASTM GRAIN SIZE NUMBER (G) OF HEAT 2 AS A FUNCTION OF
AUSTENITISING TEMPERATURE**

AUSTENISED AT 1075°C AND OIL QUENCHED					
Measurements	L_T	P	M	L_L	G
1	165	52	260	0.0122	9.425
2	165	50	260	0.0127	9.312
3	165	52	260	0.0122	9.425
4	165	53	260	0.0120	9.480
5	165	49	260	0.0130	9.254
95% confidence interval					0.12
Average ASTM grain size number, G					9.379
AUSTENISED AT 1100°C AND OIL QUENCHED					
Measurements	L_T	P	M	L_L	G
1	141	34	320	0.0130	9.252
2	141	29	320	0.0152	8.793
3	141	28	320	0.0157	8.692
4	141	29	320	0.0152	8.793
5	141	27	320	0.0163	8.587
95% confidence interval					0.3
Average ASTM grain size number, G					8.823
AUSTENISED AT 1130°C AND OIL QUENCHED					
Measurements	L_T	P	M	L_L	G
1	148	20	250	0.0296	6.869
2	148	22	250	0.0269	7.144
3	148	23	250	0.0257	7.272
4	148	18	250	0.0329	6.565
5	148	19	250	0.0312	6.721
95% confidence interval					0.4
Average ASTM grain size number, G					6.914
AUSTENISED AT 1150°C AND OIL QUENCHED					
Measurements	L_T	P	M	L_L	G
1	145	10	260	0.0558	5.041
2	145	9	260	0.0620	4.737
3	145	12	260	0.0464	5.567
4	145	9	260	0.0620	4.737
5	145	11	260	0.0507	5.316
95% confidence interval					0.45
Average ASTM grain size number, G					5.080



AUSTENISED AT 1175°C AND OIL QUENCHED					
Measurements	L_T	P	M	L_L	G
1	144	5	240	0.1200	2.830
2	144	6	240	0.1000	3.356
3	144	7	240	0.0857	3.801
4	144	7	240	0.0857	3.801
5	144	6	240	0.1000	3.356
95% confidence interval					0.5
Average ASTM grain size number, G					3.429
AUSTENISED AT 1200°C AND OIL QUENCHED					
Measurements	L_T	P	M	L_L	G
1	145	5	240	0.1208	2.810
2	145	7	240	0.0863	3.781
3	145	5	240	0.1208	2.810
4	145	7	240	0.0863	3.781
5	145	5	240	0.1208	2.810
95% confidence interval					0.7
Average ASTM grain size number, G					3.199

APPENDIX C - VICKERS HARDNESS MEASUREMENTS

MEASURED HARDNESS VALUES OF HEAT 1

HEAT TREATMENT CONDITION	VICKERS HARDNESS WITH A 10 KG LOAD, HV10					AVERAGE	95% CONF. LEVEL
AS-RECEIVED	216	206	214	207	203	209	7
AUSTENITISED AT 1000°C							
Austenitised and oil quenched	660	665	650	670	676	664	12
AUSTENITISED AT 1050°C							
Austenitised and oil quenched	672	688	674	687	669	678	9
AUSTENITISED AT 1075°C							
Austenitised and oil quenched	680	689	675	695	680	684	10
AUSTENITISED AT 1100°C							
Austenitised and oil quenched	658	656	654	642	655	653	8
Austenitised, oil quenched and sub-zero treated	802	800	778	810	793	797	15
AUSTENITISED AT 1130°C							
Austenitised and oil quenched	467	481	477	470	476	474	7
Austenitised, oil quenched and sub-zero treated	737	748	749	727	736	739	11
Austenitised, oil quenched, sub-zero treated and tempered at 550°C	677	665	675	678	672	673	6
Austenitised, oil quenched, sub-zero treated and tempered at 700°C	365	371	380	376	369	372	7
AUSTENITISED AT 1150°C							
Austenitised and oil quenched	308	301	309	314	310	308	6
Austenitised, oil quenched and tempered at 550°C	292	296	308	292	308	299	10
Austenitised, oil quenched and tempered at 650°C	359	350	380	363	360	362	14
Austenitised, oil quenched and tempered at 750°C	550	552	570	569	568	560	10
Austenitised, oil quenched and double tempered at 650°C	492	510	511	498	494	500	9
Austenitised, oil quenched and double tempered at 750°C	315	313	312	320	328	320	7
Austenitised, oil quenched and sub-zero treated	698	695	698	720	689	700	15
Austenitised, oil quenched, sub-zero treated and tempered at 550°C	637	650	653	648	668	651	14
Austenitised, oil quenched, sub-zero treated and tempered at 700°C	380	373	378	381	379	378	4
AUSTENITISED AT 1175°C							
Austenitised and oil quenched	276	281	282	276	280	279	4
Austenitised, oil quenched and tempered at 550°C	292	290	271	294	271	284	14
Austenitised, oil quenched and tempered at 650°C	417	397	415	398	416	409	13
Austenitised, oil quenched and double tempered at 550°C	286	307	293	307	284	295	14
Austenitised, oil quenched and double tempered at 650°C	402	390	384	378	382	388	9
Austenitised, oil quenched and sub-zero treated	713	714	686	690	705	702	16
Austenitised, oil quenched, sub-zero treated and tempered at 550°C	653	641	658	642	653	649	9
Austenitised, oil quenched, sub-zero treated and tempered at 700°C	366	371	374	380	368	372	7
AUSTENITISED AT 1200°C							
Austenitised and oil quenched	278	262	282	260	268	270	12

MEASURED HARDNESS VALUES OF HEAT 2

HEAT TREATMENT CONDITION	VICKERS HARDNESS WITH A 10 KG LOAD, HV10					AVERAGE	95% CONF. LEVEL
AS-RECEIVED	197	191	193	199	193	195	4
AUSTENITISED AT 1000°C							
Austenitised and oil quenched	646	628	647	634	638	639	10
AUSTENITISED AT 1050°C							
Austenitised and oil quenched	674	654	656	670	675	665	9
AUSTENITISED AT 1075°C							
Austenitised and oil quenched	667	666	685	684	666	674	12
AUSTENITISED AT 1100°C							
Austenitised and oil quenched	630	635	647	643	639	639	8
Austenitised, oil quenched and sub-zero treated	791	775	774	794	793	785	12
AUSTENITISED AT 1130°C							
Austenitised and oil quenched	615	622	625	618	616	620	4
Austenitised, oil quenched and sub-zero treated	764	745	739	728	730	741	18
Austenitised, oil quenched, sub-zero treated and tempered at 550°C	624	627	630	626	622	626	4
Austenitised, oil quenched, sub-zero treated and tempered at 700°C	332	334	333	330	334	333	2
AUSTENITISED AT 1150°C							
Austenitised and oil quenched	599	620	612	603	611	609	10
Austenitised, oil quenched and tempered at 550°C	505	520	506	518	510	513	9
Austenitised, oil quenched and tempered at 650°C	471	480	495	473	492	482	14
Austenitised, oil quenched and tempered at 750°C	398	402	412	390	400	400	10
Austenitised, oil quenched and double tempered at 650°C	366	357	357	360	362	360	5
Austenitised, oil quenched and double tempered at 750°C	296	297	286	290	299	294	7
Austenitised, oil quenched and sub-zero treated	764	757	758	756	745	756	9
Austenitised, oil quenched, sub-zero treated and tempered at 550°C	635	642	642	655	644	644	9
Austenitised, oil quenched, sub-zero treated and tempered at 700°C	329	330	328	329	334	330	3
AUSTENITISED AT 1175°C							
Austenitised and oil quenched	485	491	485	486	489	488	3
Austenitised, oil quenched and tempered at 550°C	440	447	448	452	445	446	5
Austenitised, oil quenched and tempered at 650°C	465	447	456	446	455	455	8
Austenitised, oil quenched and double tempered at 550°C	517	528	521	525	520	522	5
Austenitised, oil quenched and double tempered at 650°C	334	345	352	342	348	344	6
Austenitised, oil quenched and sub-zero treated	761	729	749	755	759	751	16
Austenitised, oil quenched, sub-zero treated and tempered at 550°C	640	644	630	650	660	647	12
Austenitised, oil quenched, sub-zero treated and tempered at 700°C	323	319	329	330	328	326	6
AUSTENITISED AT 1200°C							
Austenitised and oil quenched	460	457	458	461	460	459	2

APPENDIX D – ADDITIONAL MICROGRAPHS

THE EFFECT OF AUSTENITISING TEMPERATURE ON MICROSTRUCTURE

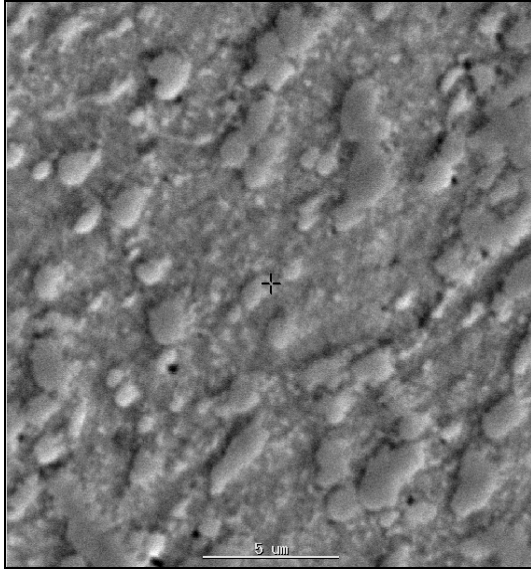


Figure D.1: Scanning electron micrograph of HEAT 1, austenitised at 1000°C for 15 minutes and oil quenched. The microstructure consists of coarse $M_{23}C_6$ carbides in a martensite matrix. (Hardness: 664 ± 12 HV). (Magnification: 500x).

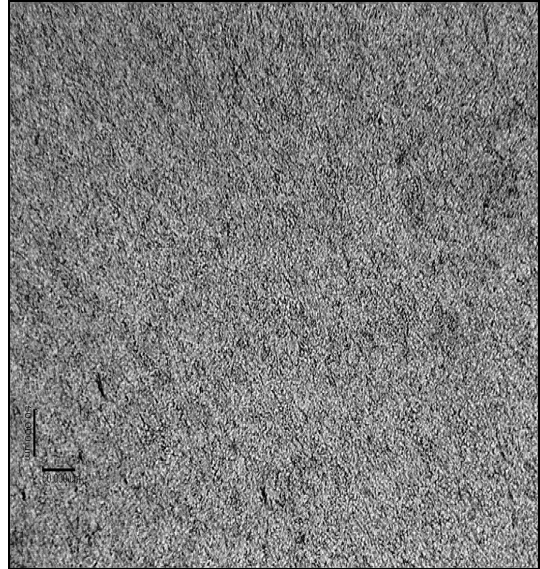


Figure D.2: Optical micrograph of HEAT 2, austenitised at 1000°C for 15 minutes and oil quenched. The microstructure consists of coarse $M_{23}C_6$ carbides in a martensite matrix. (Hardness: 639 ± 10 HV). (Magnification: 100x).

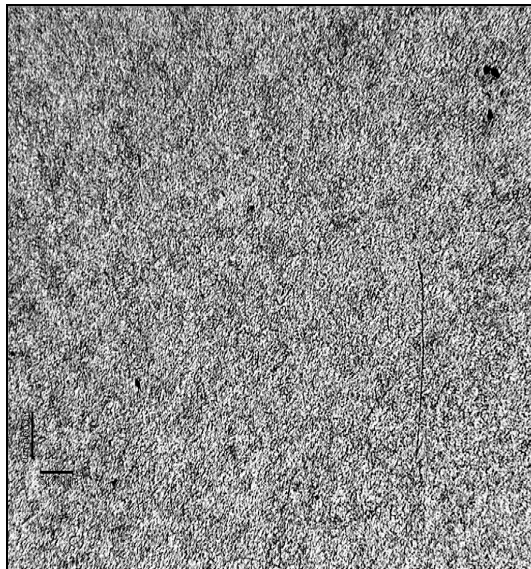


Figure D.3: Optical micrograph of HEAT 2, austenitised at 1050°C for 15 minutes and oil quenched. The microstructure consists of coarse $M_{23}C_6$ carbides in a martensite matrix. (Hardness: 665 ± 19 HV). (Magnification: 100x).

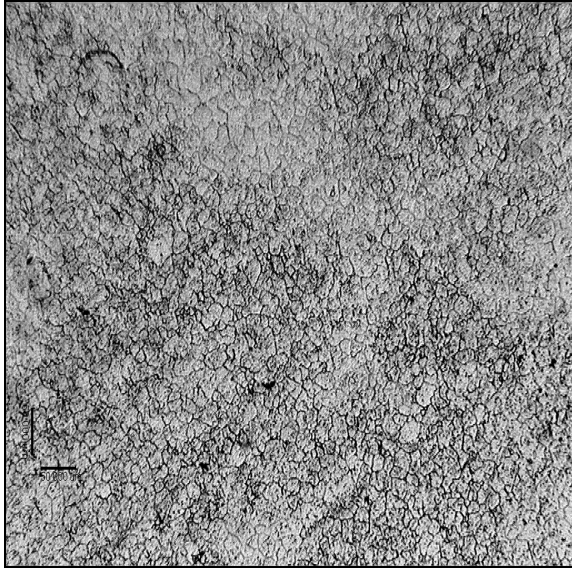


Figure D.4: Optical micrograph of HEAT 1, austenitised at 1075°C for 60 minutes and oil quenched. The microstructure consists of $M_{23}C_6$ carbides and retained austenite in a martensite matrix. (Hardness: 665 ± 16 HV). (Magnification: 100x).

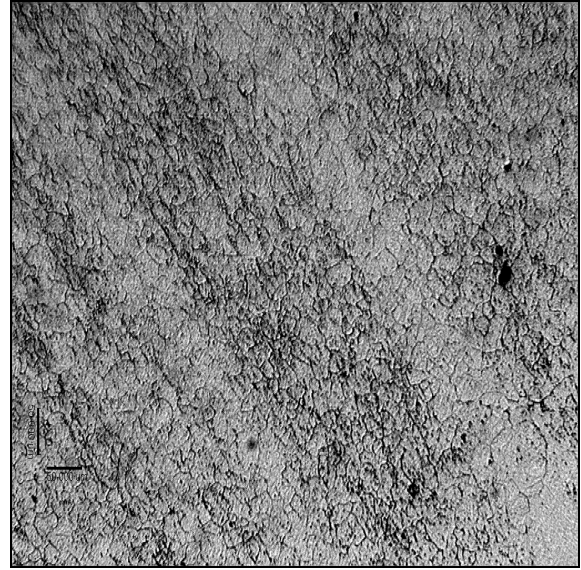


Figure D.5: Optical micrograph of HEAT 2, austenitised at 1075°C for 120 minutes and oil quenched. The microstructure consists of $M_{23}C_6$ carbides and retained austenite in a martensite matrix. (Hardness: 681 ± 9 HV). (Magnification: 100x).

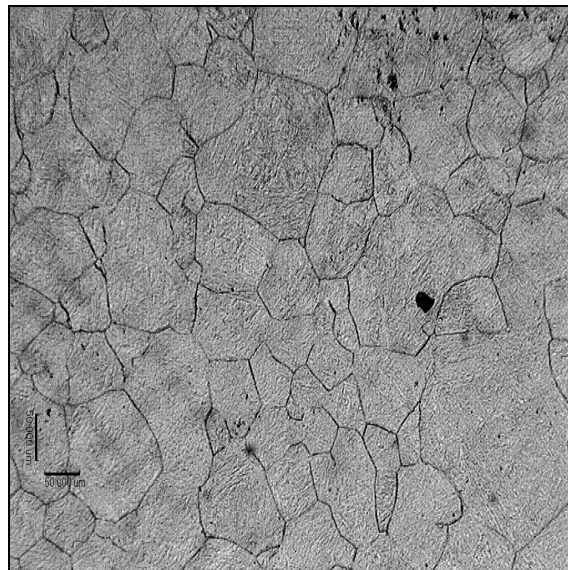


Figure D.6: Optical micrograph of HEAT 2, austenitised at 1150°C for 15 minutes and oil quenched. The microstructure consists of coarse $M_{23}C_6$ carbides in a martensite matrix. (Hardness: 609 ± 15 HV). (Magnification: 100x).

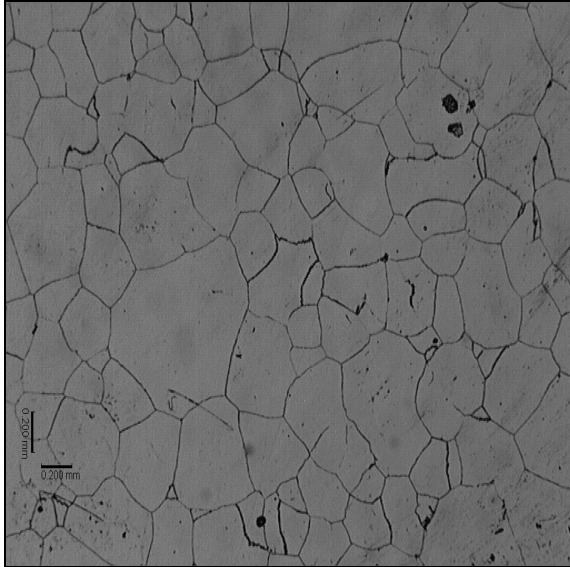


Figure D.7: Optical micrograph of HEAT 1, austenitised at 1175°C for 15 minutes and oil quenched. The microstructure consists of retained austenite in a martensite matrix. (Hardness: 279±4 HV). (Magnification: 50x).

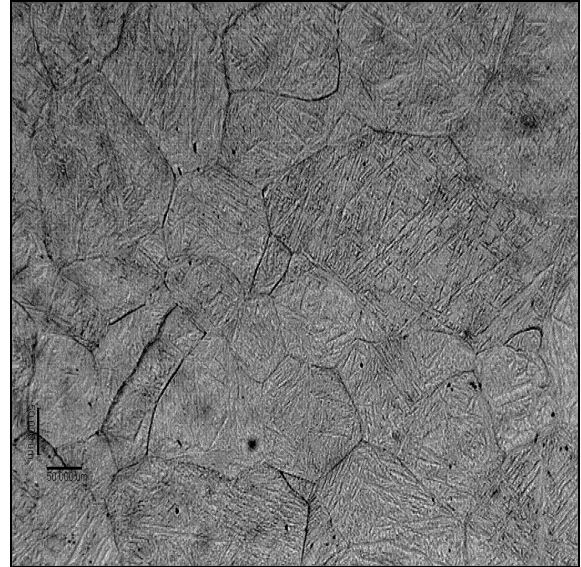


Figure D.8: Optical micrograph of HEAT 2, austenitised at 1175°C for 15 minutes and oil quenched. The microstructure consists of retained austenite in a martensite matrix. (Hardness: 488±63 HV). (Magnification: 100x).

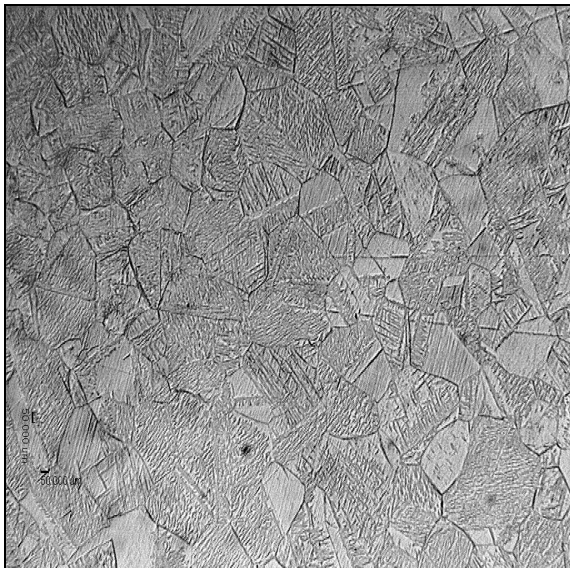


Figure D.9: Optical micrograph of HEAT 1, austenitised at 1200°C for 15 minutes and oil quenched. The microstructure consists of retained austenite in a martensite matrix. (Hardness: 270±12 HV). (Magnification: 50x).

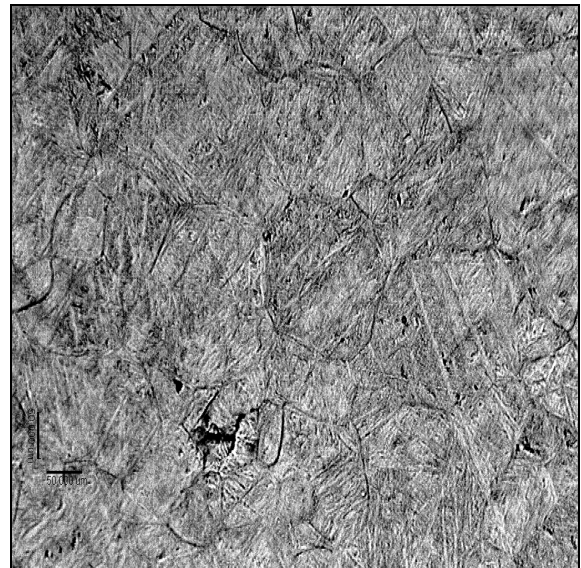


Figure D.10: Optical micrograph of HEAT 2, austenitised at 1200°C for 15 minutes and oil quenched. The microstructure consists of retained austenite in a martensite matrix. (Hardness: 459±2 HV). (Magnification: 100x).

THE EFFECT OF TEMPERING TEMPERATURE ON MICROSTRUCTURE

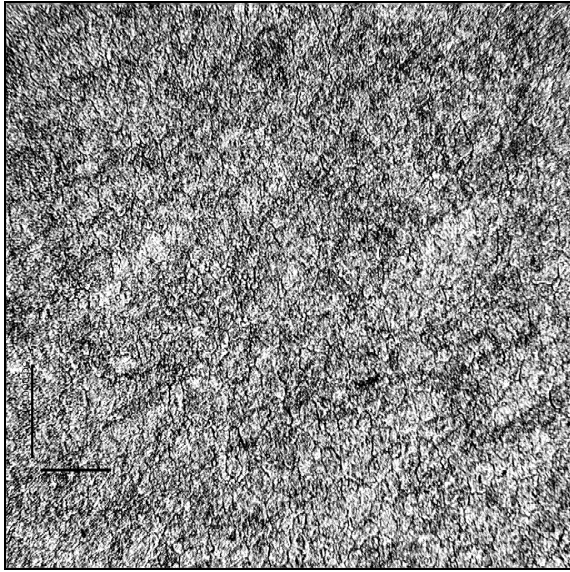


Figure D.11: Optical micrograph of HEAT 1, austenitised at 1075°C for 15 minutes, oil quenched and tempered at 400°C for 120 minutes. The microstructure consists of retained austenite in a martensite matrix. (Hardness: 589±9 HV). (Magnification: 100x).

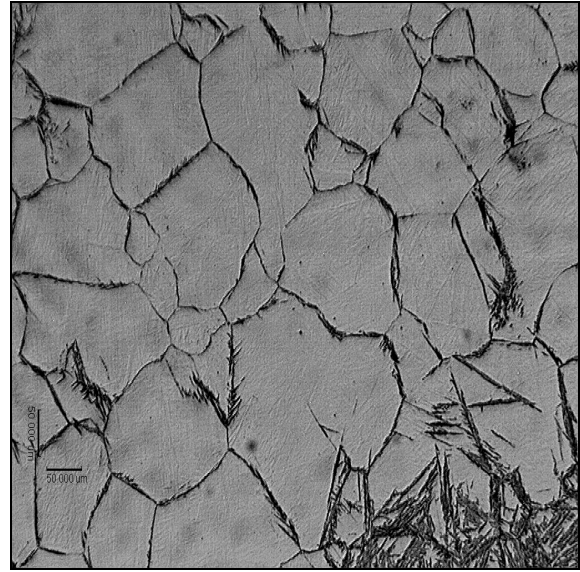


Figure D.12: Optical micrograph of HEAT 1, austenitised at 1150°C for 15 minutes, oil quenched and tempered at 550°C for 30 minutes. The microstructure consists of retained austenite in a martensite matrix. (Hardness: 299±10 HV). (Magnification: 100x).

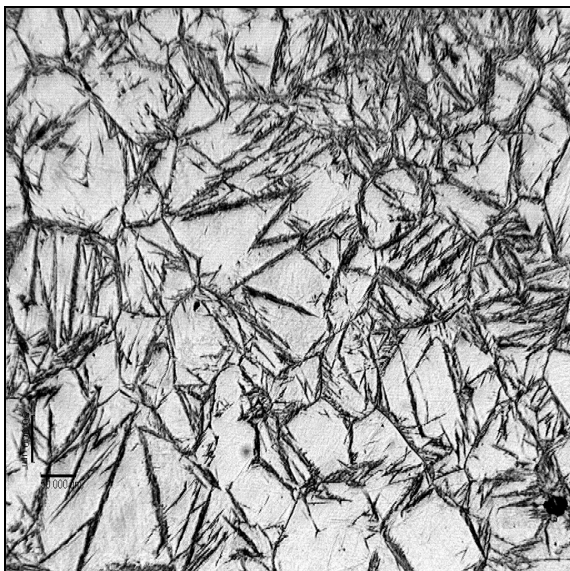


Figure D.13: Optical micrograph of HEAT 2, austenitised at 1150°C for 15 minutes, oil quenched and tempered at 550°C for 30 minutes. The microstructure consists of retained austenite in a martensite matrix. (Hardness: 513±9 HV). (Magnification: 100x).

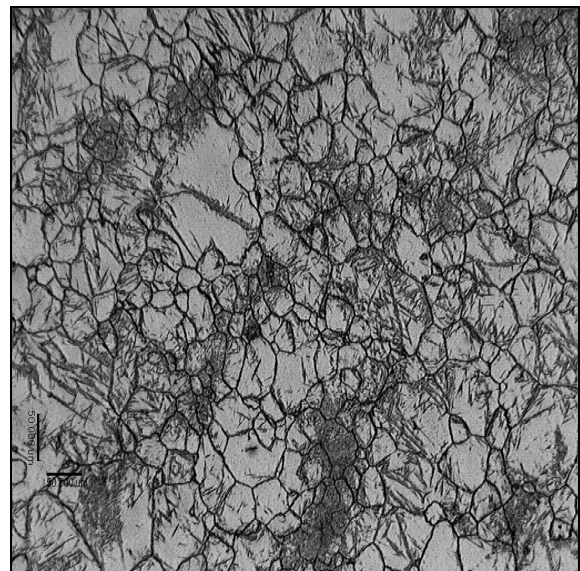


Figure D.14: Optical micrograph of HEAT 2, austenitised at 1175°C for 15 minutes, oil quenched and tempered at 550°C for 30 minutes. The microstructure consists of retained austenite in a martensite matrix. (Hardness: 446±5 HV). (Magnification: 100x).

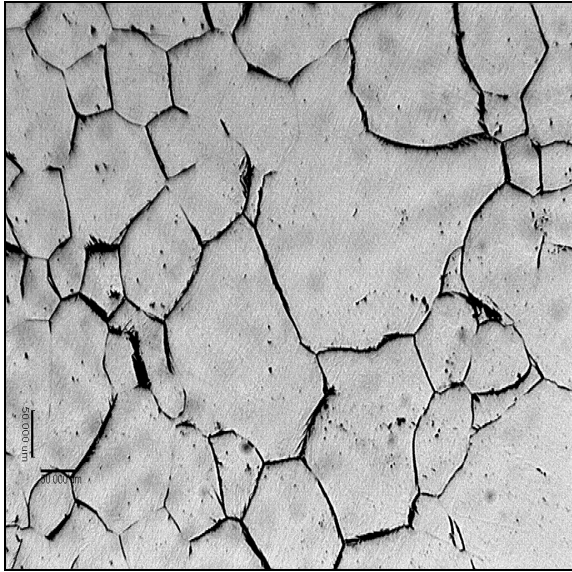


Figure D.15: Optical micrograph of HEAT 1, austenitised at 1150°C for 15 minutes, oil quenched and tempered at 650°C for 30 minutes. The microstructure consists of retained austenite in a martensite matrix. (Hardness: 362 ± 14 HV). (Magnification: 100x).

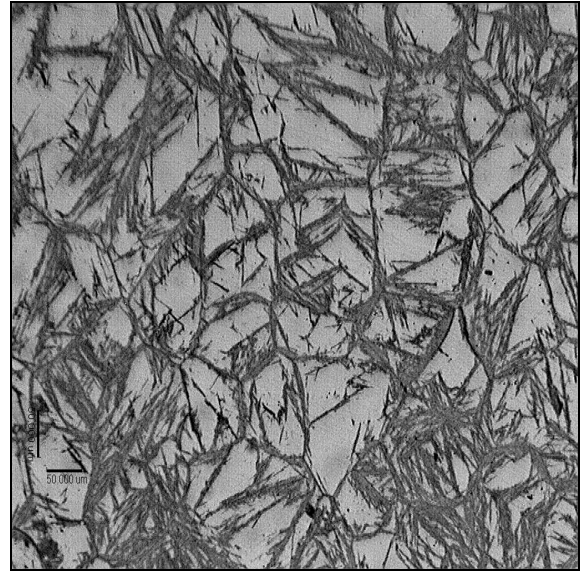


Figure D.16: Optical micrograph of HEAT 2, austenitised at 1150°C for 15 minutes, oil quenched and tempered at 650°C for 30 minutes. The microstructure consists of retained austenite in a martensite matrix. (Hardness: 482 ± 14 HV). (Magnification: 100x).

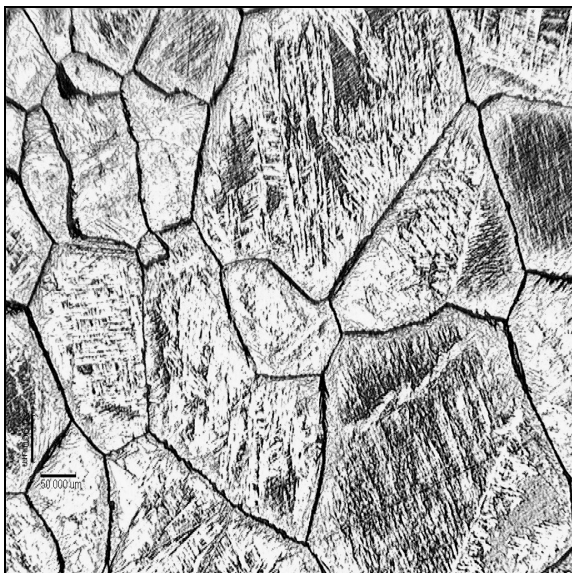


Figure D.17: Optical micrograph of HEAT 1, austenitised at 1175°C for 15 minutes, oil quenched and tempered at 650°C for 30 minutes. The microstructure consists of retained austenite in a martensite matrix. (Hardness: 409 ± 13 HV). (Magnification: 100x).

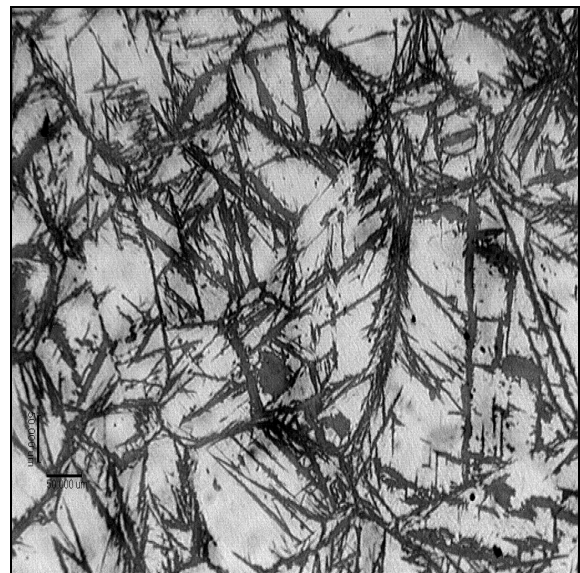


Figure D.18: Optical micrograph of HEAT 2, austenitised at 1175°C for 15 minutes, oil quenched and tempered at 650°C for 30 minutes. The microstructure consists of retained austenite in a martensite matrix. (Hardness: 455 ± 8 HV). (Magnification: 100x).

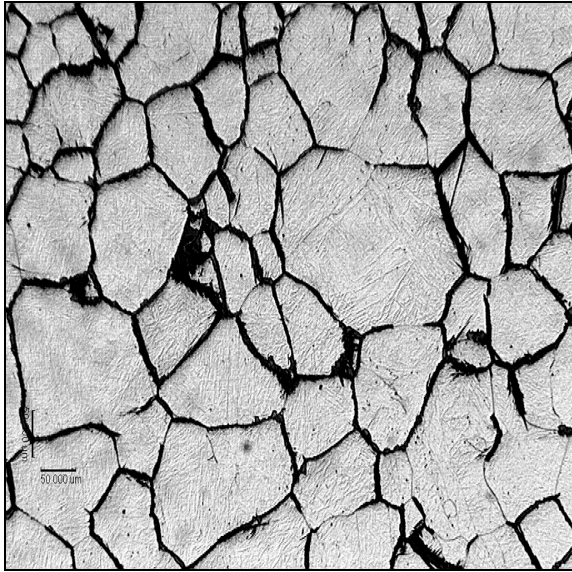


Figure D.19: Optical micrograph of HEAT 1, austenitised at 1150°C for 15 minutes, oil quenched and tempered at 750°C for 30 minutes. The microstructure consists of retained austenite in a martensite matrix. (Hardness: 560 ± 10 HV). (Magnification: 100x).

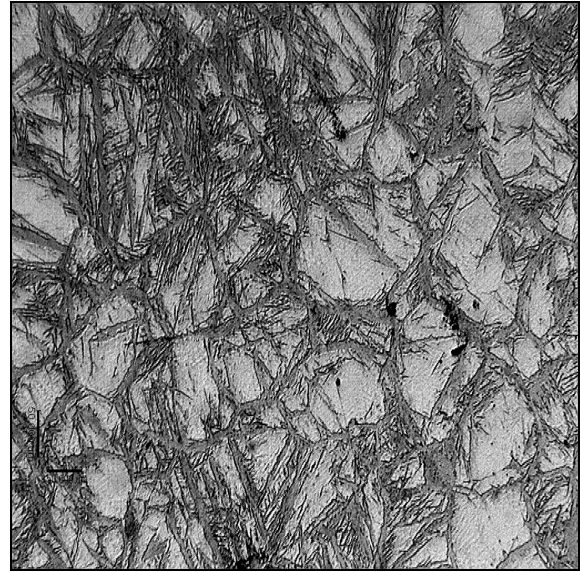


Figure D.20: Optical micrograph of HEAT 2, austenitised at 1150°C for 15 minutes, oil quenched and tempered at 750°C for 30 minutes. The microstructure consists of retained austenite in a martensite matrix. (Hardness: 400 ± 10 HV). (Magnification: 100x).

THE EFFECT OF DOUBLE TEMPERING ON MICROSTRUCTURE

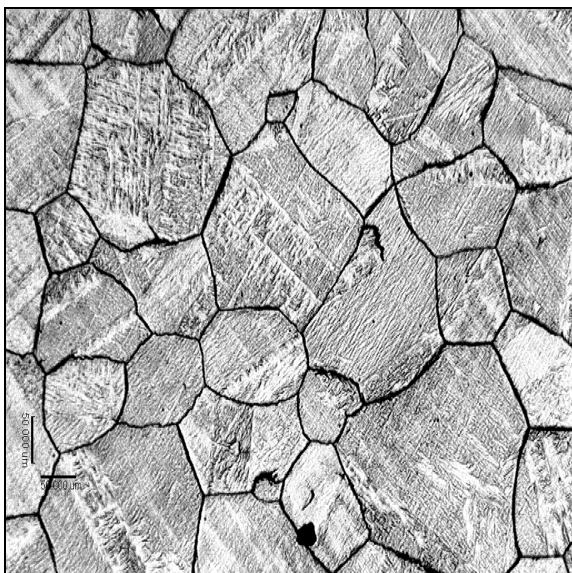


Figure D.21: Optical micrograph of HEAT 1, austenitised at 1175°C for 15 minutes, oil quenched, and double tempered at 550°C for 30 minutes. The microstructure consists of retained austenite in a martensite matrix. (Hardness: 295 ± 14 HV). (Magnification: 100x).

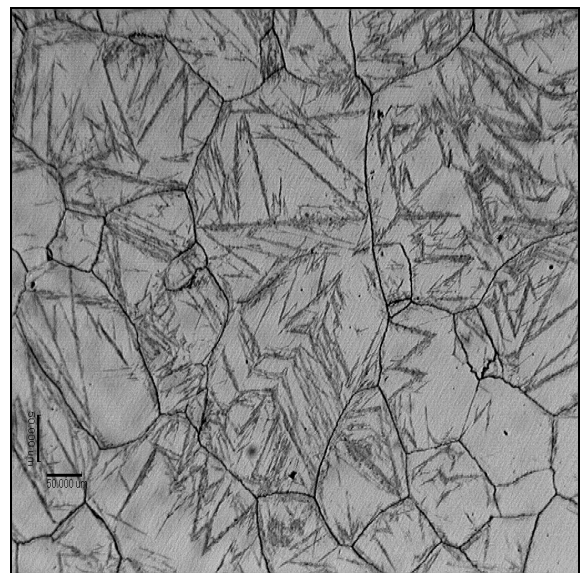


Figure D.22: Optical micrograph of HEAT 2, austenitised at 1175°C for 15 minutes, oil quenched and double tempered at 550°C for 30 minutes. The microstructure consists of retained austenite in a martensite matrix. (Hardness: 522 ± 5 HV). (Magnification: 100x).

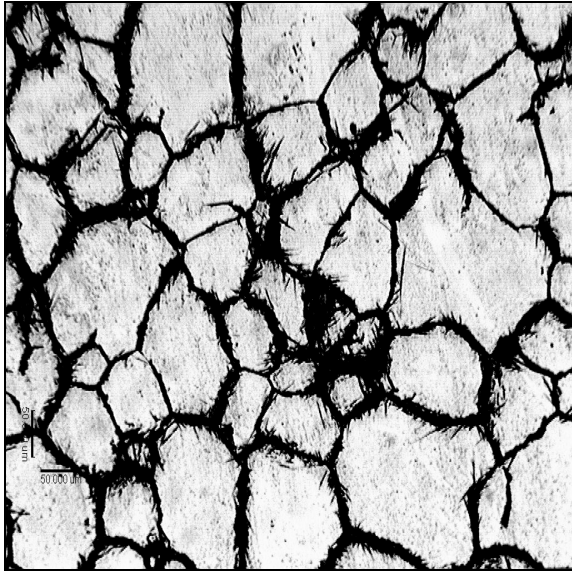


Figure D.23: Optical micrograph of HEAT 1, austenitised at 1150°C for 15 minutes, oil quenched, and double tempered at 650°C for 30 minutes. The microstructure consists of retained austenite in a martensite matrix. (Hardness: 500±9 HV). (Magnification: 100x).

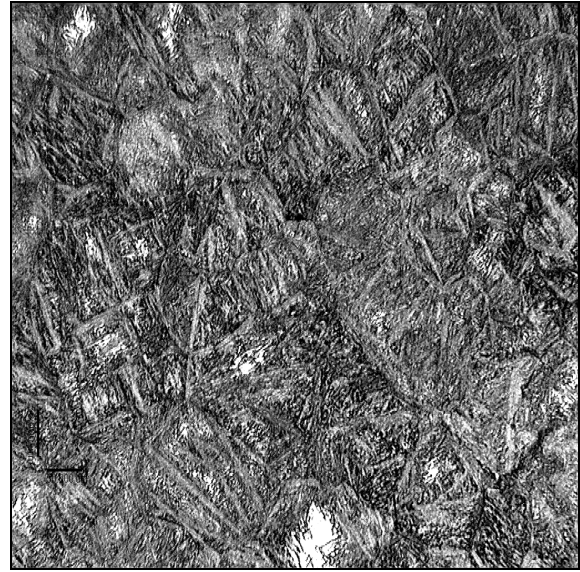


Figure D.24: Optical micrograph of HEAT 2, austenitised at 1150°C for 15 minutes, oil quenched and double tempered at 650°C for 30 minutes. The microstructure consists of retained austenite in a martensite matrix. (Hardness: 360±5 HV). (Magnification: 100x).

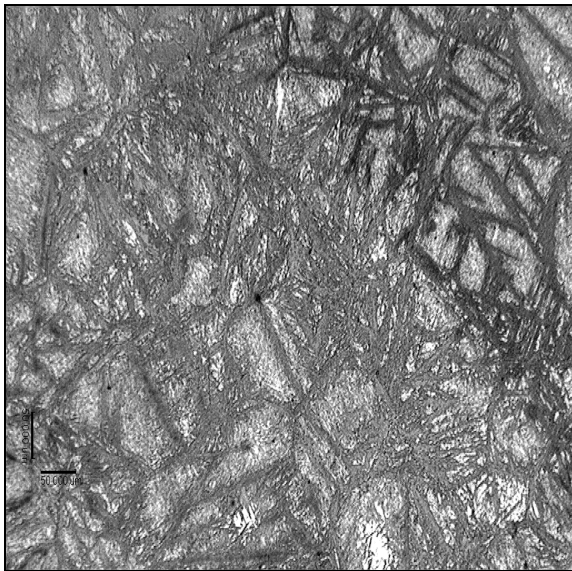


Figure D.25: Optical micrograph of HEAT 2, austenitised at 1175°C for 15 minutes, oil quenched, and double tempered at 650°C for 30 minutes. The microstructure consists of retained austenite in a martensite matrix. (Hardness: 344±6 HV). (Magnification: 100x).

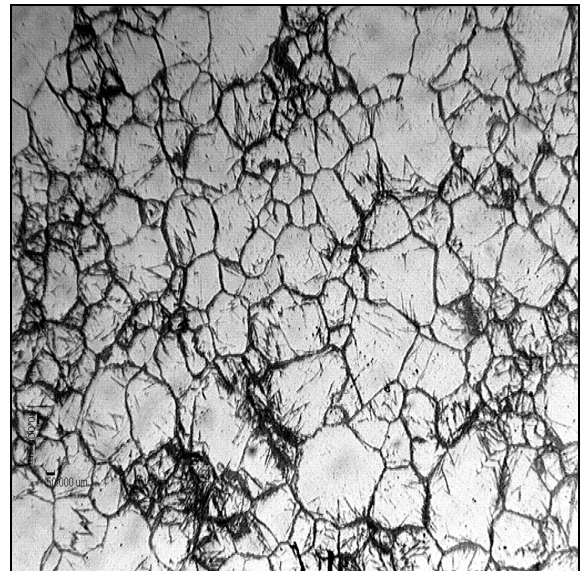


Figure D.26: Optical micrograph of HEAT 1, austenitised at 1150°C for 15 minutes, oil quenched and double tempered at 750°C for 30 minutes. The microstructure consists of retained austenite in a martensite matrix. (Hardness: 320±7 HV). (Magnification: 100x).

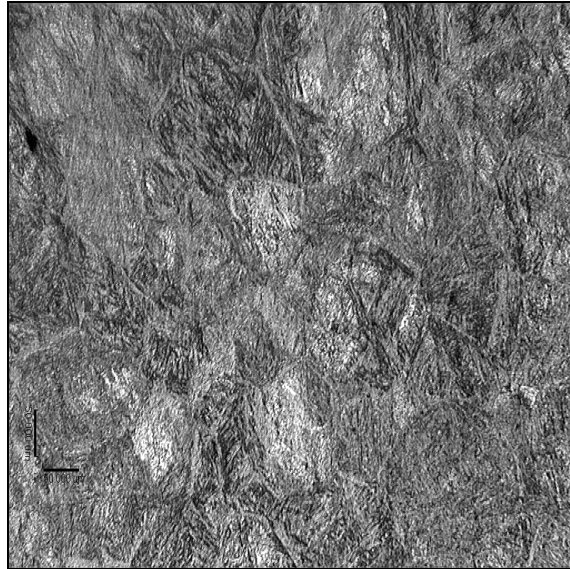


Figure D.27: Optical micrograph of HEAT 2, austenitised at 1150°C for 15 minutes, oil quenched and double tempered at 750°C for 30 minutes. The microstructure consists of retained austenite in a martensite matrix. (Hardness: 294±7 HV). (Magnification: 100x).

THE EFFECT OF SUB-ZERO TEMPERING ON MICROSTRUCTURE

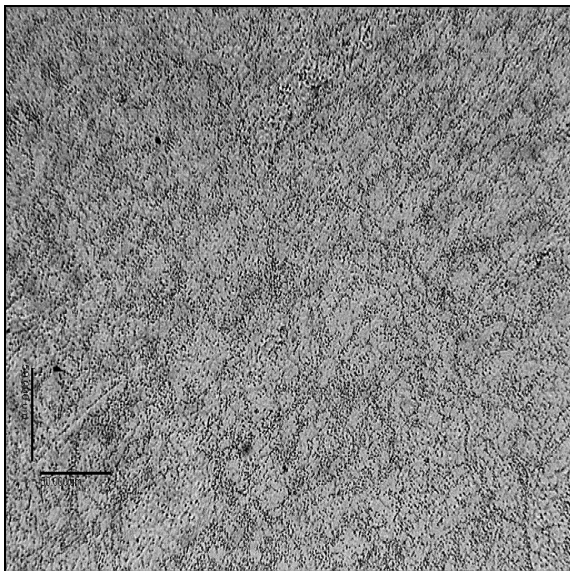


Figure D.28: Optical micrograph of HEAT 1, austenitised at 1050°C for 15 minutes, oil quenched, and sub-zero treated at -75°C. The microstructure consists of M₂₃C₆ carbides and retained austenite in a martensite matrix. (Hardness: 660±8 HV). (Magnification: 200x).

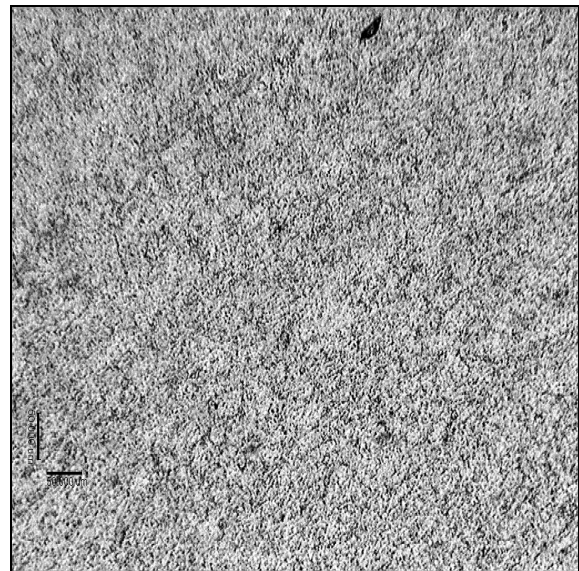


Figure D.29: Optical micrograph of HEAT 2, austenitised at 1050°C for 15 minutes, oil quenched and sub-zero treated at -75°C. The microstructure consists of M₂₃C₆ carbides and retained austenite in a martensite matrix. (Hardness: 673±8 HV). (Magnification: 100x).

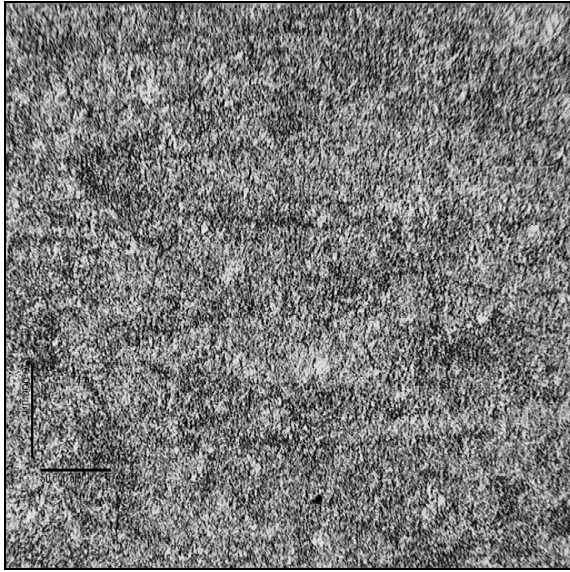


Figure D.30: Optical micrograph of HEAT 1, austenitised at 1100°C for 15 minutes, oil quenched, and sub-zero treated at -196°C. The microstructure consists of $M_{23}C_6$ carbides and retained austenite in a martensite matrix. (Hardness: 797 ± 15 HV). (Magnification: 200x).

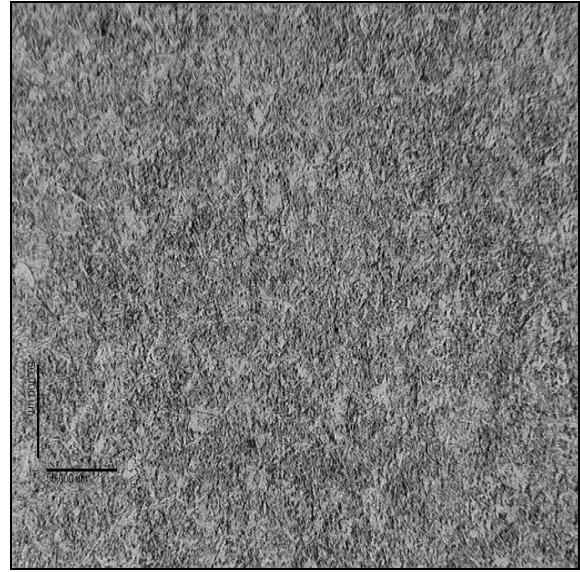


Figure D.31: Optical micrograph of HEAT 2, austenitised at 1100°C for 15 minutes, oil quenched, and sub-zero treated at -196°C. The microstructure consists of $M_{23}C_6$ carbides and retained austenite in a martensite matrix. (Hardness: 785 ± 12 HV). (Magnification: 200x).

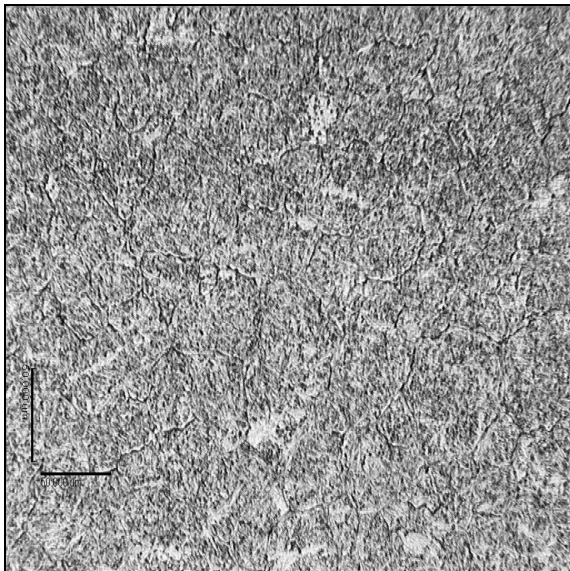


Figure D.32: Optical micrograph of HEAT 1, austenitised at 1130°C for 15 minutes, oil quenched, and sub-zero treated at -196°C. The microstructure consists of retained austenite in a martensite matrix. (Hardness: 739 ± 11 HV). (Magnification: 200x).



Figure D.33: Optical micrograph of HEAT 1, austenitised at 1150°C for 15 minutes, oil quenched, and sub-zero treated at -196°C. The microstructure consists of retained austenite in a martensite matrix. (Hardness: 700 ± 15 HV). (Magnification: 200x).

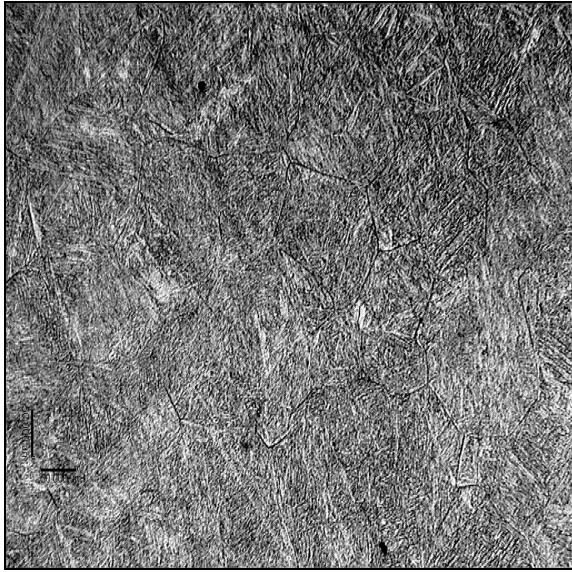


Figure D.34: Optical micrograph of HEAT 2, austenitised at 1150°C for 15 minutes, oil quenched, and sub-zero treated at -196°C. The microstructure consists of retained austenite in a martensite matrix. (Hardness: 756±9 HV). (Magnification: 100x).

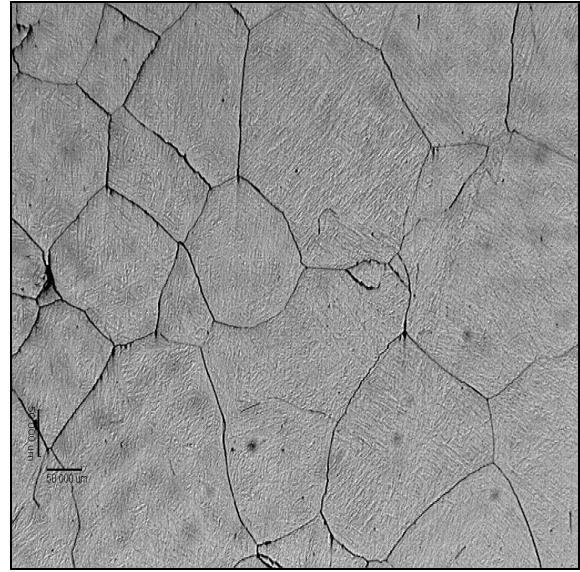


Figure D.35: Optical micrograph of HEAT 1, austenitised at 11750°C for 15 minutes, oil quenched and sub-zero treated at -196°C. The microstructure consists of retained austenite in a martensite matrix. (Hardness: 702±16 HV). (Magnification: 100x).

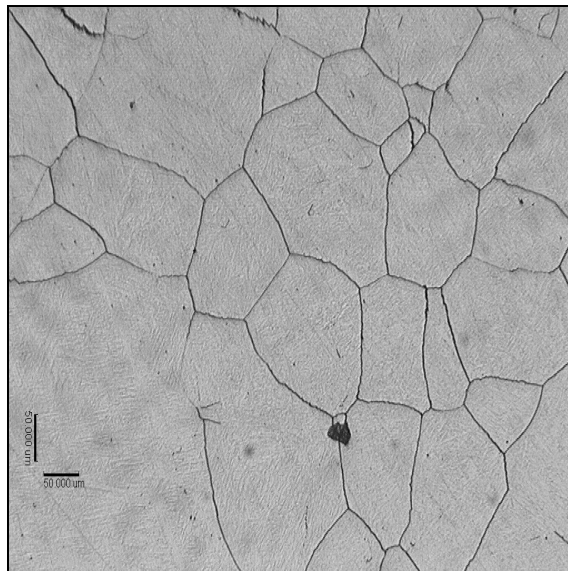


Figure D.36: Optical micrograph of HEAT 2, austenitised at 1175°C for 15 minutes, oil quenched, and sub-zero treated at -196°C. The microstructure consists of retained austenite in a martensite matrix. (Hardness: 751±16 HV). (Magnification: 100x).

SUB-ZERO TEMPERING FOLLOWED BY TEMPERING

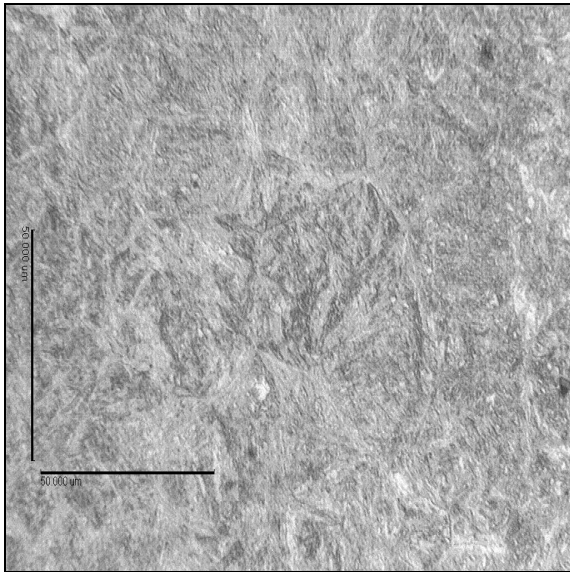


Figure D.37: Optical micrograph of HEAT 1, austenitised at 1130°C for 15 minutes, oil quenched, sub-zero treated at -196°C and tempered at 700°C. The microstructure consists of retained austenite in a martensite matrix. (Hardness: 327 ± 7 HV). (Magnification: 500x).

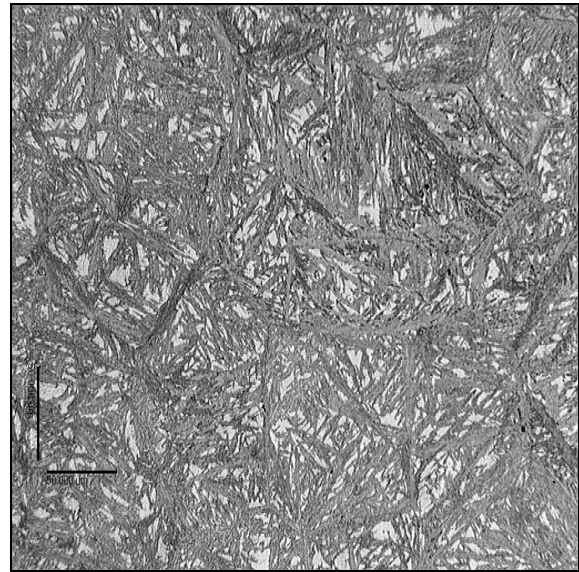


Figure D.38: Optical micrograph of HEAT 1, austenitised at 1150°C for 15 minutes, oil quenched, sub-zero treated at -196°C and tempered at 700°C. The microstructure consists of retained austenite in a martensite matrix. (Hardness: 380 ± 4 HV). (Magnification: 200x).

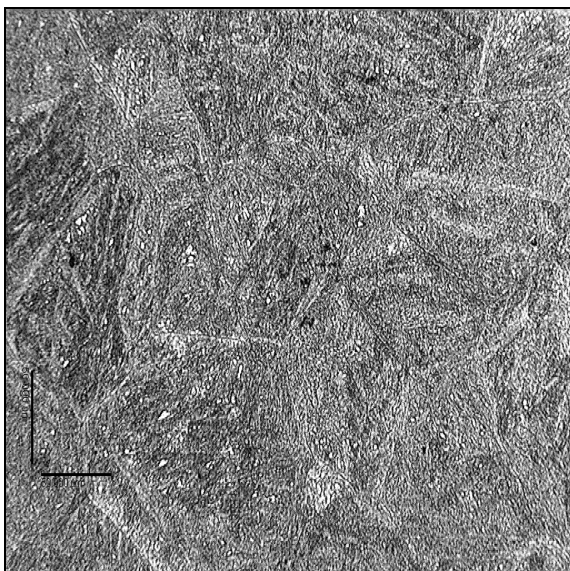


Figure D.39: Optical micrograph of HEAT 2, austenitised at 1150°C for 15 minutes, oil quenched, sub-zero treated at -196°C and tempered at 700°C. The microstructure consists of retained austenite in a martensite matrix. (Hardness: 330 ± 3 HV). (Magnification: 200x).

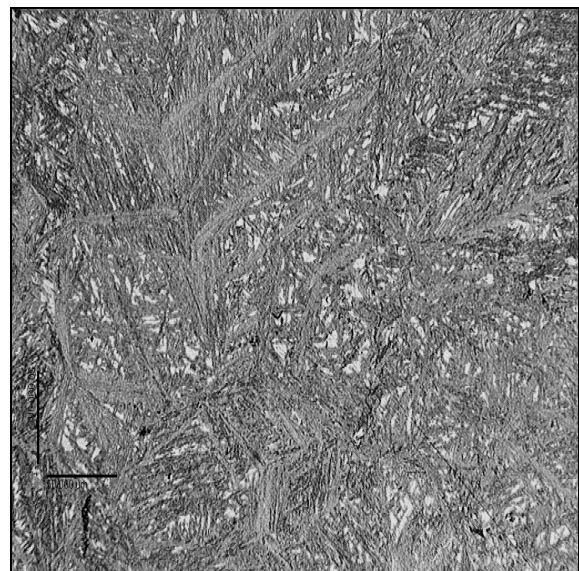


Figure D.40: Optical micrograph of HEAT 1, austenitised at 1175°C for 15 minutes, oil quenched, sub-zero treated at -196°C and tempered at 700°C. The microstructure consists of retained austenite in a martensite matrix. (Hardness: 327 ± 7 HV). (Magnification: 200x).

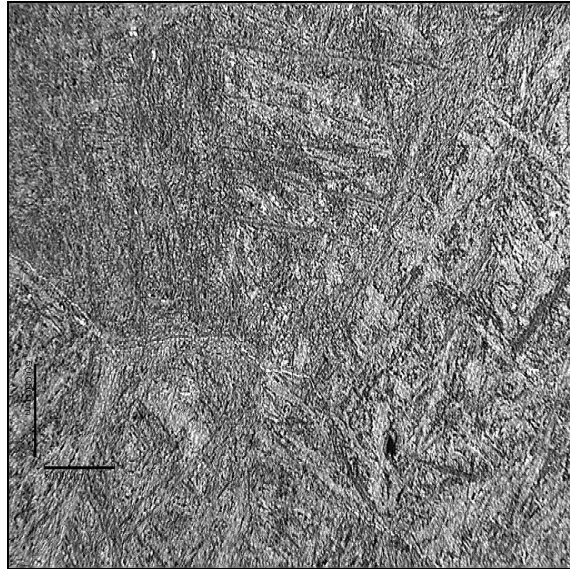


Figure D.41: Optical micrograph of HEAT 2, austenitised at 1175°C for 15 minutes, oil quenched, sub-zero treated at -196°C and tempered at 700°C. The microstructure consists of retained austenite in a martensite matrix. (Hardness: 326 ± 6 HV). (Magnification: 200x).